



Master of Science in Civil Engineering

Design of field trial with stabilized granular mixtures
containing recycled aggregate from construction and
demolition waste.

Supervisors:

Prof. Marco BASSANI
Ing. Luca TEFA

Candidate:

Lorenzo LERDA

Academic year 2021/2022

March 2022

LIST OF CONTENTS

1. Introduction.....	1
1.1. State of the art	2
1.1.1. CDW stabilized with non-traditional binders	3
1.1.2. Field performance of cement stabilized CDW aggregates.....	4
1.2. Objectives.....	4
2. Materials and methods	7
2.1. Experimental design.....	7
2.1.1. Laboratory tests.....	7
2.1.2. Field trial test design.....	7
2.2. Materials.....	8
2.2.1. Natural and recycled aggregates	8
2.2.2. Binders.....	9
2.2.3. Mixtures.....	11
2.3. Methods – Laboratory tests.....	12
2.3.1. Proctor study	13
2.3.2. Specimen preparation by the gyratory shear compactor	16
2.3.3. Cyclic triaxial test.....	19
2.3.4. Unconfined compression strength (UCS)	22
2.3.5. Indirect tensile strength (ITS)	24
2.4. Methods – Field investigation.....	25
2.4.1. Light weight deflectometer (LWD) test.....	25

2.4.2. Plate load test	27
2.4.3. In-place density with sand-cone test:	28
3. Results and discussion of Laboratory tests.....	31
3.1. Proctor study.....	31
3.2. Workability.....	34
3.3. Cyclic triaxial test (Resilient modulus)	36
3.4. Unconfined compression strength and indirect tensile strength	41
4. Preliminary field trial	45
4.1. LWD test simulation	45
4.1.1. LWD test simulation: results and discussion	46
4.2. On-site tests	48
4.2.1. On-site tests: results and discussion.....	53
5. Design of the field trial.....	59
5.1. Materials.....	59
5.2. Operation schedule	61
5.3. Quantities estimation.....	69
6. Conclusions	73
7. References	77
8. Attachments.....	83
8.1. Proctor test.....	83
8.2. Gyratory shear compaction.....	84
8.3. Cyclic triaxial test.....	89

8.3.1. Resilient modulus dyagrams	99
8.4. UCS and ITS	101
8.5. Preliminary site operations.....	107
8.5.1. LWD test simulation.....	107
8.5.2. LWD test on multi-layer	112

1. INTRODUCTION

Civil works require considerable amount of natural resources and produce large amounts of waste. For many years, the construction industry has been following a model of extraction, production, use and discard. In the last decades, the awareness about sustainability bringing us to consider development model based on a circular economy. The concept of a sustainable economy is centred on the reduction of the generation of waste, and on the reuse of materials by means of recycling. Considering the construction industry, national and international authorities started to move to a cradle-to-cradle approach, which accounts for the whole life cycle of the materials from the production to their recovery and recycling process. The European Union has introduced the waste framework directive (European Parliament, Waste Framework Directive 2008/98/EC, 2008) which requires the member states to achieve a minimum of 70% construction and demolition waste (CDW) reuse. The ISPRA report (ISPRA, 2021) states that in 2019, in Italy the total production of CDW stands at about 52.1 million tons, while the total recovery of the material reaches 40.7 million tons. Hence, the percentage of CDW recovery is at 78.1%, which is above the 70% target set by the European directive.

The waste material deriving from the construction and demolition process, if specifically processed, can be reused as aggregates for the construction of new civil works. In the road pavement industry, CDW aggregates are already used in the formation of subgrades or for the production of asphalt mixtures, providing satisfactory and promising solutions (Ossa et al., 2016). Despite these encouraging results, the widespread use of recycled CDW aggregates is still hampered in Italy. One of the main reasons is the lack of confidence in the products derived from waste, combined with a poor knowledge of technical characteristics of the same. Moreover, low taxes on mining activities and landfills do not yet allow adequate competitiveness of recycled aggregates compared to virgin ones (Iacobaea et al., 2019).

The recycling process of CDW aggregates is usually inexpensive and can bring high advantages like:

- reduction of the amount of waste destined to landfills;
- reduction of extraction and consumption (preservation) of non-renewable primary (and natural) resources;
- cost reduction, since waste materials are cheaper compared to virgin aggregate.

An improvement in the environmental sustainability of pavement construction will be possible only if complemented by scientific and technological support aimed at demonstrating the feasibility of employing CDW materials. The research activities described in this thesis are part of the INTREC (Innovative technologies for recycled aggregates from construction and demolition waste in road construction) Project. This study aims at developing stabilized granular mixtures with recycled aggregates for the formation of subbase layers of road pavements. The study adds a contribution to the development of a wider knowledge on the use of recycled aggregates stabilised with alternative binders and their in-situ performances.

1.1. State of the art

CDW is generated by construction and demolition activities of buildings, civil works or road infrastructures. CDW is a strongly heterogeneous material whose composition depends on multiple factors such as (i) local construction types and techniques, (ii) raw materials and (iii) the construction products locally available. The composition of CDW mainly consists of concrete, bricks, bituminous mixtures, natural aggregates and excavated soil. Moreover, undesired materials such as metals, plastic, wood and glass can also be present.

This material can be processed to create CDW recycled aggregates. The transformation of a waste product into a commercial one is obtained through analysis, treating and by a third-parties control process. If performed correctly, these steps lead to the CE marking of the recycled aggregate, which is a fundamental requirement for its placing on the market. According to the EU regulation, the suitability and homogeneity of the material are guaranteed when it is provided with the CE marking (EU regulation n. 305/2011).

CDW recycled granular material is already used as filling material in the road embankments formation (Zhang et al., 2020), and the construction of unbound pavement layers for low-traffic roads (Pourkhorshidi et al., 2020; Arulrajah et al., 2013a). Many studies advocated that the mechanical properties of mixed recycled aggregates, such as resilient modulus (RM) and California Bearing Ratio (CBR) are comparable to virgin aggregates when used in unbound layers of road pavements. (Leite et al., 2011; Arulrajah et al., 2013a).

As well as natural aggregates, also in the case of CDW aggregates, mechanical properties can be improved by recurring to stabilization techniques (Beja et al., 2020; Del Rey et al., 2016). Stabilization can be performed with traditional binders as lime and cement. Taha et al. (2002) and Puppala et al. (2011) demonstrated that the mechanical properties of recycled aggregates stabilized mixtures increase remarkably with respect to unstabilised mixtures. Traditional binders

like Portland cement are expensive and their production process is responsible for the production of a huge amount of CO₂ (Zhang et al. 2014). A valid alternative to the stabilization with traditional binders is the use of by-products coming from industrial processes like fly-ash, cement kiln dust, or the stabilization through alkaline activation.

1.1.1. CDW stabilized with non-traditional binders

The use of recycled aggregates in substitution of the natural ones aims at reducing the environmental impact of road constructions. The same goal has to be pursued when non-traditional binders are considered. The environmental sustainability of a binder can be evaluated in terms of local availability, transportation costs and CO₂ emissions. The sustainability of a binder must be evaluated also in terms of mechanical properties, a reasonably limited amount of binder has to provide the mixture with sufficient strength over time. In this context, the research on new solutions in the field of binders is becoming of pivotal role.

Interesting results have been achieved with the stabilisation of CDW aggregates through alkaline activation of fly ash (FA) or blast furnace (BF). Mohammadinia et al. (2016) assessed the suitability of this solution when employed in base and subbase layers of road pavements. The CDW aggregates were composed of recycled asphalt product (RAP), crushed bricks (CB) and recycled concrete aggregates (RCA). The stabilisation was obtained by mixing the CDW aggregates with different combinations of FA or BF and by adding different percentages of an alkaline solution to activate the chemical reactions. The values observed in the unconfined compression test (UCS) showed an improvement in mechanical strength proportional to the content of BF or FA added, to the percentage of RCA contained in the aggregates, and to the alkaline solution content.

Of particular interest in terms of environmental sustainability is the study of Bassani et al. (2019), which demonstrated that CDW fine powders containing crushed concrete and ceramic material can react in an alkaline environment increasing in strength without the addition of external reactive precursors. In the study, the fine fraction of the granular mix was used to stabilize the coarse aggregates thanks to the reaction induced by the alkaline environment. In the formation of stabilized subbase layers made of CDW aggregates, this solution can be advantageous from an economical and environmental point of view since it does not require the use of any conventional binder and promote the innovative use of CDW aggregates with adequate mechanical properties comparable to those of traditional cement-stabilized natural granular materials.

1.1.2. Field performance of cement stabilized CDW aggregates

Interesting results have been observed with the use of recycled aggregates in road pavements.

The experimental study of Agrela et al. (2012) involved the construction of three trial sections 300 m long with a pavement structure composed of a 30 cm-thick cement-stabilized soil as subgrade, 20 cm of cement-treated subbase (with 3% of CEM II/B) and a top bituminous mixture of 15 cm layer. The three sections were identical in composition except for the subbase layer in which were used natural aggregates (NA) in the first section, in the second section were used a mix of recycled aggregates composed of RCA and CB in equal proportions (MixRA-15), in the last section were used CC and CM with a proportion of 34 % and 64 % respectively (MixRA-22). On the subbase layer were performed impact deflectometer tests after 28 days, a 67 kN load was applied on a 450 mm diameter plate. The surface deflection of the cement-treated recycled aggregates sub-base (both MixRA-15 and MixRA-22) was equal to 0.10 mm, while the section with NA had a mean deflection equal to 0.21 mm on its surface. Moreover, the 28 days unconfined compressive strength performed on cored samples, showed a mean value of 4.17 MPa in the section with natural aggregates, 4.51 MPa in the MixRA-15 section, and 4.25 MPa in the MixRA-22 section. These results confirm that recycled aggregates in stabilised subbase layers can reach similar or higher performances with respect to the natural ones, in terms of stiffness and strength.

Similarly, Perez et al. (2013) investigated the mechanical response of two different road sections, in which the subgrade layer was the same for both, while the first subbase consisted of a 21 cm-thick cement-treated recycled concrete aggregate layer (CT-RCA), and the second one consisted of a cement-treated natural aggregate layer (CT-NA) of the same thickness. In both cases, the mixtures were stabilised with 3.5 % of CEM II/A. The surface deflection was measured through an impact deflectometer by applying a 67 kN load on a 450 mm diameter plate. The results showed that a deflection equal to 0.317 mm was obtained on the CT-RCA layer and 0.398 mm on the CT-NA. Also in this case, the recycled aggregates stabilised mixture reported a higher value of stiffness with respect to the natural aggregates mixture.

1.2. Objectives

The use of recycled materials such as aggregates deriving from CDW, replacing virgin natural resources, is increasing in popularity in road construction. Several studies have shown that CDW aggregates can replace natural mixtures in the subgrade and subbase layers of the pavement. Although several successful applications are documented, recycled materials are still viewed with

some distrust. This can be related to several reasons such as the large availability of virgin natural resources, the reduced durability concerning the degradation phenomena produced by traffic and the environment, and to a lack of scientific knowledge which brings distrust from the authorities (Iacobaea et al., 2019).

The experimental investigation described in this thesis partly covers the gap in knowledge on the properties of these materials.

INTREC (Innovative Technologies for RECycled aggregates from construction and demolition waste in road constructions) project aims at promoting the reuse of this alternative source of aggregate through the investigation of stabilized and non-stabilized mixtures. The objective of INTREC is to increase the economic and environmental sustainability of road constructions. The project plans at developing stabilized granular mixtures with recycled aggregates for the formation of sustainable road subbase layers. The project is organized into three Work Packages (WP). WP1 concerns the laboratory study and experimental characterization of innovative stabilized mixtures, obtained from natural and recycled aggregates. WP1 includes the design, in terms of geometry and operation, of an experimental field trial (to be developed in WP2). WP2 aims to test the mechanical performance of the innovative materials at a real scale. During WP2, the mechanical performance will be tested in the experimental site, and the environmental and economic sustainability of the materials will be monitored and evaluated. Finally, in WP3 an experimental road section will be built. In WP3, structural and environmental investigations will be carried out to demonstrate the applicability of the technological solutions of the INTREC project.

The experimental investigation of this thesis is included in the WP1 of INTREC, and the main objectives follow:

the laboratory study of the CDW granular mixtures stabilised with non-traditional binders (paragraph **Errore. L'origine riferimento non è stata trovata.**) through optimum water content, the maximum dry density, the resilient modulus, the UCS and the indirect tensile strength (ITS) determinations;

the selection of the materials to be investigated in real-scale;

the implementation of preliminary site operation in order to test the equipment (lightweight deflectometer) evaluating the sensibility of the measured dynamic modulus with respect to the variation of the applied stress and to the different levels of compaction, and testing the procedures in view of the experimental field trial;

the design of the experimental field trial section, which included the geometry and structural design, the material quantity estimation, the schedule definition and the programming of the performance monitoring system.

2. MATERIALS AND METHODS

2.1. Experimental design

In line with the objectives, the experimental plan was divided into two stages: (i) the laboratory tests and (ii) the design of the experimental field trial. In the first stage (laboratory test), the composition of the mixtures was defined and their mechanical properties were investigated. In the second stage (experimental field trial design), the geometric characteristics of the site were designed and the in-situ investigations were planned. In addition, it was developed a preliminary testing box in which the equipment and procedures for the field activities of WP2 were tested.

2.1.1. Laboratory tests

The laboratory investigation aimed at determining the mechanical characteristics of stabilized CDW mixtures with different types of binders. In order to compact specimens at their maximum densification, the optimum water content and the maximum dry density as per the Proctor method. The mechanical characterisation of the mixtures was focused on the determination of the RM and UCS after 7 and 28 days of curing, and ITS after 7 days of curing only. The analysis of laboratory results allowed to select the mixtures to be used in the field trial test. Since the length of the testing site was defined and referring to the mechanical properties determined during the previous stage, three innovative mixtures, two unbound mixtures and two reference mixtures were selected.

2.1.2. Field trial test design

The field trial test is aimed at investigating the in-situ properties of the stabilised and unbound mixtures that were selected in the previous stage of the study. The mixtures will be employed as subbase layer of the field trial road section. In this thesis, the design of the field trial and the programming of the activities necessary to investigate the properties of the examined materials was carried out. The geometrical design of the road was provided by Cavit, while the thickness of the pavement layers was determined through a structural analysis employing a mechanical model. The field tests to be developed on-site were defined on the basis of national prescriptions such as the CIRS regulations (*CIRS e Ministero delle Infrastrutture e dei Trasporti, 2° edizione*) and consulting reliable guidelines such as the “*Quaderni tecnici*” of ANAS (ANAS 2019). During the execution of the preliminary field trial operations, it was possible to test equipment and methods to be implemented in the field trial, moreover, the sensitivity of the LDW device was assessed. The material quantities necessary to build the field trial were determined on the basis of

the experimental site dimensions and the thickness of the pavement layers established in the structural analysis. The final stage was dedicated to the scheduling of construction operations.

The logical scheme of the experimental site design is shown in Figure 1.

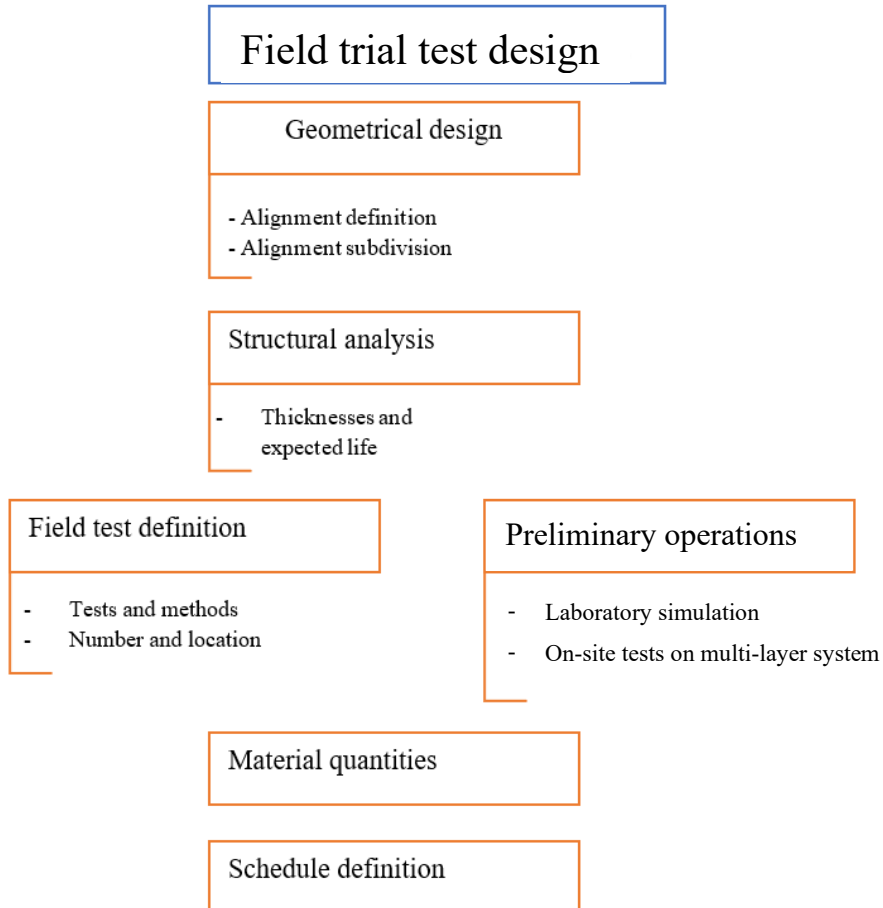


Figure 1: Experimental design, conceptual scheme of the experimental site design

2.2. Materials

2.2.1. Natural and recycled aggregates

Recycled aggregates from CDW were provided by Cavit S.p.A. (La Loggia, Torino). The recycling plant has a production capacity of 250,000 tons per year. The recycling process begins with the recovery and collection of construction waste from civil works. The material is mainly composed of concrete, bricks, bituminous mixtures, natural aggregates and excavation soil, but metal materials, plastics, wood and glass are also present in minimal quantities. As the CDW

arrives at the Cavit plant, it must be selected. At first, it is transported to a control station where wood, plastic sheets and iron elements are separated. Subsequently, the material is sieved and the components that exceed 40 mm in size are separated and sent to an additional crushing process. The finest fraction is subjected to mud removal, then, air blowers allow eliminating the lightest material such as plastics. In this phase also the metallic scraps are removed with a magnetic device. At the end, the material is sieved and separated into different piles depending on the grain sizes (0-10, 0-8, 8-40 and 40-100 mm). The materials are marked with CE certification required by law. In this study, only the material passing through 25 mm was used, since larger particles are unsuitable to prepare cylindrical samples with a diameter of 100 mm.

In the case of natural aggregates, the material was provided by Cave Germaire (Carmagnola, Italy); grains passing at 25 mm was used also in this case.

Table 1 reports the physical parameters of the aggregates.

Table 1: Physical parameters of the aggregates (Investigated by Avellino and Gugliotta (2021)).

PARAMETER	NATURAL	CDW
SHAPE INDEX [%]	13	14
FLATTENING INDEX [%]	14	12
DENSITY [kg/m ³]	2669	2597
ABSORPTION [%]	0.9	3.7

2.2.2. Binders

In the study, the attention was focused on innovative and environmentally sustainable binders. To provide a reliable comparison of the mechanical properties, traditional binders like Portland type II cement were used. The characteristics of the binders used are reported as follows.

CEMENT

Cements were provided by Holcim S.p.A. During the experimental investigation, the following cements were employed:

CEM II/B-LL 32,5 R: Portland limestone cement, compliant with regulations UNI EN 197-1:2011 (*Ente nazionale italiano di unificazione*, 2011), with 67-79% of clinker and 21-35% of limestone. Its density is equal to 2930 kg/m³ (Holcim S.p.A. 2020a);

CEM IV/B: following the quantities defined by the reference standard UNI EN 197-1:2011 (*Ente nazionale italiano di unificazione*, 2011), contains from 45% to 64% of clinker and from 36% to

55% of calcined clay as an industrial pozzolan, with minor components in quantities not exceeding 5%, the density was assumed to be equal to the one of CEM II/B, 2930 kg/m³;
HYBRID CEMENT: mixture obtained by mixing 50% by weight of CEM IV/B and 50% of calcined clay, the density was assumed to be equal to the one of CEM II/B, 2930 kg/m³.

ALKALI-ACTIVATE CDW FINES

As reported in paragraph 1.1.1, stabilized CDW aggregate mixtures can be stabilised without the addition of traditional binders. The stabilization is possible thanks to the addition of alkaline liquids that activate chemical binding reactions between aluminosilicates and alkaline metal silicates present both in the fine CDW fine fraction and in the alkaline solution used. The alkaline solution is composed of 20% by weight of hydrated sodium hydroxide (NaOH) and 80% by weight of hydrated sodium silicate (Na₂SiO₃).

In the study, three alkaline solutions (AS) were adopted to trigger the alkali-activation of CDW fines:

AS1: aqueous solution obtained in the lab by mixing 20% by weight of 50%-concentrated sodium hydroxide (NaOH) solution and 80% by weight of sodium silicate (38/40 Bé R3.3) (Na₂SiO₃);
 AS2: aqueous solution composed of sodium silicate (44 Bé R1.65) present in a ratio SiO₂/Na₂O of about 1.65, the liquid is obtained by a hydrothermal process performed in the Ingessil S.r.l. plant;

AS3: is a solution identical to the AS2 one but with the addition of a surfactant to reduce the viscosity.

BONDAFIX FH 130

In the investigation, a commercial binder named Bondafix FH 130 (Barzaghi s.r.l.) was investigated for the production of stabilized CDW aggregates. It is a composite agglomerating polymer of natural origin. It is a powder with a density equal to 1000-1100 kg/m³ (Barzaghi s.r.l. 2020); when mixed with water it provides binding properties. Table 2 reports the characteristics summary of the binders.

Table 2: Characteristics of the binders

BINDER	DENSITY [kg/m ³]	COMPOSITION
CEM II/B-LL 32,5 R	2930	67-79% clinker, 21-35% limestone

CEM IV/B	2930	45%-64% clinker, 36%-55% calcined clay
HYBRID CEMENT	2930	50% CEM IV/B, 50% calcined clay
CDW fines + ALKALINE SOLUTION (AS1, AS2, AS3)	-	Sodium hydroxide and sodium silicate
Bondafix	1000-1100	Polymers

2.2.3. Mixtures

BLEND WITH NATURAL AGGREGATES

The properties of natural aggregates mixtures were investigated in a previous study by Avellino and Gugliotta (2021). In this study, these mixtures were considered for comparison purposes.

In particular, mixtures stabilised with 3 % by weight of CEM II/B, denominated as NAT+3CEM-II/B, and the unbound natural aggregate denominated as “NAT and water” were considered. Both of the mixtures present an Optimal Moisture Content (OMC) equal to 6.5 %, and the Maximum Dry Density (MDD) is 2.253 Mg/m³ and 2.248 Mg/m³ for the stabilised mixture and the unbound one respectively. These materials were employed as a reference to compare the mechanical properties of the mixtures containing recycled aggregates.

BLEND WITH CDW AGGREGATES

Regarding the Bondafix binder, three solutions containing 4 %, 8 % and 12 % by weight of binder were tested. The blends were named respectively CDW+4BF, CDW+8BF and CDW+12BF.

Concerning the mixtures stabilised with alkali-activated CDW fines, three mixtures combinations were investigated. Previous studies defined the properties of the mixtures stabilised with AS1 (Avellino and Gugliotta, 2021), the OMC was found to be 8.5 %, which corresponds to an MDD of 2.155 Mg/m³. This mixture was denominated CDW+AS1. The same OMC and MMD were assumed for the mixtures stabilised with AS2, which were denominated CDW+AS2. In the case of AS3, the solution containing surfactant, OMC and MDD were determined during this study, the denomination for this blend is CDW+AS3.

To compare the mechanical properties between the mixtures stabilised with traditional and non-traditional binders, the one stabilised with 3% by weight of CEM II/B (CDW+3CEM-II/B) showed an OMC equal to 8.5% and an MDD of 2.119 Mg/m³ (Avellino and Gugliotta 2021).

Two mixtures containing CEM IV/B were investigated, the first one was denominated as CDW+3CEM-IV/B, it contains 3% by weight of CEM IV/B, the OMC and the MDD were assumed to be the same as for the mixture CDW+3CEM-II/B (Avellino and Gugliotta 2021). The second one contains 3% by weight of “hybrid” cement (50% CEM IV/B and 50% calcinated clay), also in this case the OMC and the MDD were assumed to be the same as for the mixtures CDW+3CEM-II/B, the blends were denominated as CDW+3IB.

Finally, the unbound granular mixture with OMC equal to 8.5% and an MDD of 2.121 Mg/m³ (Avellino and Gugliotta 2021). The mixture was denominated “CDW and water” was considered. Table 3 resumes the characteristics of the mixtures.

Table 3: Studied mixtures (studied by Avellino and Gugliotta (2021)).

MIXTURE NAME	AGGREGATE	BINDER	BINDER %
NAT and water *	NAT	-	-
CDW and water *	CDW	-	-
NAT+3CEM-II/B *	NAT	CEM II/B	3
CDW+3CEM-II/B *	CDW	CEM II/B	3
CDW+3CEM-IV/B	CDW	CEM IV/B	3
CDW+3IB	CDW	HYBRID CEMENT	3
CDW+AS1 *	CDW	CDW fines + AS1	8.5 AS1
CDW+AS2	CDW	CDW fines + AS2	8.5 AS2
CDW+AS3	CDW	CDW fines + AS3	4-6-8-8.5-10-12 AS3
CDW+4BF	CDW	Bondafix	4
CDW+8BF	CDW	Bondafix	8
CDW+12BF	CDW	Bondafix	12

2.3. Methods – Laboratory tests

This paragraph describes the methods adopted to perform the laboratory tests on mixtures. A specific Proctor study to determine OMC and MDD was performed. The Optimal Moisture Content (OMC) and the Maximum Dry Density (MDD) were used as inputs in the recipes used to mix the constituents of mixtures and prepare the samples through the gyratory shear compactor.

In addition, during the compaction the workability parameters were recorded. The mechanical properties of stabilized mixtures were evaluated in terms of Resilient Modulus (RM) through the cyclic triaxial test and compressive and tensile strengths in the Unconfined Compressions Strength (UCS) on slim samples and the Indirect Tensile Strength (ITS) tests on stubby samples.

2.3.1. Proctor study

The Proctor study allows investigating the degree of compaction that a granular mixture (or a soil) can achieve when a specific water content is added. The objective of the test is to determine the OMC that induces the MDD of the mixture ($\gamma_{d, \text{Max}}$). According to UNI EN 13286-2 (2010), the modified procedure was adopted (mould type B, hammer mass of 4.5 kg and 56 blows per layer). In Figure 2 the equipment used is shown.



Figure 2: Proctor compaction machinery

The procedure starts with the preparation of the mixture in a metallic bowl, which is then sealed with a plastic coat and left to rest. After, the first layer of material is laid in the Proctor mould. The compaction consists of 56 blows per layer. For each blow, the mass is first lifted and then fallen at an elevation of 457 mm above the sample. At the end of the compaction, five uniform layers are obtained in a sample. The material contained in the mould of known volume is weighed and dried to estimate the MDD and through the measurement of the effective water content. Figure 3 shows some significant steps of the test.

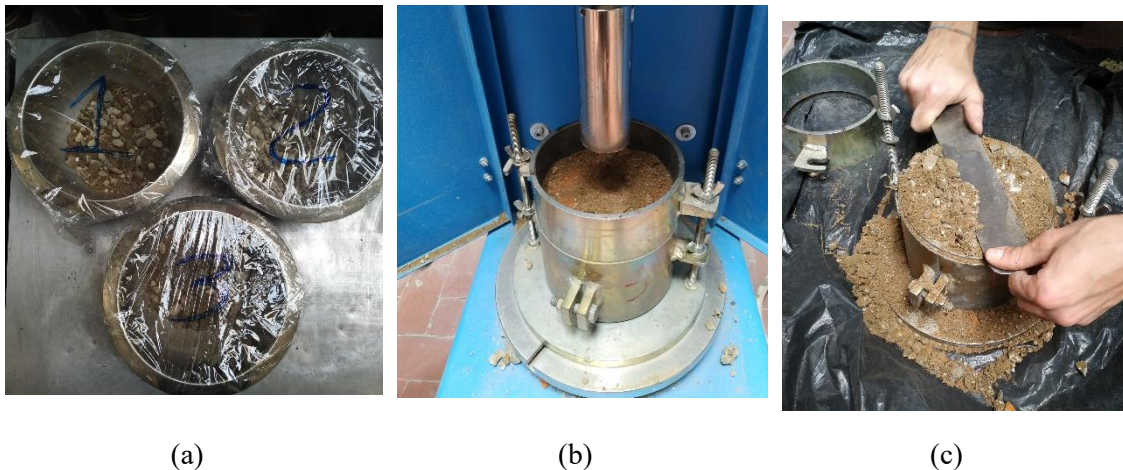


Figure 3: (a) Preparation of the mixture; (b) Compaction; (c) Mass measurement operations

The dry density is obtained from the following relation:

$$\gamma_d = \frac{\gamma_w}{(1+w)} \text{ [kg/m}^3\text{]}$$

where:

$$\gamma_w = \frac{\text{Wet sample mass}}{\text{Sample volume}} \text{ [kg/m}^3\text{]}: \text{wet density}$$

$$w = \frac{\text{Water mass}}{\text{Dry solid mass}} \text{ [%]: water content}$$

By varying the water content (w) in the mixture, it is possible to draw the Proctor curve and determine the maximum dry density. Table 4 lists the stabilized mixture undergone to Proctor study in the INTREC project.

Table 4: Mixtures tested with Proctor compaction

Aggregate type	Binder	W [%]	Mixture name
NAT	Unbound	2 - 4 - 6 - 6.6 - 8 - 10 %	NAT and water *
	2% CEM II/B	2 - 4 - 6 - 7 - 8 - 10 %	NAT+2CEM-II/B *
	3% CEM II/B	2 - 4 - 6 - 7 - 8 - 10 %	NAT+3CEM-II/B *
	4% CEM II/B	2 - 4 - 6 - 6.5 - 8 - 10 %	NAT+4CEM-II/B *
CDW	Unbound	4 - 6 - 8 - 10 - 12 %	CDW and water *
	2% CEM II/B	5 - 7 - 9 - 9.5 - 11 - 13 %	CDW+2CEM-II/B *
	3% CEM II/B	5 - 7 - 8.5 - 9 - 11 - 13 %	CDW+3CEM-II/B *
	4% CEM II/B	5 - 8 - 9 - 11 - 14.5 %	CDW+4CEM-II/B *
	AS 1	6 - 8 - 10 - 12 %	CDW+AS1 *
	4% Bondafix	4 - 6 - 9 - 10.1 - 12 %	CDW+4BF
	8% Bondafix	4 - 6 - 8 - 10 - 12 %	CDW+8BF
	12% Bondafix	4 - 6 - 8 - 10 - 12 %	CDW+12BF
	AS 3	4 - 6 - 8 - 10 - 12 %	CDW+AS3

* tested by Avellino and Gugliotta (2021)

2.3.2. Specimen preparation by the gyratory shear compactor

The gyratory shear compactor allows to produce cylindrical samples of different sizes and to obtain the workability parameters. During compaction, the actual height of the specimen is recorded for each gyration in order to determine the workability parameters: self-compaction (C_1) and workability (k). The compaction degree (C_n) is calculated at every gyration, and it is defined as the ratio between the density of the material and the maximum density achievable (measured with the Proctor study). C_1 and k describe the compaction degree as a function of the number of cycles (Figure 4). The compaction ends when the layer of material reaches the predefined height or when the maximum number of gyrations is reached.

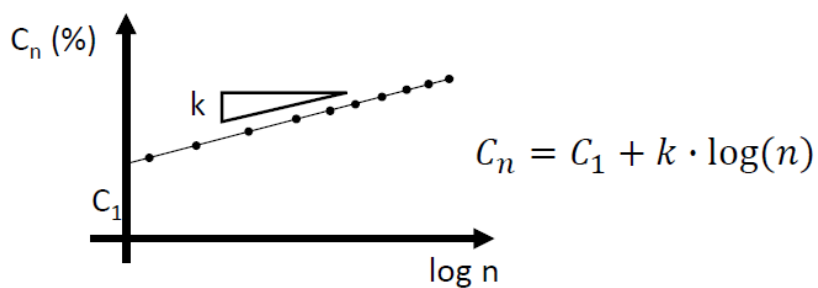


Figure 4: Workability curve and parameters.

where:

C_n = Degree of compaction at the n^{th} cycle expressed as a percentage;

C_1 = Self-compaction, compaction of the material due to its weight;

k = Workability of the mixture identified by the angular coefficient of the compaction curve;

n = Number of revolutions.

Two different sets of samples were prepared: (i) slender samples of 186 mm height and 100 mm of diameter were produced for both UCS tests and RM, and (ii) stubby samples 100 mm height and 100 mm of diameter for indirect tensile tests. Specimens were compacted in different layers to obtain a uniform compaction along the entire height. The slender samples were compacted into three layers of 62 mm in height each, while the stubby ones in two layers of 55 mm and 45 mm height. After compaction, the specimens were cured at room temperature in humid conditions ($\text{RH} > 95\%$), Figure 5 shows the steps of the specimen preparation.

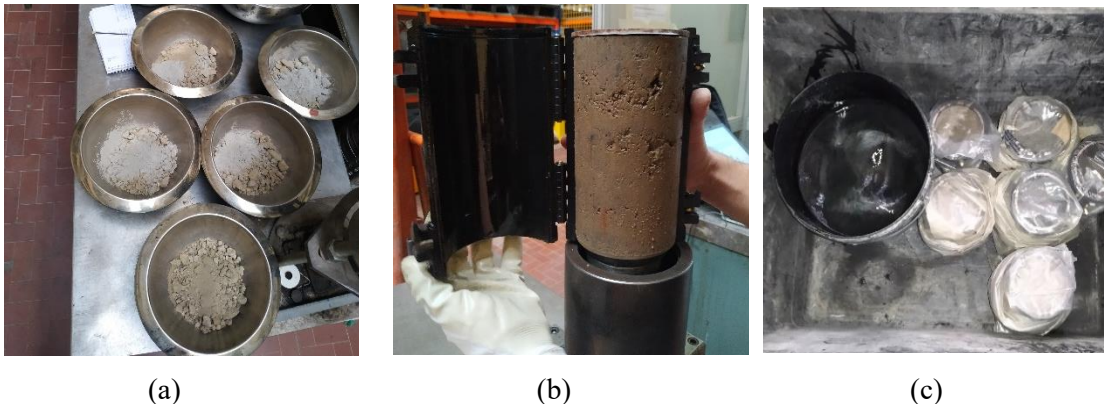


Figure 5:(a) Mixture preparation; (b) Sample sealing; (c) Box for curing in a humid environment.

Table 5 reports the parameters adopted for the preparation of slender samples, while Table 6 reports the parameters adopted in the preparation of stubby samples of the mixtures stabilised with Bondafix. In Table 7 the same parameters used in the preparation of stubby samples for the mixtures stabilised with hybrid cement and alkali-activated CDW fines are shown. In Table 8 the total number of samples produced for each mixture type is reported.

Table 5: Parameters to produce slender samples 100x186 mm

Binder type	Bondafix			Hybrid cement	AS2	AS3
Mixture name	CDW+4BF	CDW+8BF	CDW+12BF	CDW+3IB	CDW+AS2	CDW+AS3
Sample	γ_d [kg/m ³]	2046.6	2038.5	2031.1	2119.0	2155.0
	w_{opt} [%]	8.5%	8.5%	8.5%	8.5%*	8.0%*
	Binder [%]	4.0%	8.0%	12.0%	3.0%	*
	Diam. [mm]	100	100	100	100	100
	h_{sample} [mm]	186	186	186	186	186
	V_{sample} [m ³]	0.00146	0.00146	0.00146	0.00146	0.00146
	M_{solid} [kg]	2.990	2.978	2.967	3.096	3.148
	M_{agg} [kg]	2.875	2.757	2.649	3.005	3.148
	M_{binder} [kg]	0.120	0.238	0.356	0.093	*
	M_{water} [kg]	0.254	0.253	0.252	0.263	0.268*
Layer	h_{layer} [mm]	62	62	62	62	62
	M_{solid} [kg]	0.997	0.993	0.989	1.032	1.049
	M_{agg} [kg]	0.958	0.919	0.883	1.002	1.049
	M_{binder} [kg]	0.040	0.079	0.119	0.031	*
M_{water} [kg]						0.082*

* For AS2 and AS3, the water content is referred to the alkaline solution.

Table 6: Parameters to produce stubby samples (Bondafix)

Binder type		Bondafix					
Mixture name		CDW+4BF		CDW+8BF		CDW+12BF	
γ_d	[kg/m ³]	2046.6		2038.5		2031.1	
w_{opt}	[%]	8.5%		8.5%		8.5%	
Binder	[%]	4.0%		8.0%		12.0%	
Diameter	[mm]	100		100		100	
h_{sample}	[mm]	100		100		100	
V_{sample}	[m ³]	0.00079		0.00079		0.00079	
M_{solid}	[kg]	1.607		1.601		1.595	
M_{agg}	[kg]	1.546		1.482		1.424	
M_{binder}	[kg]	0.064		0.128		0.191	
M_{water}	[kg]	0.137		0.136		0.136	
h_{layer}	[mm]	55	45	55	45	55	45
M_{solid}	[kg]	0.884	0.723	0.881	0.720	0.877	0.718
M_{agg}	[kg]	0.850	0.696	0.815	0.667	0.783	0.641
M_{binder}	[kg]	0.035	0.029	0.070	0.058	0.105	0.086
M_{water}	[kg]	0.075	0.061	0.075	0.061	0.075	0.061

Table 7: Parameters to produce stubby samples (Hybrid cement, AS2, AS3)

Binder type		Hybrid cement		AS2		AS3	
Mixture name		CDW+3IB		CDW+AS2		CDW+AS3	
γ_d	[kg/m ³]	2119.0		2155.0		2111.0	
w_{opt}	[%]	8.5%		8.5%		8.0%	
Binder	[%]	3.0%		*		*	
Diameter	[mm]	100		100		100	
h_{sample}	[mm]	100		100		100	
V_{sample}	[m ³]	0.00079		0.00079		0.00079	
M_{solid}	[kg]	1.664		1.693		1.658	
M_{agg}	[kg]	1.616		1.693		1.658	
M_{binder}	[kg]	0.050		*		*	
M_{water}	[kg]	0.141		0.144*		0.133*	
h_{layer}	[mm]	55	45	55	45	55	45
M_{solid}	[kg]	0.915	0.749	0.931	0.762	0.912	0.746
M_{agg}	[kg]	0.889	0.727	0.931	0.762	0.912	0.746
M_{binder}	[kg]	0.027	0.022	0.000	0.000	0.000	0.000
M_{water}	[kg]	0.078	0.064	0.079	0.065	0.073	0.060

* For AS2 and AS3, the water content is referred to the alkaline solution.

Table 8: Number of samples produced for each mixture type

Curing [d]	Dimensions [mm x mm]	Bondafix 4%	Bondafix 8%	Bondafix 12%	Hybrid cement 3%	AS2 8.5%	AS3 8%
7	100 x 186	3	3	3	4	3	3
7	100 x 100	3	3	3	3	5	3
28	100 x 186	-	3	-	4	3	3
							Total 52

2.3.3. Cyclic triaxial test

Cyclic triaxial test is used to determine the RM of a granular unbound or stabilized mixture. The test was carried out by means of the Nottingham Asphalt Tester, applying repeated pulse loads to the specimen. The cyclic triaxial test was performed according to AASHTO T307-99:2007 (AASHTO 2007).

The RM corresponds to the stiffness of non-linear granular materials, and it is used as an input parameter for the structural design of road pavements. Hence, RM depends on the stress state to which the granular material is subjected, and the test is performed in a triaxial chamber under different stress conditions. The resilient modulus is defined as the ratio between the deviatoric stress and the vertical recovered deformation:

$$RM = \frac{\sigma_d}{\varepsilon_r}$$

where:

$\sigma_d = \sigma_1 - \sigma_3$ is the deviatoric stress;

σ_1 and σ_3 are the principal stress in the vertical and radial direction respectively;

ε_r is the vertical resilient (recovered) strain.

Due to the stress-dependency of RM, the AASHTO T307 suggests measuring it in fifteen different loading conditions as per those reported in Table 9. During each loading sequence, the material is subjected to a constant radial pressure (σ_3), while the vertical pressure (σ_1) is applied with periodic pulses of 0.1 s of load and 0.9 s of rest. The first loading sequence, composed of a thousand load cycles, allows to pre-conditionate the sample. The following fifteen sequences are composed of one hundred cycles.

Table 9: Cyclic load sequences (AASHTO T307)

Sequence No.	Confining Pressure, S_3		Max. Axial Stress, S_{max}		Cyclic Stress, S_{cyclic}		Constant Stress, $0.1S_{max}$		No. of Load Applications
	kPa	psi	kPa	psi	kPa	psi	kPa	psi	
0	103.4	15	103.4	15	93.1	13.5	10.3	1.5	500-1000
1	20.7	3	20.7	3	18.6	2.7	2.1	0.3	100
2	20.7	3	41.4	6	37.3	5.4	4.1	0.6	100
3	20.7	3	62.1	9	55.9	8.1	6.2	0.9	100
4	34.5	5	34.5	5	31.0	4.5	3.5	0.5	100
5	34.5	5	68.9	10	62.0	9.0	6.9	1.0	100
6	34.5	5	103.4	15	93.1	13.5	10.3	1.5	100
7	68.9	10	68.9	10	62.0	9.0	6.9	1.0	100
8	68.9	10	137.9	20	124.1	18.0	13.8	2.0	100
9	68.9	10	206.8	30	186.1	27.0	20.7	3.0	100
10	103.4	15	68.9	10	62.0	9.0	6.9	1.0	100
11	103.4	15	103.4	15	93.1	13.5	10.3	1.5	100
12	103.4	15	206.8	30	186.1	27.0	20.7	3.0	100
13	137.9	20	103.4	15	93.1	13.5	10.3	1.5	100
14	137.9	20	137.9	20	124.1	18.0	13.8	2.0	100
15	137.9	20	275.8	40	248.2	36.0	27.6	4.0	100

Experimental results of RM testing were fitted with the M-EPDG (Mechanistic-Empirical Pavement Design Guide) model:

$$RM = k_1 \cdot p_a \cdot \left(\frac{\theta}{p_a} \right)^{k_2} \cdot \left(\frac{\tau_{oct}}{p_a} + 1 \right)^{k_3}$$

where:

RM = Resilient modulus, in MPa;

k_i = Regression parameters;

p_a = Atmospheric pressure, 0.1013 MPa;

θ = Bulk stress = $\sigma_1 + \sigma_2 + \sigma_3$

τ_{oct} = Octahedral stress, in MPa, under axial symmetry conditions, equal to:

$$\tau_{oct} = \frac{\sqrt{2}}{3} \cdot \sigma_d = \frac{\sqrt{2}}{3} \cdot |\sigma_1 - \sigma_3|$$

In order to obtain the regression coefficients k_i , the least-squares method was applied in an Excel spreadsheet. The goodness of the fitting was evaluated by means of the following parameters:

R^2 = Coefficient of determination;

R_{adj}^2 = Adjusted coefficient of determination, which takes into account the number of variables in the model;

S_e/S_y = Ratio between the standard estimation error and the standard deviation.

The R^2 parameter is considered as good as much it gets closer to one, while the S_e/S_y parameter is as good as much as it is close to zero, Table 10 provides a reference in the estimation of the goodness.

Table 10: Evaluation of the goodness of the fitting parameters (Witczak et al. 2002)

CRITERIA	R^2	S_e/S_y
Excellent	> 0.90	< 0.350
Good	0.70–0.89	0.36–0.55
Fair	0.40–0.69	0.56–0.75
Poor	0.20–0.39	0.76–0.90
Very Poor	< 0.19	> 0.90

Figure 6 reports the NAT apparatus and the steps performed during the triaxial test



Figure 6: (a) Nottingham asphalt tester (NAT) during the testing of a sample; (b) Equipment; (c) Sample preparation.

2.3.4. Unconfined compression strength (UCS)

The UCS test defines the maximum compressive stress that the specimen can withstand in the absence of lateral confinement. The test was performed according to the UNI EN 13286-41:2006 (Ente Nazionale Italiano di Unificazione 2006a).

The test was performed by applying a constant displacement rate of 0.5 mm/min on the specimen. The load cell, with a capacity of 50 kN, recorded at the frequency of 5 Hz the applied force, while a strain transducer evaluated the vertical deformation.

The stress-strain curve recorded during the test allowed to obtain several parameters:

- σ_{\max} : is the maximum strength that the sample exhibits under a compression state of stress, it is obtained by dividing the maximum force applied by the area of the specimen section, in MPa;
- E_{sec} : is the secant elastic modulus, which is identified by the slope of the straight line passing through the initial deformation and the maximum stress, in MPa;
- E_{tan} : is the tangent elastic modulus, which is obtained by evaluating the slope of the stress-strain curve in its linear part, in MPa.
- T : is the toughness (energy at failure), graphically can be defined as the area under the stress-strain curve, in kPa mm/mm.

The maximum compressive strength and the two elastic moduli were determined after 7 and 28 days of curing. Figure 7 shows the stress-strain curve and the parameters obtained from the UCS test.

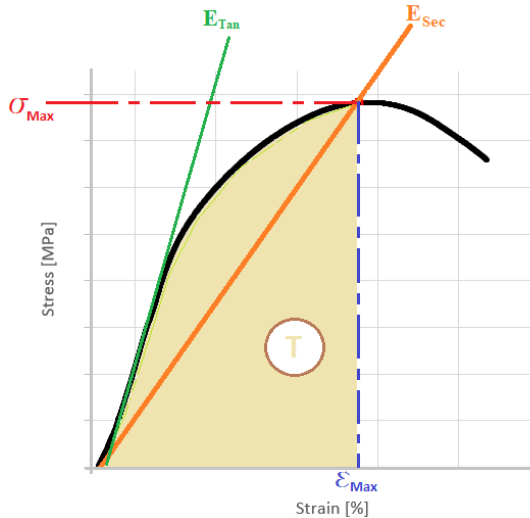


Figure 7: Graphical representation of the UCS parameters.

In the elastic phase, the stresses increase with a linear dependence with respect to the strains. As the applied stress approaches the maximum value, the plastic strains become more evident, and the stress-strain curve shows a non-linear behaviour until it reaches the peak (σ_{Max}). At this point, cracks are visible on the sample which is not able to support an additional load (Figure 8).

After the test, the sample is weighed and dried at 105 °C to determine the water content in the material.

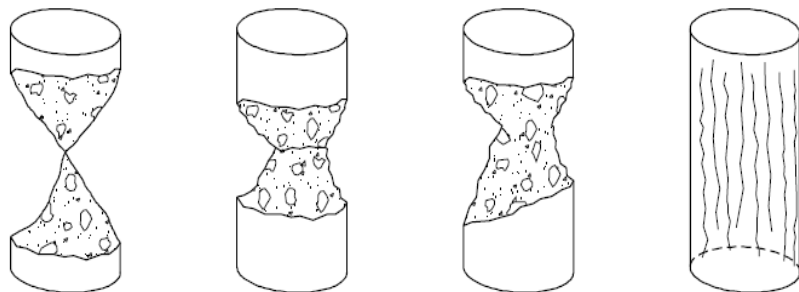


Figure 8: Examples of satisfactory failures of specimens UNI EN 13286-41

Figure 9 shows the UCS testing equipment and the execution of the test.

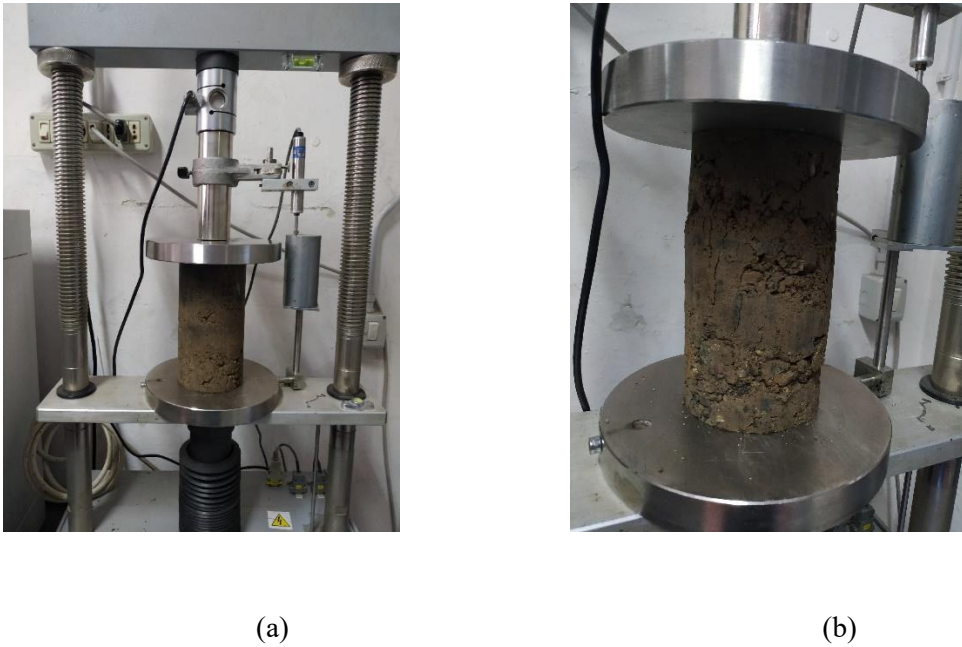


Figure 9: (a) UCS test equipment; (b) Cracked sample during the test.

2.3.5. Indirect tensile strength (ITS)

Indirect tensile strength (ITS) test was carried out according to the standard UNI EN 13286-42 (2006b). The test was performed on cylindrical samples of 100 mm in diameter and height (Figure 10) after 7 days of curing. The ITS is a static test performed at the displacement rate of 0.5 mm/min. The indirect tensile stress is then obtained from the equation:

$$\sigma_t = \frac{2 P}{\pi d h}$$

where:

σ_t = Indirect tensile strength, in MPa

d = Diameter of the specimen, in mm;

h = Height of the specimen, in mm;

P = Maximum applied force, in N.



Figure 10 : (a) ITS test machinery; (b) Crack in the sample after the test

2.4. Methods – Field investigation

2.4.1. Light weight deflectometer (LWD) test

The Light Weight Deflectometer (LWD) equipment consists of a falling weight, a dumper device at the bottom and a loading plate, and a series of sensors to measure the load and the vertical displacement of the loading plate. The mass is dropped from a predetermined height on the circular loading plate, and a load impulse is transmitted to the pavement top. The sensors measure the applied load impulse intensity and shape, and the deflections of the plate in function of time. The load impulse is measured through a load cell and the deflection under the centre of the plate is measured with a geophone. Two additional geophones may be added to measure the deflection profile, and then calculate the stiffness of the layered systems. In the assessment carried out in this study, the LWD was used with three geophones. The test allows to determine the dynamic surface modulus, the stiffness modulus of pavement layers and the degree of compaction of soils. These parameters are universally assumed as fundamental parameters in the final evaluation of the performance of road construction. The tests were conducted according to the American standard ASTM E2583–07 (2015).

The LWD employed during field trials is the Dynatest 3032, whose characteristics follows:

- main unit with integral load cell and central deflection sensor;

- 300 mm diameter plate and a rubber pad of the same size; this unit includes also 100, 150, and 200 mm plates;
- two additional geophones;
- a guide shaft;
- buffer pads;
- 10 kg weight plus two additional 5 kg weights.

Figure 11 shows a schematic representation of the LWD.

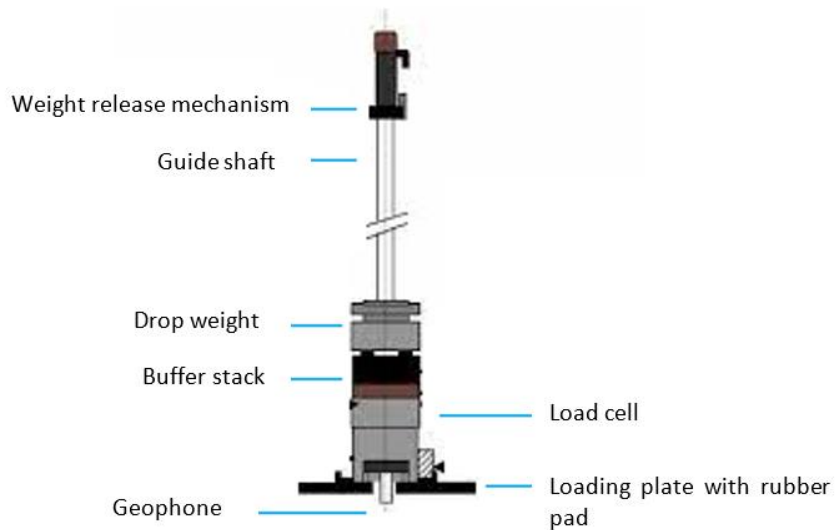


Figure 11: LWD description

According to the standard ASTM E2583–07 and the supplier manual, the first step is to fix the dimensions of the load plate and the value of the height from which the weight is dropped, to define the applied stress. The applied pressure is defined as the maximum force divided by the plate area. Varying the weight of the falling mass, the diameter of the load plate, the drop height and the buffer configuration, the user can control both the intensity and the duration of the stressing pulse. The weight is lifted and fixed to the required height, and then released to impart the impulse. Generally, the first 3 falls are used to ensure good contact between the plate and the surface and were then excluded from the computation.

The surface modulus at the centre of the plate is determined according to Boussinesq theory:

$$E_0 = \frac{f \cdot (1 - \nu^2) \cdot \sigma_0 \cdot r}{d_0}$$

where:

E_0 = Surface modulus, in MPa;

f = Plate stiffness factor (2 for uniform distribution, $\pi/2$ for rigid plate);

ν = Poisson ratio of the soil;

σ_0 = Maximum contact pressure, in MPa;

r = Plate radius, in mm;

d_0 = Maximum deflection at the centre of the plate, in mm.

The surface modulus represents a composite value for the pavement rather than a single layer. The measured deflection depends on the response of the material inside the displacement basin of influence, i.e., the portion of soil in which the stresses are significant. The depth of this basin depends on the plate diameter and on the stiffness of the soil.

2.4.2. Plate load test

The plate load test as per the Italian standard BU CNR 146/92 allows to determine the deformation modulus (M_d). The deformation modulus represents a conventional measure of the bearing capacity of pavements, it is determined through a load test with a circular plate and it is expressed as per the following relation:

$$M_d = \frac{\Delta P}{\Delta D} \cdot \varphi \text{ [MPa]}$$

where:

- ΔP [MPa] = Increase in the pressure on the rigid circular plate;
- φ [mm] = Diameter of the circular plate (300 mm);
- ΔD [mm] = Increase in the settlement of the loaded layer.

The test requires a contrast which is generally constituted of a truck or an excavator. During the test, the plate is placed on a thin layer of sand that serves to even out the support surface, then, a preload of 0.02 MPa is applied. When the settlement of the plate is completed (i.e., the difference between two readings at a distance of one minute < 0.02 mm), a 0.05 MPa stress is applied and the first displacement is measured. Further measurements are recorded applying successive increments of 0.05 MPa until reaching 0.20 MPa on the top of a subgrade, or increments of 0.10 MPa until reaching 0.35 MPa on the top of a subbase.

M_d is determined by posing ΔP equal to $0,1 \text{ MPa}$ and determining ΔD considering the interval of ΔP between $0,05$ and $0,15 \text{ MPa}$ for subgrades and embankments, or between $0,15$ e $0,25 \text{ MPa}$ for subbases.

After this procedure, the plate is unloaded and second moduli, M'_d is evaluated with the same modality presented before. The ratio between M_d and M'_d is called compaction degree. The compaction degree is as close to 1 as the material is compacted.

2.4.3. In-place density with sand-cone test:

The in-place density is determined with the sand-cone test following the standard ASTM D 1556-00 (2000). The apparatus used is reported in Figure 12.

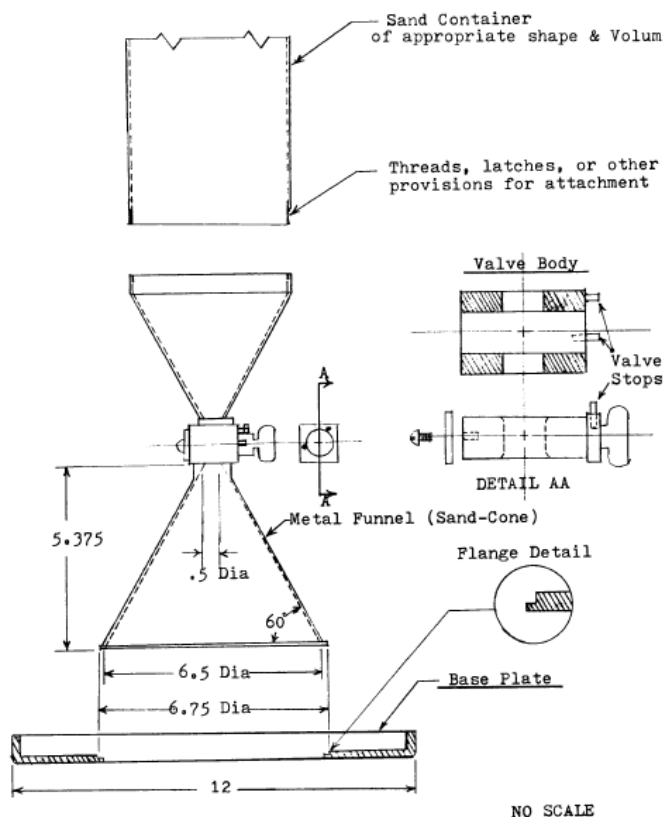


Figure 12: In-place density apparatus (ASTM D 1556-00)

The test uses sand with known density to determine the in-situ density of a soil. The sand is inserted in a hand-excavated hole, knowing the density and the mass of the sand, the volume of the hole is calculated. The mass and water content of the removed soil are measured, therefore the wet and dry density can be computed.

The dry density is obtained as follows:

Hole volume: $V = (M_1 - M_2)/\rho_1$

where:

- V: Test hole volume [cm^3];
- M_1 : Mass of sand used to fill the test hole, funnel and base plate [g];
- M_2 : Mass of sand used to fill the funnel and base plate [g];
- ρ_1 : Bulk density of sand [$\frac{\text{g}}{\text{cm}^3}$].
- Dry mass of material removed from the test hole:
$$M_4 = 100 M_3 / (w + 100)$$
- w: Water content of the material removed from the hole;
- M_3 : Wet mass of material removed from the test hole [g];
- M_4 : Dry mass of the material removed from the test hole [g].
- Wet and dry in-situ density of the tested material: $\rho_w = M_3/V$ $\rho_d = M_4/V$
- ρ_w : Wet density [$\frac{\text{g}}{\text{cm}^3}$];
- ρ_d : Dry density [$\frac{\text{g}}{\text{cm}^3}$].

3. RESULTS AND DISCUSSION OF LABORATORY TESTS

In this section, the results obtained from the Proctor study, the workability parameters and the strength tests (UCS and ITS) on the studied mixtures are discussed. Moreover, these data are compared with the outcomes obtained during the previous stages of the INTREC project.

3.1. Proctor study

The Proctor test was performed on the three Bondafix stabilized mixtures (4, 8 and 12 % by weight), and on the alkali-activated CDW fines using AS3 stabilized mixture. Figure 13 compares the Proctor curve of the three Bondafix stabilized mixtures and the unstabilised CDW mixture.

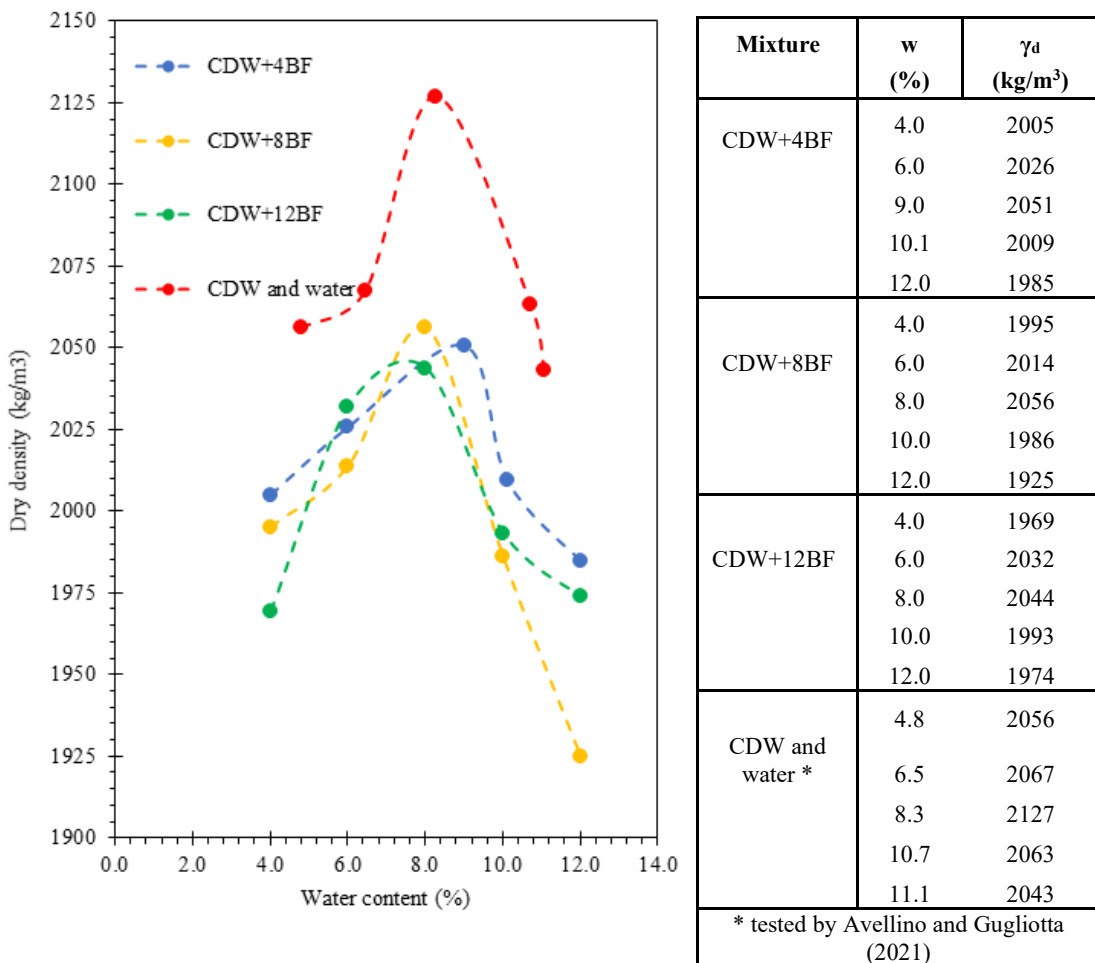


Figure 13: Proctor curves for recycled aggregates stabilized with Bondafix.

The curves presented in Figure 13 approximate parabola arcs, for each of them, the peak is achieved with water content between 8 and 10%. It is worth noting that the OMC is similar for the three mixtures stabilised with Bondafix and for the unstabilised one. However, the OMC was identified as 8.5% for the stabilised mixtures too. The MDD was higher in the CDW aggregate than in the stabilised mixtures. In fact, the relevant quantity of Bondafix, which has a much lower density with respect to the aggregates ($1000-1100 \text{ kg/m}^3$) justify such results. As can be noted from Table 11, the MDD decreases as the binder content increases, while the OMC does not vary sensibly with the addition of the binder.

Table 11: Maximum dry densities (BF = Bondafix)

Mixture	$\gamma_{d,\text{Max}}$ (kg/m ³)
CDW+4BF	2047
CDW+8BF	2038
CDW+12BF	2031
CDW and water	2121

Figure 14 shows the comparison between the Proctor curves provided by the unstabilised CDW and the mixtures stabilised with alkali-activated fines of CDW aggregates (AS1 and AS3).

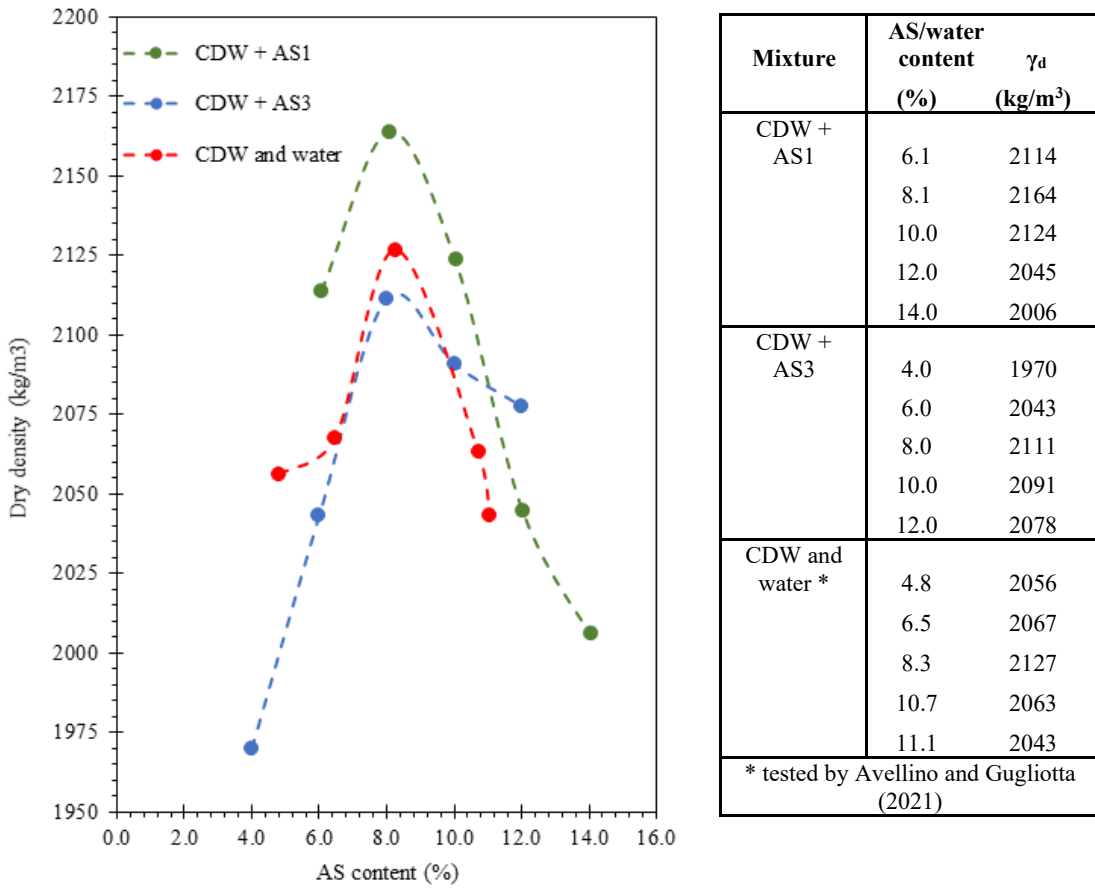


Figure 14: Proctor curves for recycled aggregates stabilized with AS1 and AS3.

The presence of the surfactant component in AS3 was expected to reduce the viscosity of the alkaline solution and to increase the compaction of the mixture. Contrary to what expected, CDW+AS3 reported a lower value of MDD compared to CDW+AS1. It can be noted also that the parabola provided by CDW+AS3 is less sharp if compared to CDW+AS1. The OMC was found to be 8.5% for CDW+AS1 and 8% for CDW+AS3. Also in this case, the OMC does not vary in a sensible way from the one of the unstabilised blend. The mixture stabilised with the original alkaline solution reported a higher maximum dry density with respect to the modified one as reported in Table 12.

Table 12: Maximum dry densities and optimum liquid content (Alkaline solutions)

Material	AS_{opt} (%)	$\gamma_{d,max}$ (kg/m³)
CDW + AS1	8.5	2155
CDW + AS3	8.0	2111

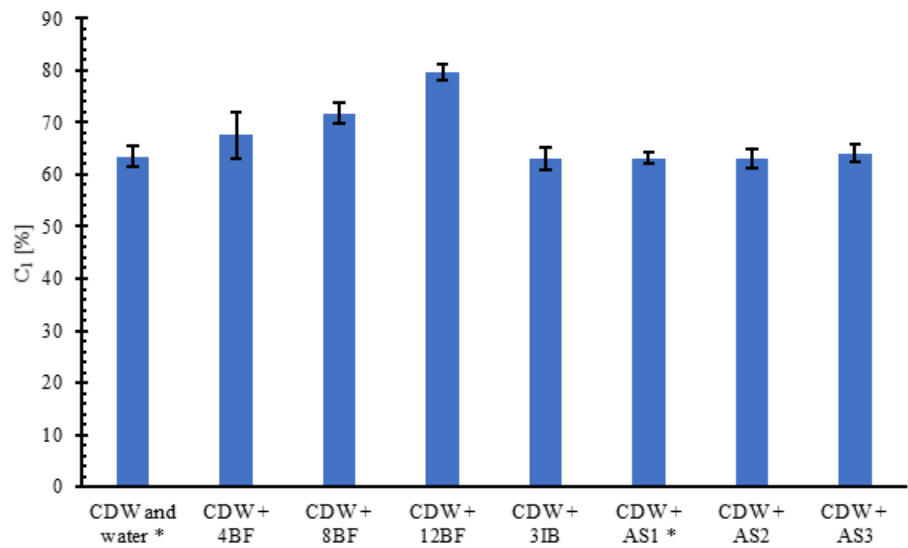
3.2. Workability

The parameters C_1 and k were computed for each sample, Table 13 reports the averaged values for each mixture type and the relative standard deviations.

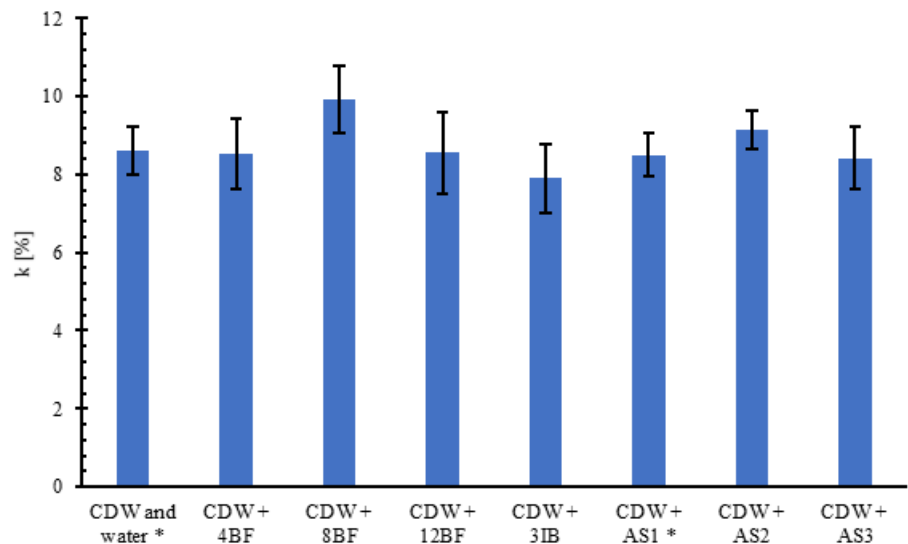
Table 13: Workability parameters

	CDW and water *	CDW + 4 BF	CDW + 8BF	CDW + 12BF	CDW + 3IB	CDW + AS1*	CDW + AS2	CDW + AS3
Binder [%]	-	4	8	12	3			
AS [%]	-	-	-	-	-	8.5	8.5	8
C_1 [%]	Avg. st.dev	63.5 2.00	67.57 4.39	71.7 2.02	79.8 1.54	62.95 2.18	63.2 1.11	62.94 1.84
k [-]	Avg. st.dev	8.6 0.62	8.52 0.9	9.92 0.85	8.56 1.04	7.9 0.89	8.5 0.55	9.14 0.49
C_{100} [%]	Avg.	80.7	84.61	91.54	96.92	78.75	80.1	81.22
v [%]	Avg.	19.3	15.39	8.46	3.08	21.25	19.8	18.78
Tested samples		-	6	9	6	11	-	9
* tested by Avellino and Gugliotta (2021)								

The values of the parameters K and C_1 are reported in the bar chart of Figure 15.



(a)



(b)

Figure 15: Average values of C_1 (a) and K (b) with the corresponding standard deviation * Tested by Avellino and Gugliotta (2021).

All the materials exhibit workability greater than 8.0 except for the mixture stabilised with “Hybrid” cement, which reported a value of 7.9. In the mixtures stabilised with 8% of Bondafix and in the one stabilized with alkali-activated CDW fines (AS2), k is above 9. Regarding the self-compaction (C_1), the mixtures stabilised with Bondafix reported an increasing value of the parameter corresponding to an increase in the binder content. The mixtures stabilised with “Hybrid” cement, alkali-activated CDW fines, and the unbound mixture reported a similar value of C_1 .

3.3. Cyclic triaxial test (Resilient modulus)

Figure 16-a and Figure 16-b represent the RM of mixtures stabilised with “hybrid” cement, Bondafix and CEM IV/B as a function of the first invariant I_1 , after 7 and 28 days of curing respectively.

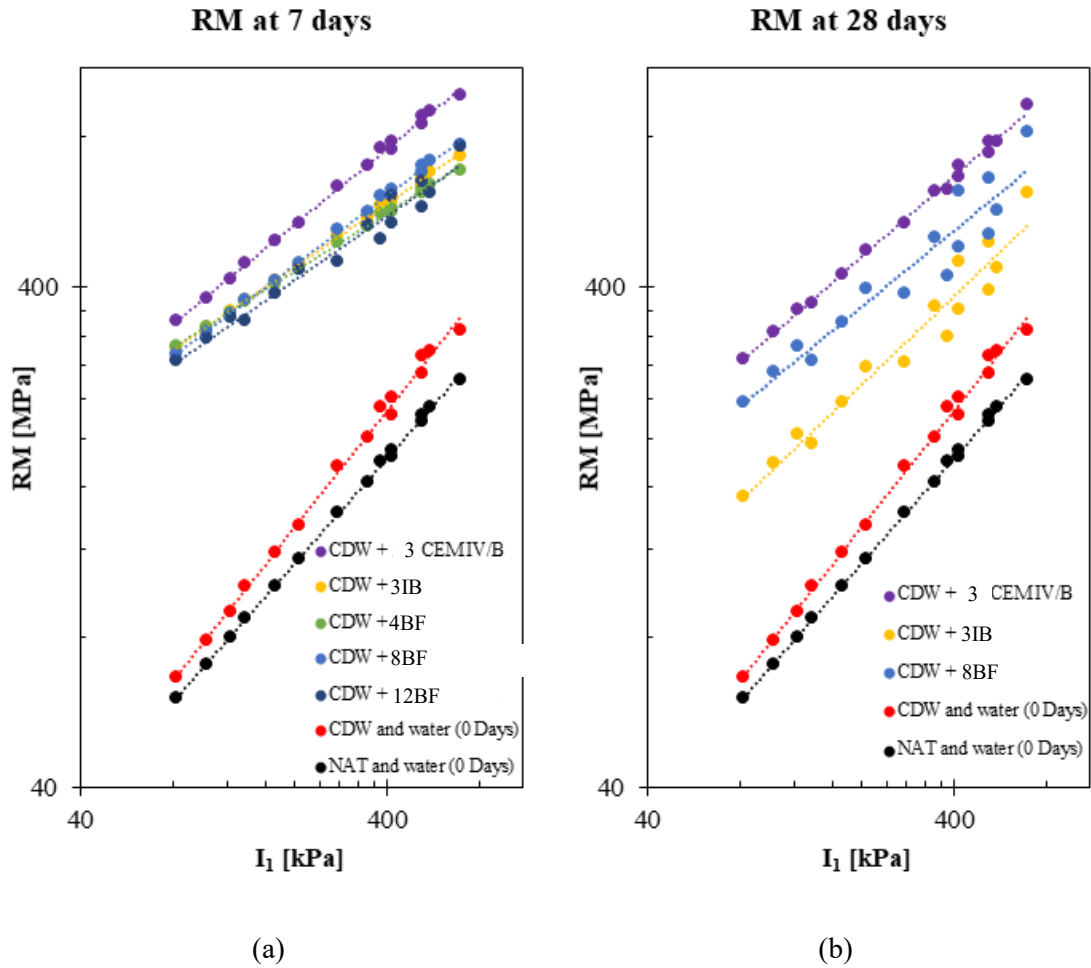


Figure 16: RM at 7 days of curing (a) and at 28 days of curing (b), mixtures stabilised with “Hybrid” cement, Bondafix and CEM IV/B.* Unstabilised mixtures (CDW and NAT) tested by Avellino and Gugliotta (2021).

The stiffness of all the materials increases as the applied stress increase, in a logarithmic scale RM has a linear behaviour with respect to I_1 . At 7 days of curing, considering a first invariant stress of 275 kPa, the resilient modulus ranges between 450 and 520 MPa for all the mixtures stabilised with Bondafix and “hybrid” cement, the mixture stabilised with CEM IV/B reported the highest value among all the tested mixtures (638 MPa). At 28 days of curing the mixtures reported a decrease in RM, in particular, CDW + 3IB exhibited a modulus equal to 283 MPa (evaluated at $I_1 = 275$ kPa), corresponding to a reduction of 44% with respect to the 7 days-cured samples. The unbound materials reported a stiffness three to four times lower than the stabilised

mixtures evaluated at 7 days of curing, while at 28 days the difference becomes lower, two times for the mixtures containing Bondafix or “hybrid” cement, and three times for the one containing CEM IV/B.

In Figure 17 are represented the average values of RM of mixtures stabilised with alkali-activated CDW fines as a function of the first invariant I_1 , after 7 and 28 days of curing time respectively.

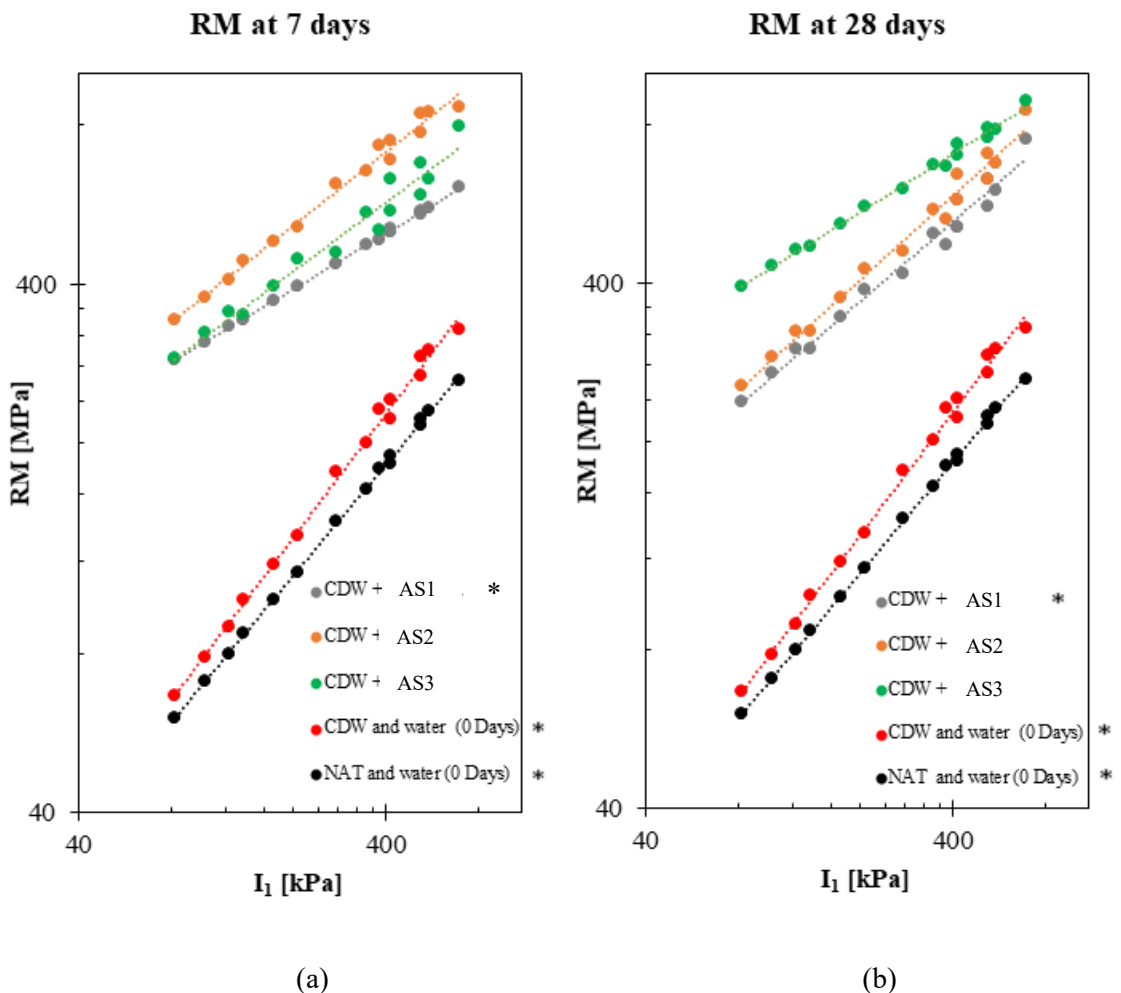


Figure 17: RM at 7 days of curing (a) and at 28 days of curing (b) for AS2 and AS3 stabilised mixtures. *Tested by Avellino and Gugliotta (2021).

Concerning the mixtures stabilised with alkali-activated CDW fines, at 7 days, the mixture containing AS2 reported a RM 35% higher than those containing AS1 or AS3 ($I_1 = 275$ MPa). After 28 days of curing, CDW + AS2 reported a reduction in RM of 25%, CDW + AS1 did not have significant variations. CDW + AS3 is the only mixture in which the stiffness was higher

after 28 days with respect to 7 days of curing, in this case the increment was 30%. In the case of the mixtures containing alkaline solution, the stabilised mixtures reported a stiffness three to four times higher than the unbound blends.

Table 14 reports the values of the K parameters of the M-EPDG model and the relative statistical accuracy.

*Table 14: M-EPDG parameters and statistical accuracy. *Tested by Avellino and Gugliotta (2021).*

	Curing	k1	k2	k3	S _c /S _y	R ²	R _{adj} ²	Goodness
NAT and water *	0 D	2677.1	0.59	-0.11	0.09	0.99	0.99	Excellent
CDW and water *	0 D	803.9	0.85	-0.29	0.15	0.98	0.98	Excellent
CDW+4 BF	7 D	3304	0.41	-0.07	0.44	0.82	0.81	Good
	28 D	-	-	-	-	-	-	
CDW+8 BF	7 D	3249	0.49	-0.11	0.44	0.81	0.81	Good
	28 D	2268	0.27	0.91	0.32	0.90	0.90	Excellent
	Δ(28-7)	-981	-0.22	+1.02				
	Δ(%)	-30	-45	+927%				
CDW+12 BF	7 D	2882	0.32	0.43	0.35	0.89	0.88	Good
	28 D	-	-	-	-	-	-	
CDW+3 IB	7 D	3297	0.44	-0.07	0.23	0.95	0.95	Excellent
	28 D	1522	0.39	0.79	0.30	0.92	0.91	Excellent
	Δ(28-7)	-1775	-0.05	+0.86				
	Δ(%)	-54%	-11%	1229%				
CDW+3 CEM IV/B *	7 D	3824	0.54	-0.14	0.36	0.88	0.87	Good
	28 D	3087	0.49	0.18	0.64	0.61	0.59	Fair
	Δ(28-7)	-737	-0.05	+0.32				
	Δ(%)	-19%	-9%	229%				
CDW+AS1 *	7 D	3035	0.34	0.04	0.29	0.92	0.92	Excellent
	28 D	2451	0.40	0.41	0.38	0.86	0.86	Good

	Curing	k1	k2	k3	S _e /S _y	R ²	R _{adj} ²	Goodness
CDW+AS2	Δ(28-7)	-584	+0.06	+0.37				
	Δ(%)	-19%	+18%	+925%				
	7 D	3868	0.54	-0.28	0.36	0.88	0.87	Good
	28 D	2641	0.43	0.40	0.10	0.99	0.99	Excellent
CDW+AS3	Δ(28-7)	-1227	-0.11	+0.68				
	Δ(%)	-32%	-20%	+243%				
	7 D	2915	0.31	0.48	0.35	0.89	0.88	Good
	28 D	4097	0.33	0.17	0.10	0.99	0.99	Excellent
CDW+3IB	Δ(28-7)	+1182	+0.02	-0.31				
	Δ(%)	+41%	+6%	-76%				

Taking into account the statistical parameters R² and S_e/S_y, according to the classification given in paragraph 2.3.3 (Witczak et al. 2002), all the models can be classified as excellent or good except for the mixture stabilised with CEM IV/B which was classified as fair.

According to the M-EPDG model, the k₁ parameter is directly proportional to RM, the parameter k₂ represents the susceptibility of RM to the variation of the bulk stress, and k₃ describes the variation of RM as a function of the octahedral stress.

From Table 14 it is possible to notice that the value of K₁ is higher at 7 days than at 28 days of curing for all the mixtures except for CDW + AS3, this is in line with the reduction of RM with the curing time. The decrease of stiffness in the 28-days cured samples may be due to the wetting of the material during the curing stages, several studies highlighted the influence of moisture content over RM, in particular, Naji (2018) showed how the RM of granular material reduces if the moisture content increases. As reported in paragraph 2.3.2, the samples were cured in a humid environment, during this time the long-time cured samples may have reached a higher moisture content with respect to the 7-days cured ones.

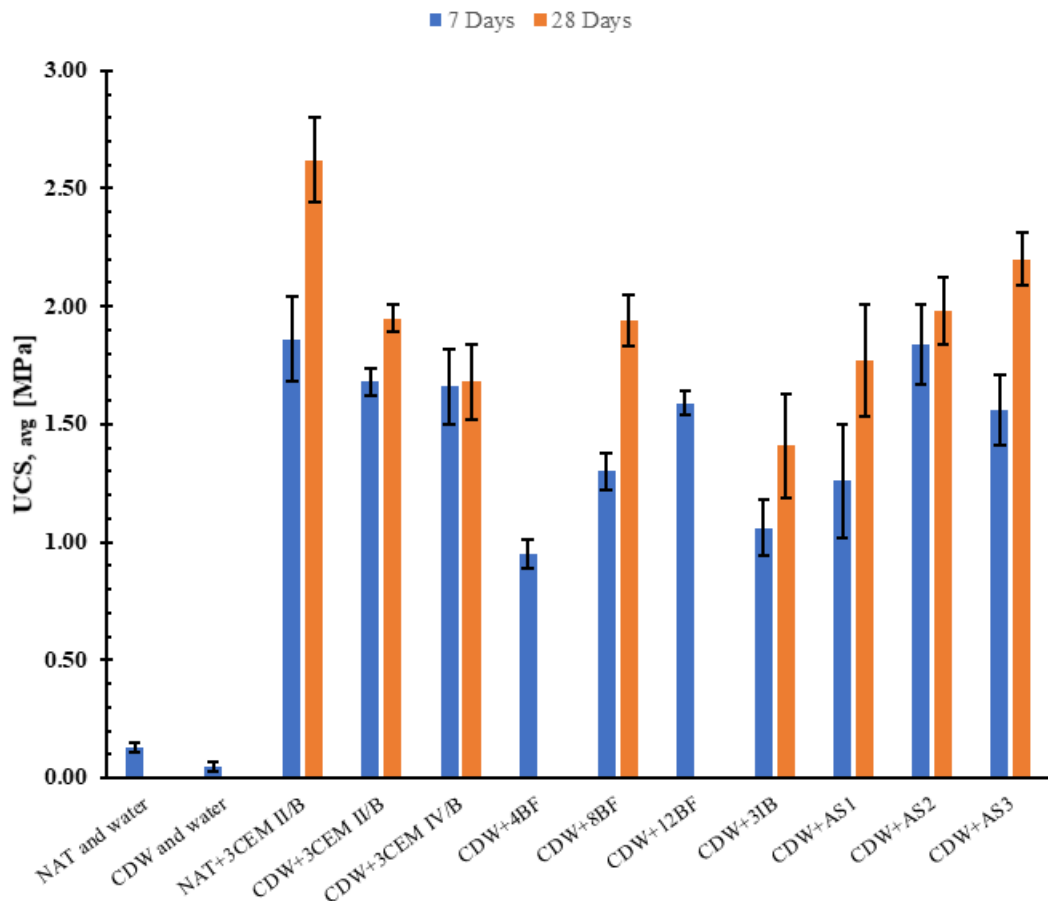
K₁ reaches the highest values (at 7 days) in the mixtures stabilised with CEM IV/B and AS2 (3824 and 3868 respectively), as these mixtures reported the highest stiffness. The reduction in RM of CDW + 3IB passing from 7 to 28 days of curing is visible also from the reduction of k₁ (from 3297 to 1522). Regarding the mixture stabilised with Bondafix, k₁ is close to 3300 for the mixtures containing 4 and 8 % of binder (at 7 days), while it decreases by 12 % in the mixture with 12 % of binder content. As expected the unbound mixtures reported the lowest value for k₁.

Most of the mixtures reported a decreasing value of k_2 when passing from 7 to 28 days of curing, this implies a reduction in time of the sensibility of RM to the stress variation. The only exceptions are represented by the mixtures CDW + AS1 and CDW + AS3 which reported an increase of about 17 and 6 % respectively. The highest k_2 value was reported by the unbound recycled aggregates mixture (0.85) while the lower value was given by the mixture stabilised with 8 % of Bondafix after 28 days (0.27).

The k_3 parameter has increased with the curing time in all the mixtures except for CDW + AS3. For most of the mixtures, it was recorded an inversion of sign (negative to positive) passing from 7 to 28 days of curing, the exceptions are represented by the mixtures stabilised with AS1, AS3 and 12 % of bondafix.

3.4. Unconfined compression strength and indirect tensile strength

The average values of UCS at 7 and 28 days are reported in Figure 18.

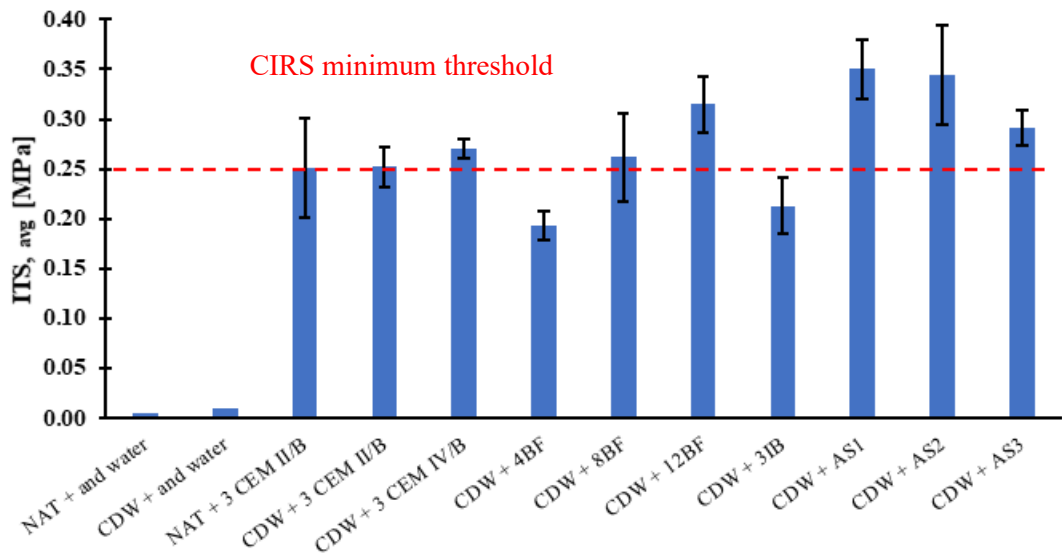


Mixture		NAT and water *		CDW and water *		NAT+3CEM II/B *		CDW+3CEM II/B *		CDW+3CEM IV/B *		CDW + 4BF
Curing	[Days]	0	0	7	28	7	28	7	28	7	28	7
$\sigma_{c,max}$	[MPa]	AVG		0.13	0.05	1.86	2.62	1.68	1.95	1.66	1.68	0.95
		St. dev		0.02	0.02	0.18	0.18	0.06	0.06	0.16	0.16	0.06

Mixture		CDW + 8BF		CDW + 12BF		CDW + 3IB		CDW + AS1 *		CDW + AS2		CDW + AS3
Curing	[Days]	7	28	7	28	7	28	7	28	7	28	7
$\sigma_{c,max}$	[MPa]	AVG		1.3	1.94	1.59	1.06	1.41	1.26	1.77	1.84	1.98
		St. dev		0.08	0.11	0.05	0.12	0.22	0.24	0.24	0.17	0.14
		0.15	0.11									0.11

Figure 18: UCS at 7 and 28 days with the corresponding standard deviation. * Tested by Avellino and Gugliotta (2021)

In Figure 19 are reported the ITS test results.



Mixture		NAT and water *	CDW and water *	NAT+3CEM II/B *	CDW+3CE M II/B *	CDW+3CE M IV/B *	CDW + 4BF
Curing	[Days]	7	7	7	7	7	7
$\sigma_{t,\max}$	AV G	0.005	0.010	0.251	0.252	0.270	0.193
	St. dev	0	0	0.050	0.020	0.010	0.015

Mixture		CDW + 8BF	CDW + 12BF	CDW + 3IB	CDW + AS1 *	CDW + AS2	CDW + AS3
Curing	[Days]	7	7	7	7	7	7
$\sigma_{t,\max}$	AV G	0.262	0.315	0.213	0.350	0.344	0.292
	St. dev	0.044	0.028	0.027	0.030	0.050	0.018

Figure 19: ITS at 7 days with the corresponding standard deviation. * Tested by Avellino and Gugliotta (2021)

Regarding the mixtures stabilized with Bondafix, it is clear from the results on the compressive strength that the strength increases as the binder content increases, only the mixture stabilized with 4% of Bondafix reported a UCS value lower than 1 MPa. In general, the strength increases with the curing time in all the tested mixtures, at 28 days, all the stabilised mixtures reported a UCS higher than 1.6 MPa, an exception is represented by the mixtures stabilized with “hybrid” cement, which exhibits a strength of 1.41 MPa. The higher UCS is achieved by the reference mixture of natural aggregates stabilised with cement type II/B, which reported a value of 2.62 MPa at 28 days of curing. The mixture stabilised with 8% of Bondafix reported a UCS of 1.3 MPa at 7 days of curing, and an increase of 50% passing to 28 days of curing. CDW + AS2 exhibited good UCS, both at 7 and 28 days of curing the strength is close to 1.9 MPa. The mixture stabilised with the modified alkaline solution (AS3) reported a compressive strength of 1.56 MPa.

at 7 days and an increase of over 40% at 28 days. Among the alkali-activated stabilised mixtures, CDW + AS1 reported the lowest UCS both for 7 and 28 days of curing (1.26 and 1.77 MPa respectively). CDW + 3IB reported the lowest compressive strength among the tested stabilised mixtures (around 1 MPa, comparable to CDW + 4BF). The unbound CDW mixture reported a UCS 20 to 50 times lower with respect to the stabilised ones.

The Italian technical specification of CIRS (*CIRS e Ministero delle Infrastrutture e dei Trasporti, 2° edizione*) set a minimum threshold value for the ITS at 7 days equal to 0.25 MPa for the mixtures of natural aggregates stabilised with cement. All the tested stabilised mixtures containing recycled aggregates achieve this requirement, except for CDW aggregates stabilized with 4% of Bondafix and 3% of “Hybrid” cement (missing 30% and 17% respectively, to reach the CIRS threshold). As for the UCS, also in the case of ITS, the mixtures stabilised with Bondafix reported an increasing strength with the binder content (0.19, 0.26 and 0.31 MPa for the mixtures containing 4, 8 and 12% of binder respectively). The highest value of ITS was achieved by the mixtures stabilised with alkaline solution, both CDW + AS1 and CDW + AS2 reached values of about 0.35 MPa, while the mixtures stabilised with AS3 and CDW fines showed an ITS of 0.29 MPa. The tensile strength of the unbound CDW is 25 times lower than the CIRS threshold.

The values of deformation at failure $\epsilon(\sigma_{C,MAX})$, elastic modulus ($E_{T,C}$ and $E_{S,C}$) and toughness (T_c) obtained from data modelling are reported in Table 15.

Table 15: Average values of strain ($\epsilon(\sigma_{C,MAX})$), tangent modulus ($E_{T,C}$), secant modulus ($E_{S,C}$) and Toughness (T_c) of mixtures subjected to UCS test.

	Curing [Days]	$\epsilon(\sigma_{C,max})$ [%]		$E_{T,C}$ [MPa]		$E_{S,C}$ [MPa]		T_c [kPa mm/mm]	
		AVG	St. dev	AVG	St. dev	AVG	St. dev	AVG	St. dev
CDW + 4BF	7	1.23	0.18	140.3	28.5	79.7	16.2	7.54	0.63
	28	-	-	-	-	-	-	-	-
CDW + 8BF	7	1.4	0.2	409	121.2	94	7.23	13.74	1.75
	28	0.95	0.11	851.2	352.9	206.8	27.3	13.77	1.83
CDW + 12BF	7	1.56	0.06	306.8	69.1	102.5	7	17.52	1.36
	28	-	-	-	-	-	-	-	-
CDW + 3IB	7	0.99	0.1	201.9	43.4	108.7	21.9	6.82	0.47
	28	0.94	0.08	226.5	28.2	149.7	21.6	8.43	1.36
CDW + AS2	7	0.7	0.18	496.5	125.8	280.4	72.4	8.73	2.06
	28	0.77	0.05	471.4	57.9	259	14.6	10.94	1.75
CDW + AS3	7	0.83	0.07	428.3	104.3	188.2	24.5	9.38	0.86
	28	0.73	0.05	1011.8	671.4	303.3	11	10.64	1.36

Similarly to the compressive strength values, also the parameters reported in Table 15 show an improvement of the performances when passing from 7 to 28 days, the maximum strain reduces, the elastic modulus and the toughness increase. An exception is represented by the mixtures containing AS2 were, passing from 7 to 28 days of curing both the tangent and secant elastic modulus decrease of about 5%.

In the 28 days cured samples the mixture stabilised with 8% of Bondafix reported an increase of 108% and 119% in the tangent and secant modulus respectively with respect to the 7 days cured ones. The CDW + 3IB reported an increase of 25% in the tangent modulus and 38% in the secant modulus. The mixture containing AS3 reported the highest increase in tangent modulus (136%) and an increment of 61% in the secant modulus.

4. PRELIMINARY FIELD TRIAL

The preliminary field trial was conceived to assess the procedures of the on-site tests to be performed during the field trial (plate load test, sand cone density and LWD measurements) and to investigate the sensibility of the LWD apparatus with respect to the variation of the input parameters such as plate diameter, drop height and impact mass. In addition, the sensitivity of the LWD device was tested on granular materials with different compaction degrees.

In order to achieve these goals, the preliminary field trial operations were divided into two stages, an LWD test simulation performed in the laboratory and an on-site test performed on a multi-layer granular material.

4.1. LWD test simulation

The capability of the device to detect the non-linear relationship between applied vertical stress and the dynamic modulus of the soil was assessed in this stage, by varying the device settings. To this purpose, a granular material layer was specifically produced and compacted in a PVC box. The layer consisted of a 25 cm-height unbound “CDW and water” mixture. The 25 cm of height were assumed to be sufficient to simulate the measurements on a homogeneous single layer with all the plate diameters available. In order to achieve sufficient homogeneity, the material was laid and compacted into three 8.3 cm-thick layers.

In Table 16 are reported the parameters necessary to produce the homogeneous layer.

Table 16:Parameters to produce the homogeneous layer

Density		
$\gamma'w_{Max}$	[kg/m ³]	2301
$\gamma'w_{85\%}$	[kg/m ³]	1956
Dimensions		
a	[m]	0.57
b	[m]	0.37
h	[m]	0.25
Volume	[m ³]	0.053
Weight		
Total	[kg]	103.1
Layer	[kg]	34.4

The compaction was uniformly performed for each layer with a manual proctor apparatus, assuming to achieve the 85% of the maximum wet density at the end of the compaction.

The test was performed with different equipment settings, varying plate diameter (150, 200 and 300 mm), weight (10, 15 and 20 kg) and drop height (13, 23 and 33 inches). Figure 20 shows the execution of the test and the different configurations of the device.

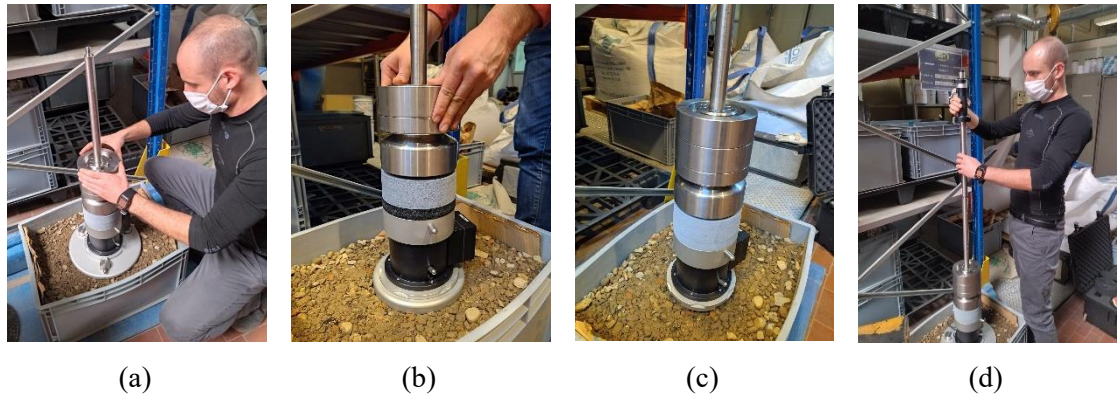


Figure 20: Assembling of the equipment in the configuration 300 mm diameter(a); Configuration 200 mm diameter and 15 kg mass (b); Configuration 150 mm diameter and 20 kg mass(c); Test execution (d)

For each settings configuration were performed eight measurements, the first four drops were applied to allow the material to exhibit only recoverable displacements. The last four measurements were recorded and used for the computation of the averaged values of the applied stress and dynamic modulus.

4.1.1. LWD test simulation: results and discussion

Table 17 reports the results of the tests performed.

Table 17: Results of the LWD test

Φ [mm]	Test	h [in]	Rubber pad [y/n]	Mass [kg]	avg stress [kPa]	st. dev. stress [kPa]	avg E ₀ [MPa]	st. dev E ₀ [MPa]
150	p18	13	no	10	201.5	3.0	32.0	0.0
	p19	23	no	10	288.8	3.8	36.3	0.4
	p20	33	no	10	388.5	4.3	43.5	0.5
	p21	13	no	15	289.0	0.7	36.8	0.4
	p22	23	no	15	453.0	2.3	47.0	0.7
	p23	33	no	15	588.0	3.5	52.0	1.2
	p24	13	no	20	389.3	2.3	42.0	0.0
	p25	23	no	20	588.0	1.6	52.3	0.8
200	p26	33	no	20	764.0	6.5	52.0	0.0
	p27	13	no	10	115.0	1.2	29.3	0.4
	p28	23	no	10	164.0	1.2	32.8	0.4
	p29	33	no	10	221.5	0.5	36.8	0.8
300	p30	13	no	15	161.3	1.5	33.0	0.7

ϕ [mm]	Test	h [in]	Rubber pad [y/n]	Mass [kg]	avg stress [kPa]	st. dev. stress [kPa]	avg E_0 [MPa]	st. dev. E_0 [MPa]
300	p31	23	no	15	251.8	1.5	39.3	0.4
	p32	33	no	15	334.3	1.3	45.3	1.6
	p33	13	no	20	218.8	3.3	35.0	0.7
	p34	23	no	20	340.0	0.0	43.3	0.4
	p35	33	no	20	441.3	1.5	48.3	0.4
	p0	13	yes	10	49.5	0.5	16.0	0.0
	p1	23	yes	10	72.3	0.8	16.3	0.4
	p2	33	yes	10	95.8	1.8	18.3	0.4
	p3	13	no	10	50.5	0.9	17.8	0.4
	p4	23	no	10	71.5	1.1	19.0	0.7
	p5	33	no	10	97.0	0.7	22.5	0.5
	p6	13	yes	15	72.0	1.0	20.3	0.4
	p7	23	yes	15	112.8	0.4	24.0	0.0
	p8	33	yes	15	149.8	0.8	24.5	2.9
	p9	13	no	15	70.5	0.9	21.0	0.0
	p10	23	no	15	112.3	1.1	24.0	0.0
	p11	33	no	15	148.0	1.2	26.8	0.4
	p12	13	yes	20	96.0	0.0	23.3	0.4
	p13	23	yes	20	151.0	1.2	27.3	1.1
	p14	33	yes	20	200.3	1.6	30.5	1.5
	p15	13	no	20	95.8	0.8	23.5	0.5
	p16	23	no	20	152.3	0.8	29.0	0.0
	p17	33	no	20	201.8	2.4	34.5	0.5

The non-linear behaviour of the granular material is clear when representing the relation between vertical stress and dynamic modulus (E_0) on a linear scale (Figure 21). The logarithmic trend shows a stress-strengthening behaviour characteristic of the granular materials, a similar behaviour was found testing the granular mixtures in the triaxial cell. It can be said that the dynamic modulus is sensitive to the applied stress and that the device is able to record this phenomenon.

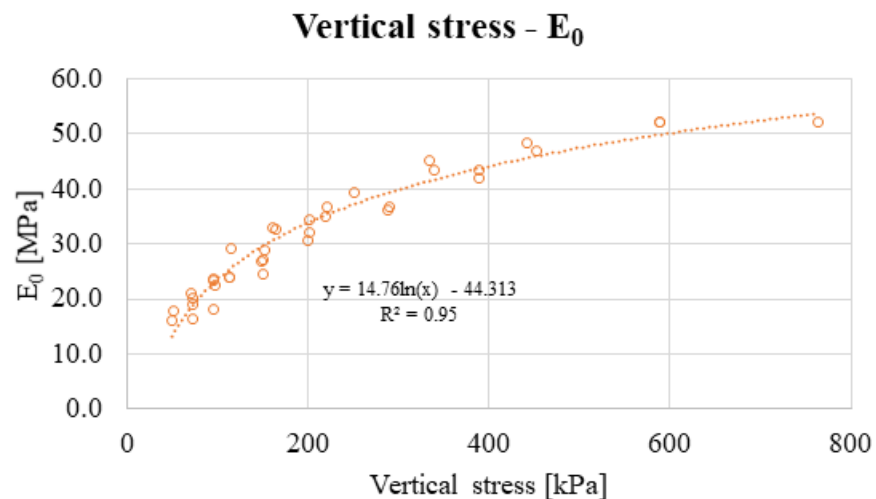


Figure 21: Vertical stress - dynamic modulus (E_0) represented in a bi-log plan

4.2. On-site tests

In this stage, the sensitivity of the LWD to different levels of compaction was tested, plate load tests and sand-cone density measurements were performed, and in the end, the results of these tests were compared.

The on-site operations were performed in the Cavit plant in La Loggia (TO), where a multi-layer granular material system was prepared for the execution of the tests. The multi-layer system consisted of a natural subgrade, a 40 cm-thick unbound CDW (layer 1), and a 30 cm thick layer of the same CDW mixture (layer 2) (Figure 22). The area occupied by the preliminary field trial is a rectangle 10 m wide and 45 m long.

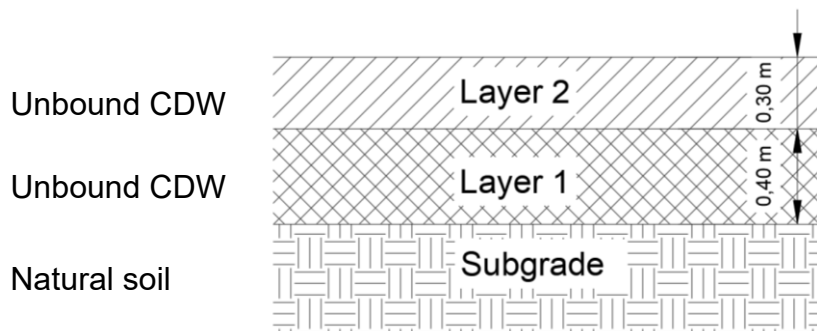


Figure 22: Multi-layer configuration

The schedule of the tests to be conducted included (i) one material sampling for each layer; (ii) LWD tests on four points of the subgrade layer, four points of the layer 1 and six points on the top layer; (iii) three plate load tests and three sand-cone density measurements on the top layer.

The operations were organised in a two-day program where for each layer were performed a sequence of tasks which included excavation procedures (for the subgrade) or material laying (for layers 1 and 2), layer compaction, and test execution. The field operations were organised as follows:

Day one: operations on subgrade and layer 1

- Subgrade:

At first, the 10 m x 45 m area was excavated to a depth of 70 cm, to this purpose an excavator, a dozer and two trucks were employed. Then the subgrade surface was compacted with 4 passes of a 200 tons dynamic roller (Figure 23).



(a)

(b)

(c)

Figure 23: Excavation procedure with excavator (a) and dozer (b); Compaction of the subgrade with a 200 tons dynamic roller (c).

During these operations, a sample of the natural soil was taken and sealed in an impermeable container, in order to determine the water content of the subgrade. After the compaction, LWD measurements were performed on 4 points located as described in Figure 24.

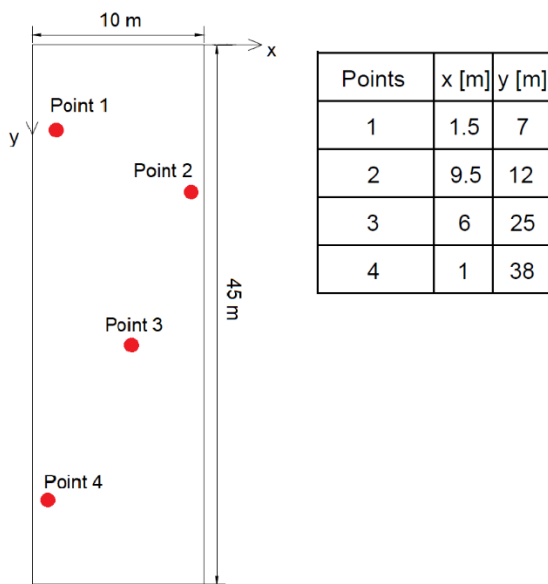


Figure 24: Tested points location

At each point, the LDW measurements were performed with a plate diameter of 300 mm, combining six apparatus settings, in particular, three drop heights (13, 23 and 33 in) and two masses (10 and 15 kg) (**Errore. L'origine riferimento non è stata trovata.**).



Figure 25: LWD device with three geophones (a); Test execution on the subgrade (b).

Although not necessary for the thesis objectives, all the field measurements conducted with LWD were performed with the three geophones configuration. In this way, further computations regarding back-calculated moduli could be done.

- Layer 1:

On the second part of day one, the first CDW layer was prepared and tested. The recycled aggregates were laid and compacted on top of the subgrade to obtain the 40 cm-thick layer. The compaction was performed with the same roller and number of passes used for the subgrade. After the layer placement operations were terminated, a sample of CDW was taken and sealed in an impermeable container, in order to determine the water content of layer 1. Then, the LWD measurements were performed at the location of points 1, 2, 3 and 4 as described in Figure 24, with the same device configurations adopted for the subgrade (plate diameter 300 mm, drop heights 13,23 and 33 in, and 10 and 15 kg mass). Figure 26 shows the execution of the operations on layer 1.



Figure 26: Placement of layer 1 (a); Test execution on layer 1(b).

Day 2: operations on layer 2

The second day was dedicated to the operations on layer 2. The layer is 30 cm thick and was divided into three 15 m-long sections with different compaction levels. The laying and compaction procedures were executed with the same procedures adopted for layer 1, except for the number of roller passes that was different for each section. Also for layer 2, a sampling of the material was performed to determine the water content. At the centre of each section were performed one plate load test and one sand-cone density measurement, while the location of the six points where the LWD tests were performed are shown in Figure 27. The same picture shows also the configuration of the sections with different levels of compaction. Sections 1, 2 and 3 were compacted with 4, 8 and 12 passes respectively. The location of points 1 to 4 are the same as the ones tested on the subgrade and layer 1, while points 5 and 6 are defined only for this layer.

The LWD measurements on layer 2 were performed in 18 configurations: plate diameters 150 and 300 mm; drop heights 13, 23 and 33 in; 10, 15, 20 kg mass).

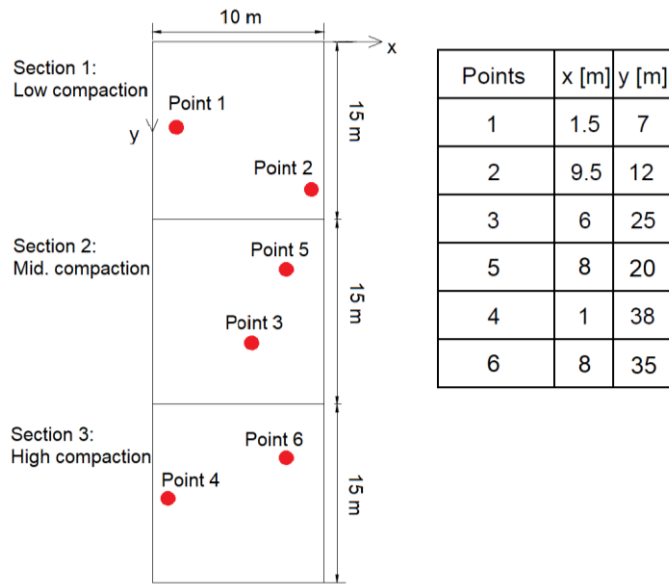


Figure 27: Compaction level configuration and location of the points tested with LWD

In Figure 28 are shown the execution of the sand cone density and plate load tests.

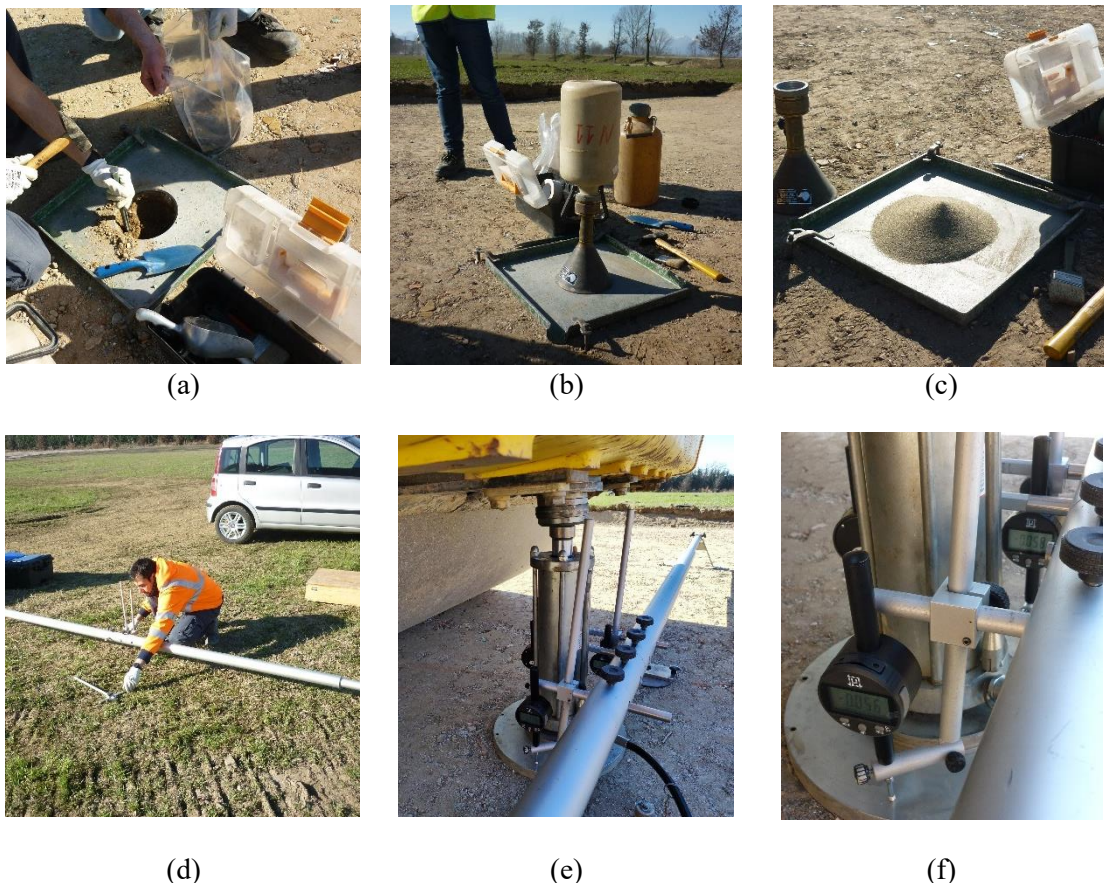


Figure 28: Sand-cone density (a) (b) (c), Plate load test (d) (e) (f).

4.2.1. On-site tests: results and discussion

LWD tests:

The LWD device was tested in different configurations to verify the sensitivity of the surface modulus to the applied vertical stress, in Figure 29 is reported, as an example, the vertical stress - surface modulus diagram obtained testing point 5 on layer 2.

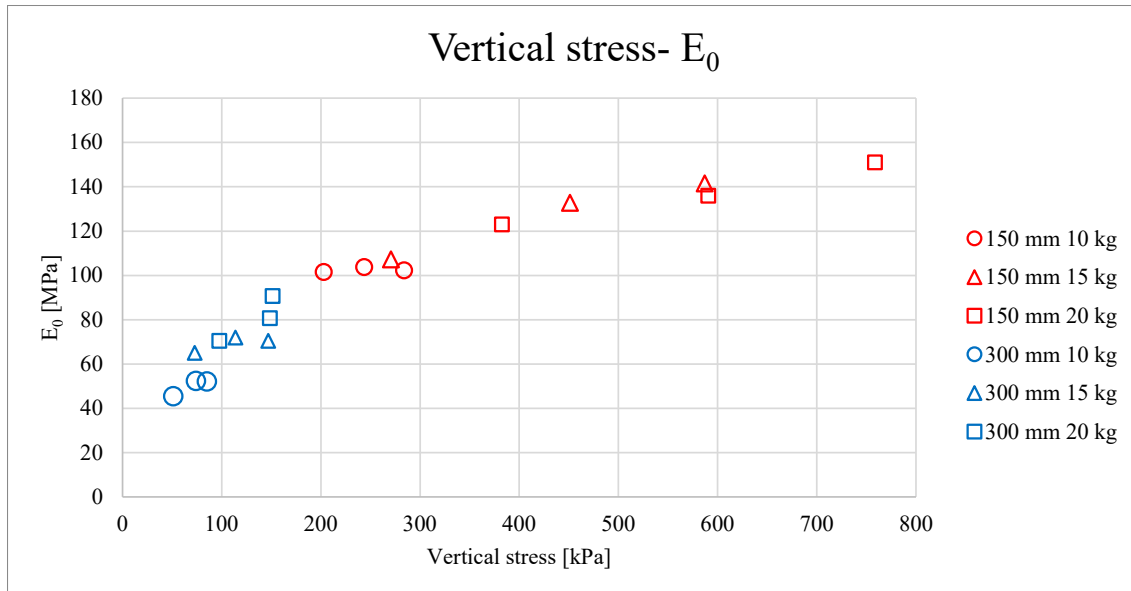


Figure 29: LWD test result of point 5 on layer 2.

The measurements were performed with different device settings, the results were represented divided by plate diameter and mass. The non-linear (stress-hardening) behaviour of the granular material is visible from this diagram, the device was able to detect different modulus in different input configurations also in a real scale multi-layer system.

At each point, the measurements were performed with different device settings as summarised in Table 18.

Table 18: Device test configurations.

Layer	Plate diameters	Masses	Drop heights	Points
Subgrade and layer 1	150 mm	10 and 15 kg	13, 23, 33 in	1, 2 , 3 and 4
Layer 2	150 and 300 mm	10, 15 and 20 kg	13, 23, 33 in	1, 2, 3, 4, 5 and 6

In the next paragraphs are shown the comparison of the LWD results between the tested points for each layer. The results are presented in histograms, where the surface modulus E_0 is evaluated in the configuration with plate diameter 300 mm and 10 kg mass, the value represented in the graphs is the average modulus obtained from all the drop heights (13, 23 and 33 in).

The LWD test on the subgrade showed that despite the same compaction level was adopted along the layer, the dynamic modulus at different points presented huge variations (Figure 30).

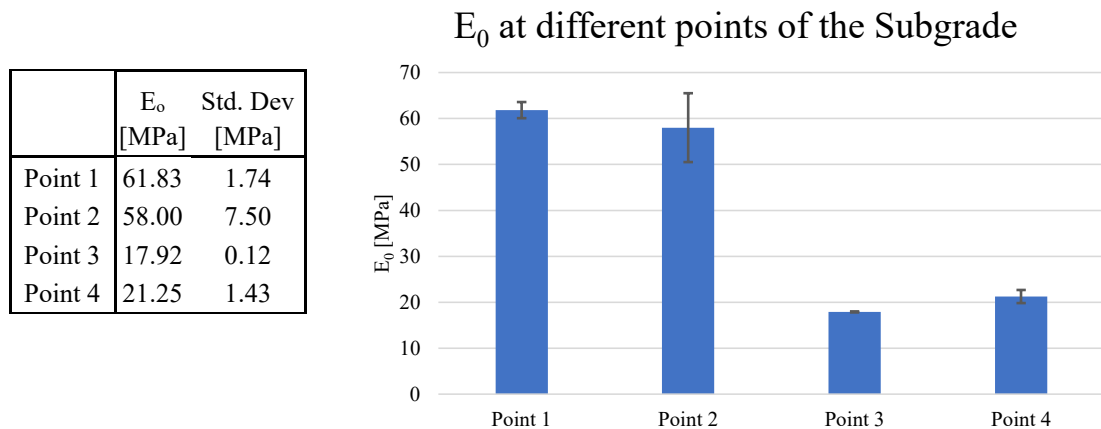


Figure 30: Comparison of E_0 on the subgrade, evaluated with configuration plate diameter = 300 mm and mass = 10 kg (average value of all the drop heights).

According to these results, the modulus of the natural subgrade is three times higher on points 1 and 2, with respect to points 3 and 4. This suggests a higher bearing capacity of the first portion of the field trial (approximately from 0 up to 15 m, according to the reference system of Figure 24) with respect to the remaining part.

In Figure 31 are reported the results on layer 1. Comparing the results on the subgrade with the ones obtained on the same locations of layer 1, it's possible to see that the modulus didn't vary for point 1, decreased by 40% for point 2, while it increased by four and two times for points 3 and 4 respectively.

	E _o [MPa]	Std. Dev [MPa]
Point 1	59.33	2.04
Point 2	34.92	0.92
Point 3	74.08	3.32
Point 4	45.17	1.55

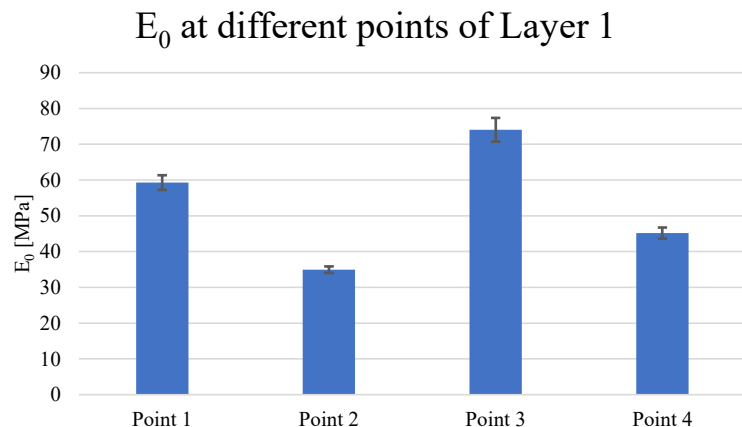


Figure 31: Comparison of E_0 on layer 1, evaluated with configuration plate diameter = 300 mm and mass = 10 kg (average value of all the drop heights).

Layer 2 was divided into three sections with different levels of compaction, points 1 and 2 are located in the lower compacted section, points 3 and 5 in the middle section, while points 4 and 6 are in the high compacted section (Figure 27). Figure 32 shows the LWD results on layer 2.

	E _o [MPa]	Std. Dev [MPa]
Point 1	72.75	2.35
Point 2	61.75	1.95
Point 3	59.67	5.09
Point 5	50.08	3.24
Point 4	132.67	8.30
Point 6	60.08	1.01

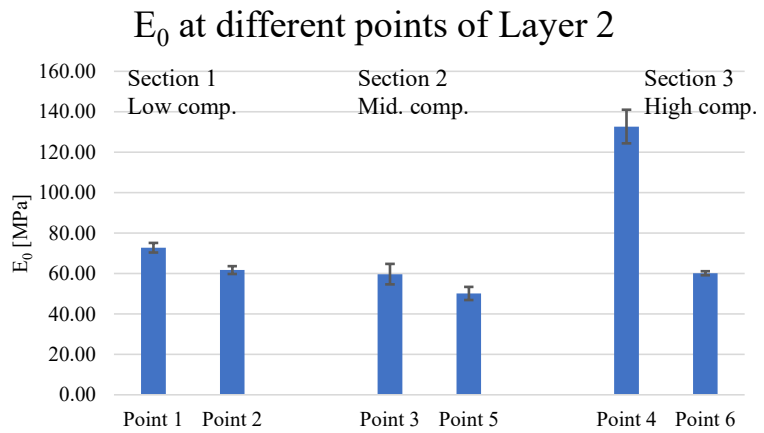


Figure 32: Comparison of E_0 on layer 2, evaluated with configuration plate diameter = 300 mm and mass = 10 kg (average value of all the drop heights).

On layer 2, the modulus ranged between 50 and 70 MPa in the first two sections and on point 6. Point 4 reported the highest value (around 130 MPa).

Sand-cone density and moisture content:

The samples of material of each layer were dried to obtain the water content, the results obtained in the lab showed a moisture content of 15.5%, 7.0% and 7.2% for the subgrade, layer 1 and layer 2 respectively. These outcomes show that the CDW material used during day one and day two had a uniform moisture content.

The sand-cone density results are reported in Table 19.

Table 19: Sand cone density results

Section	w	γ_w	γ_d	$\gamma_{d \text{ Situ}}/\gamma_{d \text{ Max}}$
	[%]	[kg/m ³]	[kg/m ³]	
1	6.2	2116.7	1994.0	95.4%
2	5.6	2196.5	2079.1	99.5%
3	4.9	2197.6	2094.3	100.2%

The $\gamma_{d \text{ Max}}$ refers to the density of the “CDW and water” mixture obtained in the Proctor curve study, corresponding to a 7.2 % of moisture content (same moisture content obtained of the sample of layer 2). As expected, higher values of density were found in the sections with a higher level of compaction.

Plate load test:

The plate load test showed an increasing modulus passing from the low-compacted section to the high-compacted one (Figure 33).

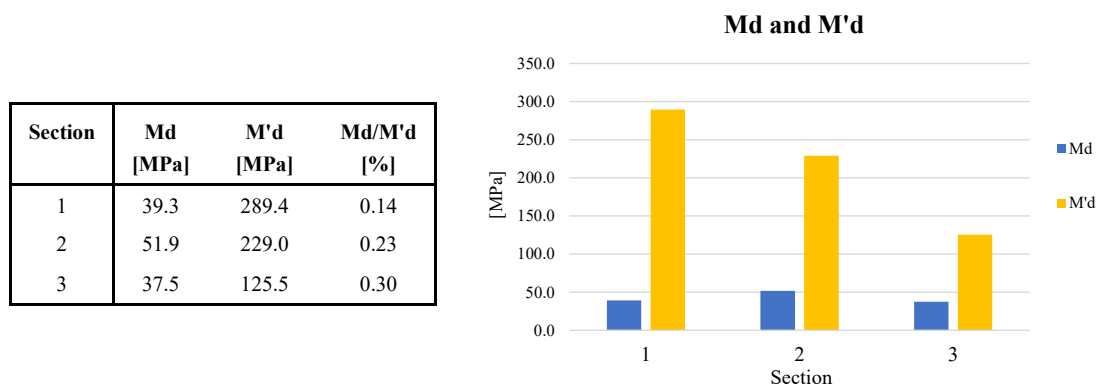


Figure 33:Plate load test results

The deformation modulus was found to be lower in the third section (although the more compacted one), this results could be affected by the lower bearing capacity of the subgrade below the highly compacted sections of layer 2 , the dynamic modulus found in section 3 was three times

lower than the one in the first section. It is possible to notice the different levels of compaction of the sections considering the ratio $M_d/M'd$, it increases as we move from a low compacted section to a high compacted one.

5. DESIGN OF THE FIELD TRIAL

In the development of the INTREC project, a field trial to investigate the mechanical properties of the mixtures in real-scale conditions will be developed. The experimental site will be located in the Cavit plant, and it will consist of a roadway 8 m wide and 320 m long. This chapter describes the design of the road, the planning and scheduling of the tests that will be performed and the computation of the amount of material necessary for the construction of the field trial.

5.1. Materials

Based on the results of the laboratory investigation (paragraph 3), seven mixtures were selected to be tested in the field trial. In particular, three mixtures composed of recycled aggregates stabilized with non-traditional binders, two mixtures stabilized with CEM II, and two unstabilized mixtures were selected.

The first mixture to be selected was CDW + AS2, among the alkali-activated stabilised mixtures, reported the highest RM and UCS at 7 days of curing, also the ITS was found to be one of the highest values. Moreover, unlike AS1, AS2 has the advantage to be a ready-made solution produced in the plant. The mixture stabilised with “Hybrid” cement reported lower mechanical properties with respect to the one containing CEM IV/B, which reported higher values of UCS and ITS of about 60 and 27% respectively. CDW + 3 CEM IV/B reported the highest stiffness at 7 days among all the mixtures stabilised with non-traditional binders. The cement type IV is obtained by mixing 50 % of cement type II with 50 % of calcinated clay, providing remarkable advantages from the sustainability point of view, it represents a good compromise between the less performing “hybrid” cement and the traditional CEM II. Regarding the mixtures stabilised with Bondafix, the best compromise between mechanical properties and amount of binder was found to be in the CDW + 8BF.

Table 20 reports the composition of mixtures.

Table 20: Mixtures for experimental site

Mixture/section n°	Aggregates	Binder	Water	Mixture name
1	CDW	CDW fines + AS2	-	CDW + AS2
2	CDW	CEM IV/B	8.5%	CDW + 3 CEM IV/B
3	CDW	Bondafix	8.5%	CDW + 8BF
4	CDW	CEM II	8.5%	CDW + 3 CEM II/B
5	NAT	CEM II	6%	NAT + 3 CEM II/B
6	NAT	-	6%	NAT and water
7	CDW	-	8.5%	CDW and water

The mixtures stabilized with CEM II (n° 4 and n° 5) will be used as a reference to compare the performance of the mixtures stabilized with non-traditional binders (n° 1, n° 2 and n° 3). The unstabilized granular mixtures (n° 6 and n° 7) will provide a reference to compare the differences between stabilised and unstabilised blends. To each of these mixtures, a section of the subbase layer of the field trial roadway will be dedicated.

The 320 m-long roadway will be subdivided into 7 sections as reported in **Errore. L'origine riferimento non è stata trovata.**

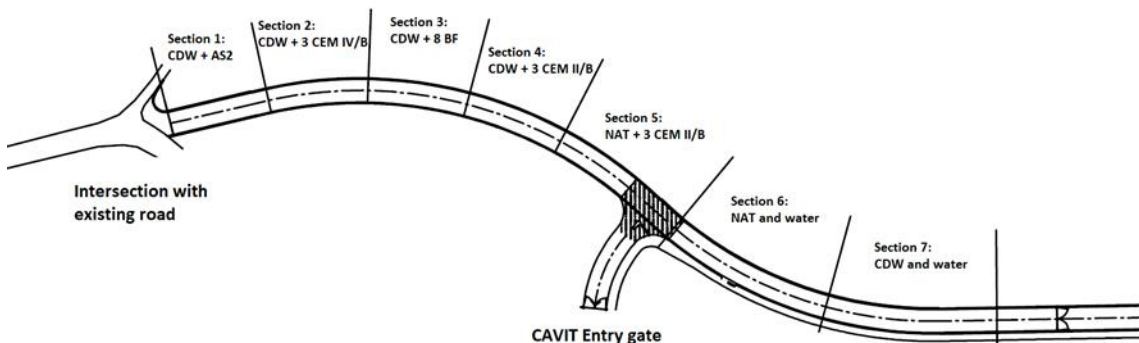


Figure 34: Field trial layout

The first 108 m will be divided into three sections of 36 m each and will be dedicated to the mixtures stabilized with non-traditional binders. Sections 4 and 5 are also 36 meters long and will house the two mixtures stabilized with CEM II. The last two sections are dedicated to the study of the unbound mixtures and each of them will be 70 m long.

5.2. Operation schedule

The construction of the field trial and the monitoring tests are organised in a 19 days schedule.

Day 1: tests on subgrade

During the first day of field tests, three operators are employed to perform the tests and sampling operations on the subgrade layer.

Two operators will carry out four Plate load tests on the subgrade layer of the field trial at different locations. The tests shall be developed on the centreline of the alignment at the distances from the starting point of the road indicated in Table 21.

Table 21: Location along the centreline of the plate load tests

Test 1	Test 2	Test 3	Test 4
25 m	75 m	125 m	200 m

The methods of the test have been described in paragraph 2.4.2.

Another operator will be involved in the ten dynamic plate tests and in-situ density measurements on the subgrade layer. The tests are planned to be carried out on the centreline of the alignment, seven tests at a distance of 20 m from each other will be performed on the section dedicated to the bound materials and three tests at a distance of 30 m from each other will be performed on the section dedicated to the unstabilised materials. The distribution of the tests is described in Table 22.

Table 22: Location along the centreline of the dynamic plate load tests

Test 1	Test 2	Test 3	Test 4	Test 5	Test 6	Test 7	Test 8	Test 9	Test 10
10 m	30 m	50 m	70 m	90 m	110 m	130 m	180 m	210 m	240 m

The two in-situ density tests will be carried out at a distance of 70 m and 120 m from the beginning of the field trial, at a distance from the centreline, to avoid interference with the plate load tests that are being developed contemporarily. The methods of the tests are described in paragraph 2.4.

The sampling of the subgrade material is also planned to investigate the characteristics of the subgrade (i.e., the granular size distribution) at the laboratory. For this purpose, a total amount of 45 kg of subgrade soil will be sampled and stoked in three bags.

Day 2: sampling raw material

Before the starting of the construction phases, raw materials for the future preparation of specimens for laboratory testing has to be sampled. Two operators are required to perform these sampling operations. Table 23 reports the volume of raw materials to be collected for each mixture to prepare the specified number of cylindrical specimens.

Table 23: Samples to be produced for each mixture type

	Sample type	Test	Quantity [-]	Diameter [mm]	h [mm]	Volume [m ³]
After 7 days	Thin sample in plastic mould	RM+UCS	3	100	186	0.00438
	Stubby sample in small metal mould	UCS	3	100	100	0.00236
	Stubby sample in large metal mould	ITS	3	150	120	0.00636
After 28 days	Thin sample in plastic mould	RM+UCS	3	100	186	0.00438

RM: Resilient modulus with triaxial cell

UCS: Unconfined compression strength

ITS: Indirect tensile strength

Total volume [m ³]	0.01748
--------------------------------	---------

The sampling will be performed on the single components of the mixture, therefore it is necessary to compute the amount of each element separately (Table 24).

Table 24: Mass content for each component of the mixture

MIXTURE	γ_d [kg/m ³]	W_{opt} [%]	Binder [%]	M_{solid} [kg]	$M_{aggregates}$ [kg]	M_{binder} [kg]	M_{water} [kg]	M_{tot} [kg]
CDW + AS2	2155	8.5%		37.676	37.676	*	3.202*	40.878
CDW + 3CEM IV B	2119	8.5%	3.0%	37.046	35.967	1.111	3.149	40.228
CDW + 8BF	2038	8.5%	8.0%	35.630	32.991	2.850	3.029	38.870
CDW + 3CEM II	2155	8.5%	3.0%	37.676	36.578	1.130	3.202	40.911
NAT + 3CEM II	2253	6.5%	3.0%	39.389	38.242	1.182	2.560	41.984
NAT and water	2248	6.5%		39.302	39.302		2.555	41.856
CDW and water	2121	8.5%		37.081	37.081		3.152	40.233

* In the case of AS2 the water content refers to the alkaline solution.

In order to have a sufficient amount of material, a safety factor equal to 1.7 is applied; the final quantity of each material to be sampled is summarized in Table 25. The table reports also the bags and/or containers that are necessary to store the materials.

Table 25: Materials quantities and necessary containers

Material	Quantity [kg]	Bags
Aggregates CDW	350	24
Aggregates NAT	140	10
Alkaline solution	5	1 container
Bondafix	5	1
Cement IV-B	2	1
Cement II	4	1

In Table 26 is reported the GAANT dyagramm for the operations of days one and two.

Table 26: GAANT activities of days one and two

MACRO ACTIVITY	Activity	Operator	DAY 1		DAY 2	
			Morning	Afternoon	Morning	Afternoon
Test on subgrade	Plate load	OP1 OP2	2 tests 2 tests			
	LWD	OP3	10 tests			
	In-situ density	OP3		2 tests		
	Sampling	OP3		3 tests		
Sampling raw material	sampling CDW aggregates	OP2			1 sampling	
	sampling NAT aggregates	OP3			1 sampling	
	sampling CEM-II/B	OP2			1 sampling	
	sampling CEM-IV/B	OP3			1 sampling	
	sampling AS2	OP2			1 sampling	
	sampling Bondafix	OP3			1 sampling	

Day 3: laying the unbound mixtures and mixtures sampling

The two sections of the subbase layer composed of unbound material (NAT and water and CDW and water) will be placed and compacted in the position described in Figure 34. For the same mixtures, material sampling will be developed.

For this task, three operators are needed, one operator will be required to supervise the laying and compaction operations, and the other two will be employed in the sampling procedures.

The amount of material to be sampled is the same as the ones reported in Table 23. The quantity by mass is calculated in Table 24. Also for this operation, the amount has been increased

with a safety factor of 1.7, therefore, for each mixture has to be sampled 70 kg. After the sampling, the fresh mixture is moved to the Cavit laboratory where will be compacted and sampled following the manual Proctor procedure. The operations to be performed are:

- Sampling of 70 kg of material for each type of mixture: the operators take the material with a wheelbarrow, and make sure to cover the mixture to avoid evaporation of water;
- In the laboratory, the operators will prepare the samples that are reported in Table 23, with a manual Proctor compactor;
- The samples are sealed and placed in a humid environment to avoid moisture loss;
- The samples are moved to the Politecnico laboratory for the tests that will be developed the next day.

In the meantime that the sampling is being performed, the second operator will be following the operations in section 6 of the field trial, where, a 30 cm thick and 70 m long layer of unbound NAT aggregates will be laid. After the layer is compacted, a CDW unbound mixture layer, of the same thickness and length, can be placed and compacted in section 7. At the end of the operations, the following tests are developed:

- Thickness control: three checks for each mixture;
- In-place density: one test for each mixture, as reported in paragraph 2.4.3

Day 4: tests on unstabilised mixtures

The laboratory and in situ tests on the unbound mixtures are performed on the day after the layers have been laid. Five operators are employed for these tasks.

Two operators are needed to perform the laboratory tests in the Politecnico laboratories, for each mixture will be performed the UCS, ITS and RM tests reported in Table 23. The tests will be performed on the cylindrical samples as described in paragraphs 2.3.3, 2.3.4 and 2.3.5.

Three operators are required in the in-situ tests on the compacted layers (CDW and NAT unbound mixtures). The following tests and repetitions are planned to be carried out:

Plate load tests: 3 tests on the NAT layer and 3 tests on the CDW layer, a Cavit vehicle will be used as a counterweight;

Dynamic plate load (LWD): 10 tests on the NAT layer and 10 tests on the CDW layer.

In Table 27 is reported the GAANT dyagramm for the operations of days three and four.

Table 27: GAANT activities of days three and four

MACRO ACTIVITY	Activity	Operator	DAY 3		DAY 4	
			Morning	Afternoon	Morning	Afternoon
LAYING UNBOUND MIXTURE Mixture 6	Sampling material	OP2	1 sampling			
	Compaction	OP3	9 Compactions			
	Laying supervision	OP1	supervision			
	In-situ density	OP1	1 test			
	Thickness check	OP1	3 tests			
	Plate load (1day)	OP4 OP5			3 tests 3 tests	
	LWD (1 day)	OP1			10 tests	
	Sample transport	OP3		transport		
	Lab tests (1day)	OP2			9 tests	9 tests
LAYING UNBOUND MIXTURE Mixture 7	Sampling material	OP3		1 sampling		
	Compaction	OP2		9 compaction		
	Laying supervision	OP1		1 supervision		
	In-situ density	OP1		1 test		
	Thickness check	OP1		3 tests		
	Plate load (1day)	OP4 OP5			3 tests 3 tests	
	LWD (1 day)	OP1			10 tests	
	Sample transport	OP3		transport		
	Lab tests (1day)	OP3			9 tests	9 tests

Day 7, 8 and 9: laying the stabilized mixtures and sampling:

In the timetable that was prepared, days 5 and 6 are supposed to be non-working days. During the following days (7, 8 and 9) will be placed the stabilised mixtures. On days 7 and 8 will be placed two mixtures per day, during day 9 it will be placed the last mixture, so to place five stabilised mixtures in total according to the scheme of Figure 34. The procedure for day 7 is described in the following paragraphs, the same procedure should be repeated on days 8 and 9.

One operator will be employed in section 1, where a 30 cm thick and 36 m long layer of the first mixture will be laid. Four additional meters of subbase will be laid in order to allow the roller to adequately compact the entire section. After the layer is compacted, the additional 4-meter segment is removed, and the adjacent subbase material can be placed and compacted with the same procedures. At the end of the operations, the following tests are developed:

- Thickness control: 3 checks for each mixture;
- In-place density: 1 test for each mixture, as reported in paragraph 2.4.3.

For both types of mixtures, the sampling operations will be performed by two operators following the same procedure as reported for the unstabilised mixtures on day 3.

In Table 28 is reported the GAANT dyagramm for the operations of day seven to day nine.

Table 28: GAANT activities of days seven to nine

MACRO ACTIVITY	Activity	Operator	DAY 7		DAY 8		DAY 9	
			Morning	Afternoon	Morning	Afternoon	Morning	Afternoon
LAYING STABILIZED MIXTURE - Mixture 1	Sampling material	OP2	1 sampling					
	Compaction	OP3		12 compaction				
	Laying supervision	OP1		supervision				
	In-situ density	OP1		1 test				
	Thickness check	OP1		3 tests				
	Sample transport	OP3					transport	
LAYING STABILIZED MIXTURE - Mixture 2	Sampling material	OP2		1 sampling				
	Compaction	OP3		12 compaction				
	Laying supervision	OP1		supervision				
	In-situ density	OP1		1 test				
	Thickness check	OP1		3 tests				
	Sample transport	OP3					transport	
LAYING STABILIZED MIXTURE - Mixture 3	Sampling material	OP2			1 sampling			
	Compaction	OP3			12 compaction			
	Laying supervision	OP1			supervision			
	In-situ density	OP1			1 test			
	Thickness check	OP1			3 tests			
	Sample transport	OP3					transport	
LAYING STABILIZED MIXTURE - Mixture 4	Sampling material	OP2			1 sampling			
	Compaction	OP3			12 compaction			
	Laying supervision	OP1			supervision			
	In-situ density	OP1			1 test			
	Thickness check	OP1			3 tests			
	Sample transport	OP3					transport	
LAYING STABILIZED MIXTURE - Mixture 5	Sampling material	OP2			1 sampling			
	Compaction	OP3			12 compaction			
	Laying supervision	OP1			supervision			
	In-situ density	OP1			1 test			
	Thickness check	OP1			3 tests			
	Sample transport	OP3					transport	

Day 10, 11 and 12: in situ tests on stabilised mixtures

The in situ tests will be developed after 3 days of curing, the following procedure refers to day 10, where will be tested the mixtures 1 and 2 (placed during day 7), the same procedure will be repeated for mixtures 3 and 4 on day 11, and mixture 5 on day 12.

Two operators are employed to perform 3 plate load tests on both sections 1 and 2. The tests will be executed on the centreline at a distance of about 10 m.

The remaining operator will perform 10 LWD tests on section 1, and 10 LWD tests on section 2. The measurements will be carried at a distance of 2.5 m from the centreline (left side and right side), with a longitudinal spacing of 3 m.

In Table 29 is reported the GAANT dyagramm for the operations of day ten to day twelve.

Table 29: GAANT activities of days ten to twelve

MACRO ACTIVITY	Activity	Operator	DAY 10		DAY 11		DAY 12	
			Morning	Afternoon	Morning	Afternoon	Morning	Afternoon
IN SITU TESTING - Mixture 1 and 2	Plate load (3 days)	OP2 OP3	3 tests 3 tests					
	LWD (3 days)	OP1	10 tests					
	Plate load (3 days)	OP2 OP3		3 tests 3 tests				
	LWD (3 days)	OP1		10 tests				
IN SITU TESTING - Mixture 3 and 4	Plate load (3 days)	OP2 OP3			3 tests 3 tests			
	LWD (3 days)	OP1			10 tests			
	Plate load (3 days)	OP2 OP3				3 tests 3 tests		
	LWD (3 days)	OP1				10 tests		
IN SITU TESTING - Mixture 5	Plate load (3 days)	OP2 OP3					3 tests 3 tests	
	LWD (3 days)	OP1					10 tests	

Day 14, 15 and 16: 7-days laboratory tests:

In the timetable that was prepared, day 13 is supposed to be a non-working day. During days 14, 15 and 16, will be performed the 7 days laboratory tests, in particular, on day 14 will be tested the mixtures 1, 2, on day 15 will be tested the mixtures 3 and 4, and on day 16 will be tested the mixture 5. It will be employed one operator to develop the UCS, ITS and RM tests reported in Table 23, the methods were described in paragraphs 2.3.3, 2.3.4 and 2.3.5.

In Table 30 is reported the GAANT dyagramm for the operations of day fourteen to day sixteen.

Table 30: GAANT activities of days fourteen to sixteen

MACRO ACTIVITY	Activity	Operator	DAY 14		DAY 15		DAY 16	
			Morning	Afternoon	Morning	Afternoon	Morning	Afternoon
LAB TESTING (7 days) - Mixture 1 and 2	Lab test mixture 1 (7 days)	OP2	6 tests	6 tests				
	Lab test mixture 2 (7 days)	OP3	6 tests	6 tests				
LAB TESTING (7 days) - Mixture 3 and 4	Lab test mixture 3 (7 days)	OP2			6 tests	6 tests		
	Lab test mixture 4 (7 days)	OP3			6 tests	6 tests		
LAB TESTING (7 days) - Mixture 5	Lab test mixture 5 (7 days)	OP2					6 tests	6 tests

Days 34, 35 and 36: 28-days lab tests:

After 28 days of curing will be tested the RM and UCS of the specimens, in particular, during day 34 will be tested the mixtures 1, 2, on day 35 will be tested the mixtures 3 and 4, and on day 36 will be tested the mixture 5. For each mixture will be tested three samples. The tests will be performed with the same methodology adopted for the 7-days laboratory tests.

In Table 31 is reported the GAANT dyagramm for the operations of day fourteen to day sixteen.

Table 31: GAANT activities of days thirty-four to thirty-six

MACRO ACTIVITY	Activity	Operator	DAY 34		DAY 35		DAY 36	
			Morning	Afternoon	Morning	Afternoon	Morning	Afternoon
LAB TESTING (28 days) - Mixture 1 and 2	Lab test mixture 1 (28 days)	OP2	3 tests	3 tests				
	Lab test mixture 2 (28 days)	OP3	3 tests	3 tests				
LAB TESTING (28 days) - Mixture 3 and 4	Lab test mixture 3 (28 days)	OP2			3 tests	3 tests		
	Lab test mixture 4 (28 days)	OP3			3 tests	3 tests		
LAB TESTING (28 days) - Mixture	Lab test mixture 5 (28 days)	OP2					3 tests	3 tests

5.3. Quantities estimation

The quantity of material needed for the construction of the field trial was estimated considering the cross-section of the road, and a safety margin of 10%. The road that needs to be built is 320 m in length and 8 m in width. The pavement layer thicknesses were designed according to a specific structural model: a fixed thickness (30 cm) of the subbase layer was maintained, while the design life of the top hot mix asphalt (HMA) layer was estimated depending on the subbase material. The design of the pavement was based on estimates of the traffic levels of heavy vehicles travelling from and to the Cavit plant. The results of pavement design in terms of design life of HMA for different subbase materials are reported in Figure 35. For sake of clarity, the structural calculations were not part of this thesis but were considered as input parameters for quantities' estimation.

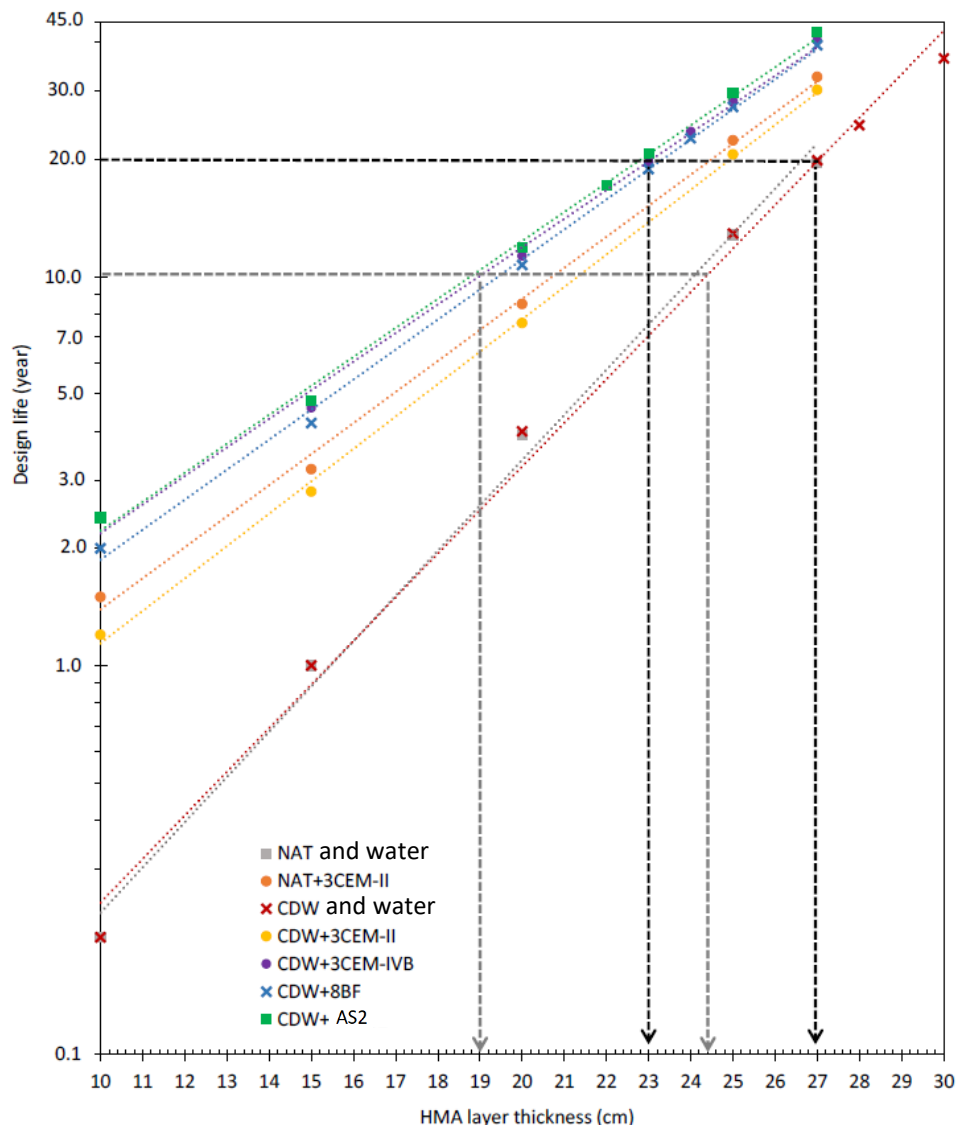


Figure 35: Pavement expected life given a 30 cm thick subbase as a function of the HMA layer thickness.

According to the results of the structural design of different pavement solutions, the HMA layer thickness was chosen to be 12 cm to balance economic requests of Cavit S.p.a and structural requirements. In conclusion, the selected pavement cross-section is composed of a compacted subgrade, a 30 cm-thick subbase and a 12 cm-thick HMA, Figure 36 shows the pavement cross-section.

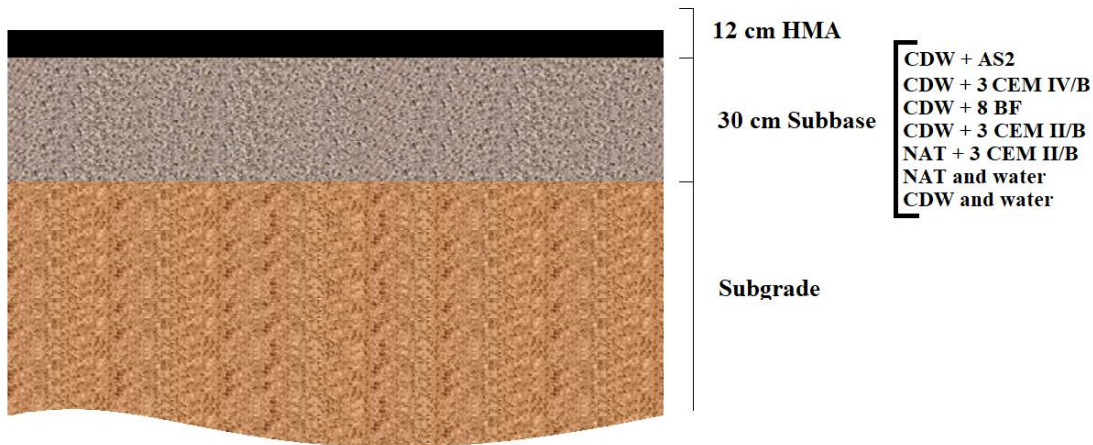


Figure 36: Pavement cross-section

The quantity of material needed for the construction of the field trial is reported in Table 32.

Table 32: Amount of material for each section

Section		1	2	3	4	5	6	7
Mixture		CDW+AS2	CDW + 8BF	CDW + 3CEM IV/B	CDW + 3CEM II	NAT + 3CEM II	NAT and water	CDW and water
Volume	Starting station	0+000	0+036	0+072	0+108	0+144	0+180	0+250
	End-station	0+036	0+072	0+108	0+144	0+180	0+250	0+320
	Length [m]	36	36	36	36	36	70	70
	Effective length [m]	40	40	40	40	40	70	70
	Subbase volume [m ³]	96	96	96	96	96	168	168
	HMA volume [m ³]	34.56	34.56	34.56	34.56	34.56	67.2	67.2
	Subbase (SF*) [m ³]	105.6	105.6	105.6	105.6	105.6	184.8	184.8
	HMA (SF*) [m ³]	38.016	38.016	38.016	38.016	38.016	73.92	73.92
	Water content [%]			8.5	8.5	8.5	6.5	6.5
	Binder content [%]	8.5	8	3	3	3		
	Subbase wet density [kg/m ³]	2271	2213	2225	2245	2313	2309	2108

	Section		1	2	3	4	5	6	7
Mass	HMA density	[kg/m ³]	2394	2394	2394	2394	2394	2394	2394
	Subbase (SF*)	[Mg]	239.8	233.7	235.0	237.1	244.3	426.7	389.6
	HMA (SF*)	[Mg]	91.0	91.0	91.0	91.0	91.0	177.0	177.0
	Aggregates (SF*)	[Mg]	221.0	199.4	210.2	212.1	222.7	400.7	359.0
	Subbase binder (SF*)	[Mg]	18.8	16.0	6.3	6.4	6.7		
	Subbase water (SF*)	[Mg]		18.3	18.4	18.6	14.9	26.0	30.5
*(SF) indicates that the safety factor equal to 1.1 was applied in the computation.									

The effective length reported in the table includes an additional four meters-long section which allows better compaction of the material at the border of the section. After the compaction will be performed, the extra material will be removed, and the next section can be laid.

In Table 33 are summarized the amount for each component.

Table 33: Summary of the quantities for each component

CDW [Mg]	NAT [Mg]	AS2 [Mg]	Bondafix [Mg]	CEM IV/B [Mg]	CEM II [Mg]	Water [Mg]	HMA [Mg]
1201.9	623.3	18.8	16.0	6.3	13.0	126.8	809.0

6. CONCLUSIONS

Civil works represent one of the main sources of waste materials. In Italy, the waste generated by construction and demolition activities is increasing. In 2019, it represented the 45.5% of the total special wastes produced (ISPRA, 2021). Recycling processes allow reusing part of this material and, in particular, the use of aggregates from construction and demolition waste (CDW) has aroused interest in the road sector. The advantages of using CDW recycled aggregates in substitution of virgin ones include the reduction of material destined to landfill, the preservation of natural resources, and the overall reduction of costs. In this context, CDW represents an opportunity for the sustainable development of pavement constructions. The use of aggregates deriving from waste material processing (CDW) has been intensifying in those construction applications that do not require high mechanical performance. An improvement in the mechanical characteristics of CDW mixtures can be achieved through stabilisation. This practice is still not common and, when implemented, it involves traditional Portland cement whose manufacture processes are expensive and generate large amounts of CO₂. For this reason, the advantages of using CDW aggregates can be compromised by the use of traditional binders. Therefore, the use of binders with reduced environmental impact is mandatory. In this framework, the INTREC project aims at developing new solutions for the formation of subbase layer of road pavements. The thesis carried out is part of INTREC, and its objective is to partly cover the gap in scientific knowledge on the properties of CDW mixtures stabilised with innovative binders.

For these purposes, different mixtures for the formation of subbase layers of roads were analyzed and compared. In particular, materials obtained both through the use of natural virgin aggregates and recycled aggregates have been considered. The aggregates have been combined with ordinary and non-traditional binders. The study was divided into two stages, the first was dedicated to the laboratory study aimed at the characterization of the mechanical properties of the mixtures, while the second one concerned the design of a field trial to test the real-scale behaviour of the materials.

The laboratory study started with the determination of the OMC and MDD of the mixtures through the Proctor study, this step allowed the production of samples by means of the gyratory shear compactor. Then, the mechanical properties such as workability, resilient modulus, UCS and ITS were tested.

The results showed that the blends stabilised with Bondafix exhibited increasingly performance in strength (UCS and ITS) as the binder content increased. In terms of stiffness, the binder dosage did not affect remarkably the results. Conversely, the curing time was found to be the main cause affecting the reduction of RM, evaluated at $I_l= 275$ kPa, the resilient modulus of CDW + 8BF decreased by 26% when passing from 7 to 28 days of curing time. The reduction of stiffness in the long-time cured samples has been found to be common in most of the mixtures types, this may be due to the increase in moisture contents of the samples that occurs in the humid environment.

Regarding the mixtures containing CEM IV/B, results from Avellino and Gugliotta (2021) on the mixture CDW + 3CEMIV/B and the one tested in this study, CDW + 3IB, were compared. CDW + 3CEM IV/B exhibited superior properties compared to CDW + 3IB; this can be due to the different amounts of calcinated clay present in the blends, 50 and 75% respectively. The first blend presented a UCS of about 1.7 MPa both at 7 and 28 days, while the second one reported 1.1 and 1.4 MPa at 7 and 28 days respectively. The CIRS threshold was reached only from the first blend with 0.27 MPa. Regarding the resilient modulus, the blend stabilised with CEM IV/B reported the highest value among all the tested mixtures, 638 MPa at 7 days ($I_l=275$ kPa). Conversely, after 7 days of curing the mixture stabilised with “hybrid” cement showed a stiffness in line with the other mixtures, but a reduction of 44% when passing to 28 days.

The last mixtures to be tested were the ones stabilised with alkali-activated CDW fines, all of these mixtures satisfied the CIRS threshold, and the blends containing AS1 and AS2 showed an ITS above 0.34 MPa. Concerning the compressive strength, at 7 days, CDW + AS2 reported a UCS similar to the reference mixture NAT + CEMII/B (1.84 and 1.86 MPa respectively). The RM of CDW + AS3 was the only one to report an increase with the curing time (30% evaluated at $I_l=275$ kPa), while the blend stabilised with AS2 reported the highest values of the M-EPDG parameters k_1 and k_2 at 7 days (3868 and 0.54 respectively).

After the laboratory tests, seven mixtures were selected to be tested on a real scale, the criteria that were adopted concerned both the evaluation of the mechanical performance and the environmental sustainability of the choice. The blend containing AS2 was selected taking into consideration the fact that it is a ready-made solution produced in the industrial plant. Regarding the CEM IV/B, despite the sustainability advantages brought by the use of the mixture CDW + 3IB, the mechanical properties turned out to be not as suitable as the ones exhibited by the blend containing “pure” cement type 4. Therefore, between these two, the choice fell on this last mixture. The Bondafix binder showed promising results and the mixtures containing it presented

an increasing performance trend together with the binder content. However, considering the impact on environmental sustainability, the choice fell on the 8% of binder content. In the end, the mixtures NAT + 3CEMII, CDW + CEM II, the unbound mixtures containing natural and recycled aggregates were selected to provide a comparison between the behaviour of the traditional materials and the studied mixtures.

Preliminary site operations were carried out in order to test the sensibility of the LWD to the different input configurations and to the different levels of compaction of the material. These activities were developed both through a laboratory simulation and through a site test on a multi-layer system. The laboratory simulation was performed on an unbound CDW layer built in a PVC box where LWD tests were developed with different device settings, the equipment recorded a non-linear stress dependence of the LWD modulus, in particular, a stress-hardening behaviour. The LWD sensitivity to different input parameters was tested on a real scale multi-layer system. The sensitivity of the device to the different levels of compaction was more difficult to be appreciated considering the great number of variables affecting the multi-layer system.

After the preliminary activities, the design of the experimental site was carried out. At first, the location of the experimental road was defined in accordance with Cavit company. Then, the schedule and the operations to be performed were defined considering the configuration of the site and the available equipment. The operations were organised avoiding the conflict of different tasks, accounting for the time needed to perform the tests, and including the necessity of testing the mixtures after a correct curing time. The planned operations included subgrade characterization and material sampling, laying and compaction supervision, static and dynamic load tests, density measurements and laboratory tests.

Since the road cross-section was defined through a structural model, the subbase and the HMA layer thickness were used for the estimation of the material quantities, these computations accounted for a safety factor.

The schedule of the experimental field trial ends with the 28-days tests of the mixtures, this allows the mechanical characterisation of the materials. However, the continuous monitoring of the pavement in time will be fundamental in order to determine the real scale behaviour of the different solutions. Only in this way, it will be possible to assess the reliability of these CDW mixtures subbase layers. To this end, the choice of the location of the experimental site was fundamental. In fact, as the road leads to the Cavit plant, will be travelled by heavy vehicles. Moreover, the traffic at which the road is subjected could precisely be determined since almost all of the heavy vehicles passing will be documented in the company records.

7. References

- AASHTO. (2007). *AASHTO T307-99: 2007 - Resilient modulus of soils and aggregate materials.*
- Agrela, F., Barbudo, A., Ramírez, A., Ayuso, J., Carvajal, M. D., & Jiménez, J. R. (2012). Construction of road sections using mixed recycled aggregates treated with cement in Malaga, Spain. *Resources, Conservation and Recycling*, 58, 98-106.
- ANAS Quaderni tecnici per la salvaguardia delle infrastrutture, Vol. 5. (2019).
- Ainchil, J.P., Cadenas, J.M., Rios, C., Cortes, C., Sampedro, A., Vazquez, E., Navarro, J.M., (2009). *Design and Execution of Soil Cement Layers with C&D Materials*, 2nd International RILEM Conference on Progress of Recycling in the Built Environment. RILEM Publications SARL, Sao Paulo, Brazil, pp. 165e173.
- Arulrajah, A., Piratheepan, J., Disfani, M. M., & Bo, M. W. (2013a). Geotechnical and Geoenvironmental Properties of Recycled Construction and Demolition Materials in Pavement Subbase Applications. *Journal of Materials in Civil Engineering*, 25
- Arulrajah, A., Mohammadinia, A., D'Amico, A., & Horpibulsuk, S. (2017). Cement kiln dust and fly ash blends as an alternative binder for the stabilization of demolition aggregates. *Construction and Building Materials*, 145, 218-225.
- ASTM D 1556 - 00. (2000) Standard Test Method for Density and Unit Weight of Soil in Place by the Sand-Cone Method
- ASTM E 2583 – 07. (2015) Standard Test Method for Measuring Deflections with a Light Weight Deflectometer
- Avellino, F., Gugliotta, F. (2021) Stabilizzazione con leganti alternativi di aggregati riciclati da costruzione e demolizione per fondazioni stradali.
- Barzaghi s.r.l. (2020). Scheda Tecnica N° 1951, BONDAFIX FH 130.
- Bassani, M., Riviera, P. P., & Tefa, L. (2017). Short-term and long-term effects of cement kiln dust stabilization of construction and demolition waste. *Journal of Materials in Civil Engineering*, 29(5), 04016286.
- Bassani, M., Tefa, L., Coppola, B., & Palmero, P. (2019). Alkali-activation of aggregate fines from construction and demolition waste: Valorisation in view of road pavement subbase applications. *Journal of Cleaner Production*, 234, 71-84.
- Beja, I. A., Motta, R., & Bernucci, L. B. (2020). Application of recycled aggregates from construction and demolition waste with Portland cement and hydrated lime as pavement subbase in Brazil. *Construction and Building Materials*, 258, 119520.
- Consiglio Nazionale delle Ricerche. (1992) BU CNR 146/92. Determinazione dei moduli di deformazione M_d e M'_d mediante prova di carico a doppio ciclo con piastra circolare.

CIRS e Ministero delle Infrastrutture e dei Trasporti. NORME TECNICHE DI TIPO PRESTAZIONALE PER CAPITOLATI SPECIALI D'APPALTO. 2a edizione.

da Conceição Leite, F., dos Santos Motta, R., Vasconcelos, K. L., & Bernucci, L. (2011). Laboratory evaluation of recycled construction and demolition waste for pavements. *Construction and building materials*, 25(6), 2972-2979.

Del Rey, I., Ayuso, J., Barbudo, A., Galvín, A.P., Agrela, F., de Brito, J. (2016b). Feasibility study of cement-treated 0-8 mm recycled aggregates from construction and demolition waste as road base layer. *Road Mater. Pavement Des.* 17, 678-692.

Dynatest. (2020). LWD 3032 User manual

EU COMMISSION https://ec.europa.eu/environment/topics/waste-and-recycling/construction-and-demolition-waste_en

Ente nazionale italiano di unificazione. (2006a). UNI EN 13286-41:2006 - Miscele non legate e legate con leganti idraulici - Parte 41: Metodo di prova per la determinazione della resistenza a compressione di miscele legate con leganti idraulici

Ente nazionale italiano di unificazione. (2006b). UNI EN 13286-42:2006 - Miscele non legate e legate con leganti idraulici - Parte 42: Metodo di prova per la determinazione della resistenza a trazione indiretta di miscele legate con leganti idraulici.

Ente nazionale italiano di unificazione. (2010) UNI EN 13286-2:2010 - Miscele non legate e legate con leganti idraulici - Parte 2: Metodi di prova per la determinazione della massa volumica e del contenuto di acqua di riferimento di laboratorio - Costipamento Proctor.

Ente nazionale italiano di unificazione. (2011). UNI EN 197-1:2011 - Cemento - Parte 1: Composizione, specificazioni e criteri di conformità per cementi comuni.

Ente nazionale italiano di unificazione. (2015). UNI EN ISO 17892-1:2015 - Indagini e prove geotecniche - Prove di laboratorio sui terreni - Parte 1: Determinazione del contenuto in acqua.

European Parliament. Waste Framework Directive 2008/98/EC. (2008).

Fernandes, E. M., Gomes, S., & Gonçalves, F. (2009). Recycled aggregates for unbound sub-base pavement layers. Elsamex Portugal, SA, Aveiro, Portugal, 15.

Iacoboaea, C., Aldea, M., & Petrescu, F. (2019). Construction and demolition waste-a challenge for the European Union?. *Theoretical and Empirical Researches in Urban Management*, 14(1), 30-52.

Ispra. Report on waste economic activities. (2021).

Mohammadinia, A., Arulrajah, A., Sanjayan, J., Disfani, M. M., Win Bo, M., & Darmawan, S. (2016). Stabilization of Demolition Materials for Pavement Base/Subbase Applications Using Fly Ash and Slag Geopolymers: Laboratory Investigation. *Journal of Materials in Civil Engineering*, 28(7), 4016033.

Naji, K. (2018). Resilient modulus–moisture content relationships for pavement engineering applications. *International Journal of Pavement Engineering*, 19(7), 651-660.

Ossa, A., García, J.L., Botero, E. (2016) Use of recycled construction and demolition waste (CDW) aggregates: A sustainable alternative for the pavement construction industry, Journal of Cleaner Production.

PFG Pavement Foundation Group. (2009). LWD Best Practice Guide – Draft version 10

Pourkhorshidi, S., Sangiorgi, C., Torreggiani, D., & Tassinari, P. (2020). Using Recycled Aggregates from Construction and Demolition Waste in Unbound Layers of Pavements. *Sustainability*, 12(22), 9386.

Puppala, A. J., Hoyos, L. R., & Potturi, A. K. (2011). Resilient moduli response of moderately cement-treated reclaimed asphalt pavement aggregates. *Journal of Materials in Civil Engineering*, 23(7), 990-998.

Silva, R. V., De Brito, J., & Dhir, R. K. (2019). Use of recycled aggregates arising from construction and demolition waste in new construction applications. *Journal of Cleaner Production*, 236, 117629.

Taha, R., Al-Harthy, A., Al-Shamsi, K., & Al-Zubeidi, M. (2002). Cement stabilization of reclaimed asphalt pavement aggregate for road bases and subbases. *Journal of materials in civil engineering*, 14(3), 239-245.

Witczak, M. W., Kaloush, K., Pellinen, T., El-Basyouny, M., & Quintus, H. Von. (2002). Simple Performance Test for Superpave Mix Design. In Transportation Research Board. http://onlinepubs.trb.org/onlinepubs/nchrp/nchrp_rpt_465.pdf

Zhang, J., Ding, L., Li, F., & Peng, J. (2020). Recycled aggregates from construction and demolition wastes as alternative filling materials for highway subgrades in China. *Journal of Cleaner Production*, 255, 120223.

Zhang, J., Liu, G., Chen, B., Song, D., Qi, J., & Liu, X. (2014). Analysis of CO₂ emission for the cement manufacturing with alternative raw materials: a LCA-based framework. *Energy Procedia*, 61, 2541-2545.

Acknowledgements

I would like to offer my special thanks to Professor Marco Bassani and Assistant Professor Luca Tefa, who supervised the research activities and supported me in the development of the thesis. I am particularly grateful for the knowledge that they were able to transfer to me during these challenging months. I would like to extend my thanks to the Cavit S.p.a company for allowing me to be part of this important research project.

Ringraziamenti

Voglio in fine ringraziare la mia famiglia e gli amici che mi hanno supportato durante questi anni impegnativi, senza il loro sostegno non sarebbe stato possibile raggiungere questo traguardo. Un grazie particolare va alla mia compagna Vanessa, che con grande pazienza mi ha accompagnato in tutto il percorso di studi e con cui ho potuto condividere le difficoltà incontrate.

8. ATTACHMENTS

8.1. Proctor test

Proctor compaction parameters

W _{initial} [%]	Mould tare [g]	Mould + material		γ _w [kg/m ³]	γ _{d,eff} [kg/m ³]	γ _{d,initial} [kg/m ³]	Tare of container [g]	Container + wet material		Wet material [g]	Dry material [g]	W _{eff} [%]
		Wet mass [g]	[g]					Container [g]	[g]			
4.0	10338.4	14760.5	4422.1	2085.3	1993.3	2065.0	401.1	2626.6	2528.4	2225.5	2127.3	4.6
6.0	10338.2	14891.7	4553.5	2147.3	2022.5	2025.8	564.9	3047.4	2903.1	2482.5	2388.2	6.2
9.0	10338.9	15079.5	4740.6	2235.5	2043.1	2050.8	402.4	3354.2	3100.1	2951.8	2697.7	9.4
10.1	10338.2	15029.9	4691.7	2212.5	2016.3	2009.3	564.5	3540	3276.2	2975.5	2711.7	9.7
12.0	10338.5	15052.1	4713.6	2222.8	2001.6	1984.6	605.7	3698.3	3390.5	3092.6	2784.8	11.1
4.0	10337.7	14737.6	4399.9	2074.9	1898.4	1995.0	1025.6	4293.1	4158.5	3267.5	3132.9	4.3
6.0	10338.2	14864.7	4526.5	2134.6	2005.3	2013.7	489.6	3651	3459.5	3161.4	2966.9	6.4
8.0	10338.3	15047	4708.7	2220.5	2065.3	2056.0	400.2	3541.2	3307.6	3141	2907.4	8.0
10.0	10338	14970.3	4632.3	2184.5	1983.9	1985.9	401	3635.2	3338.2	3234.2	2937.2	10.1
12.0	10338.1	14909.6	4571.5	2155.8	1927.1	1924.8	605.3	4187	3807	3581.7	3201.7	11.9
4.0	10337.9	14681	4343.1	2048.1	1959.7	1969.3	27.9	2492.7	2386.3	2464.8	2358.4	4.5
6.0	10338.2	14905.2	4567	2153.7	2019.2	2031.8	490	3840	3630.8	3350	3140.8	6.7
8.0	10338	15018.5	4680.5	2207.2	2038.1	2043.7	402	3128.3	2919.5	2726.3	2517.5	8.3
10.0	10337.9	14987.6	4649.7	2192.7	1975.8	1993.3	606.4	3289.4	3024.1	2683	2417.7	11.0
12.0	10337.8	15026.1	4688.3	2210.9	2000.9	1974.0	400.1	3759.6	3440.6	3359.5	3040.5	10.5
4.0	10368.2	14712.9	4344.7	2048.8	1954.1	1970.0	605.4	4148.6	4045	3543.2	3439.6	4.8
6.0	10368.1	14961	4592.9	2165.9	2087.7	2043.3	490.3	4660.8	4504	4170.5	4013.7	6.3
8.0	10367.5	15203	4835.5	2280.3	2107.5	2111.4	490.2	5093	4870	4602.8	4379.8	8.2
10.0	10368.7	15246	4877.3	2300.0	2098.7	2090.9	496.5	4855.5	4591.5	4339.0	4095	9.6
12.0	10369	15303.2	4934.2	2326.8	2101.4	2077.5	1039.3	5569.5	5286.5	4530.2	4247.2	10.7

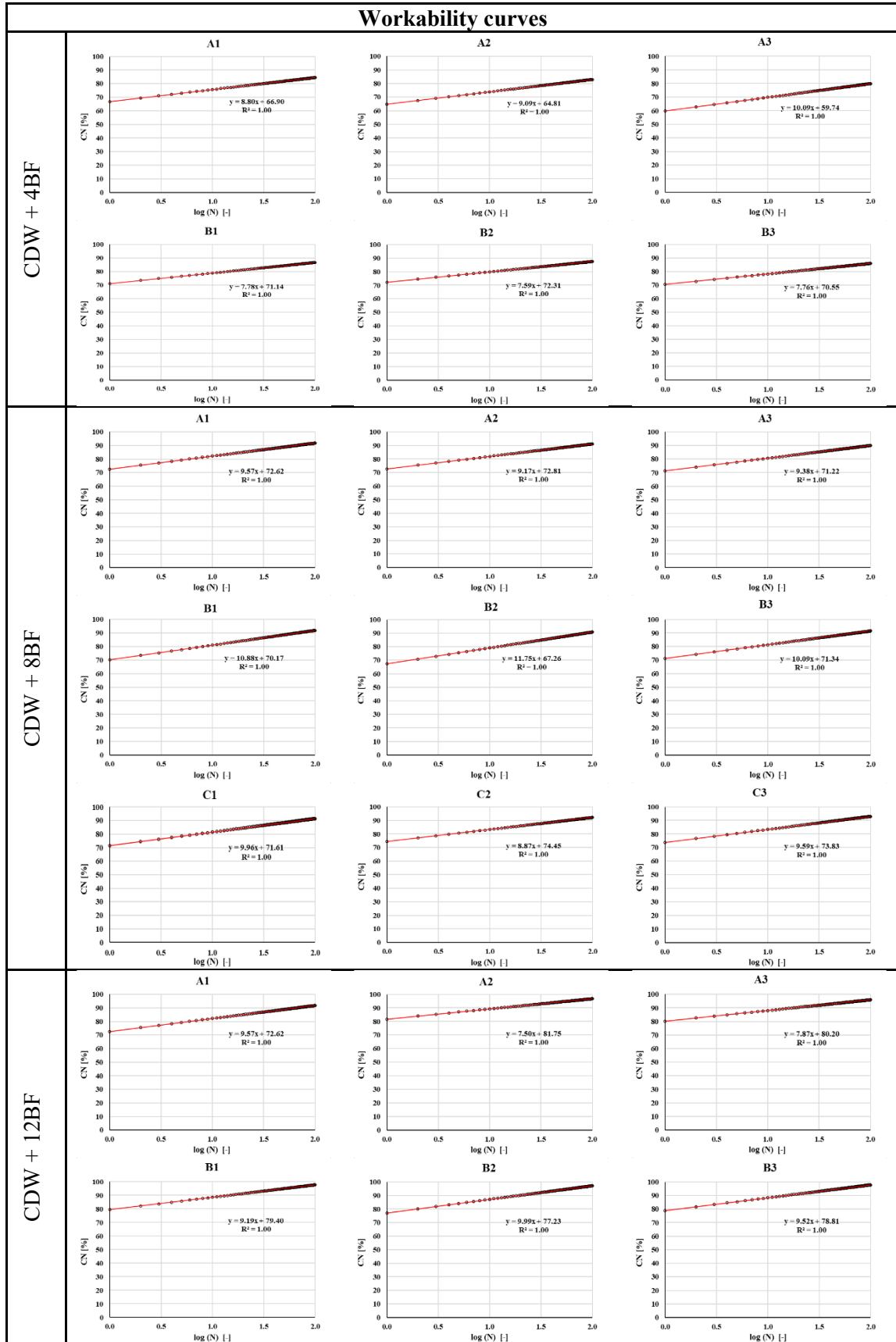
8.2. Gyratory shear compaction

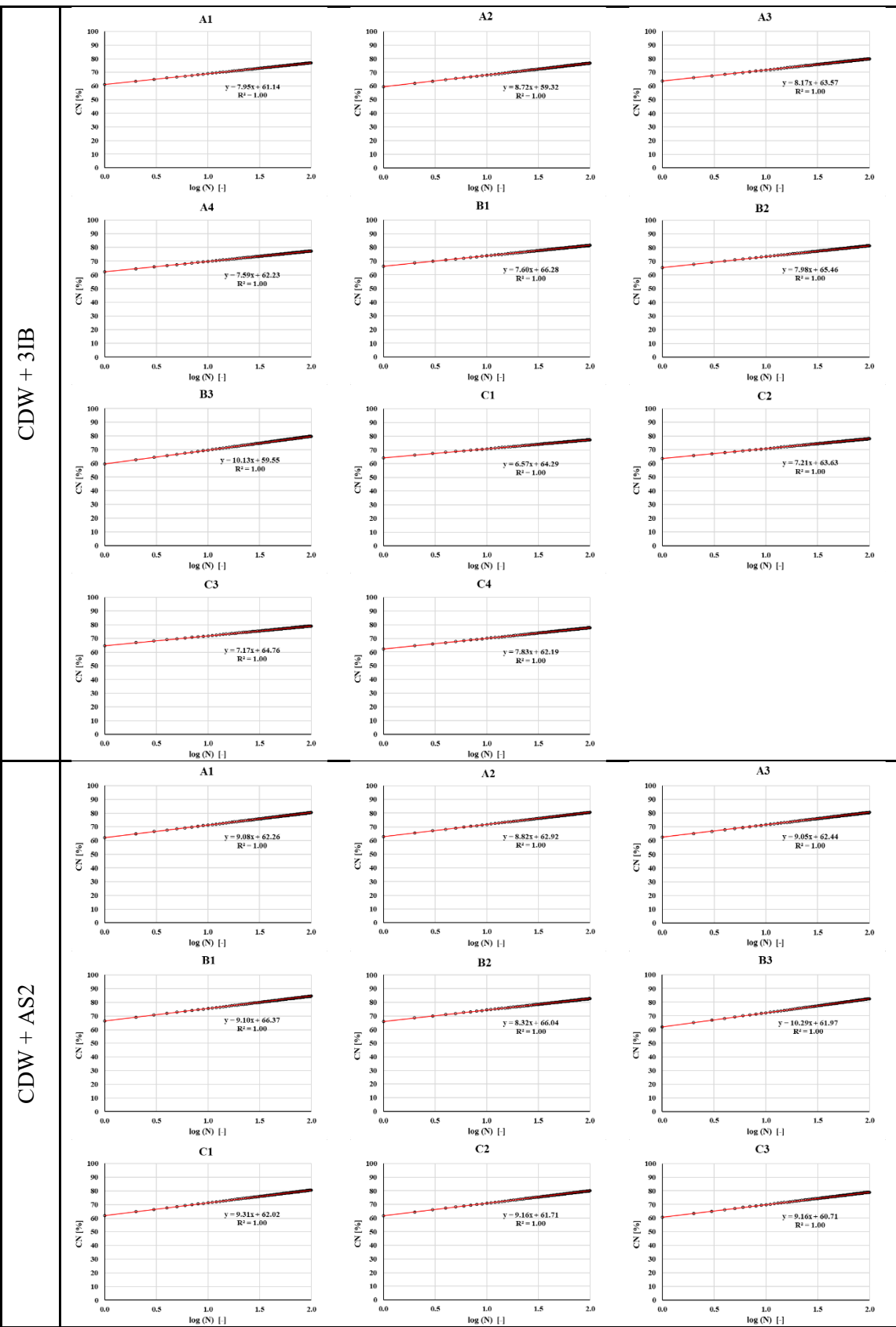
Sampling parameters

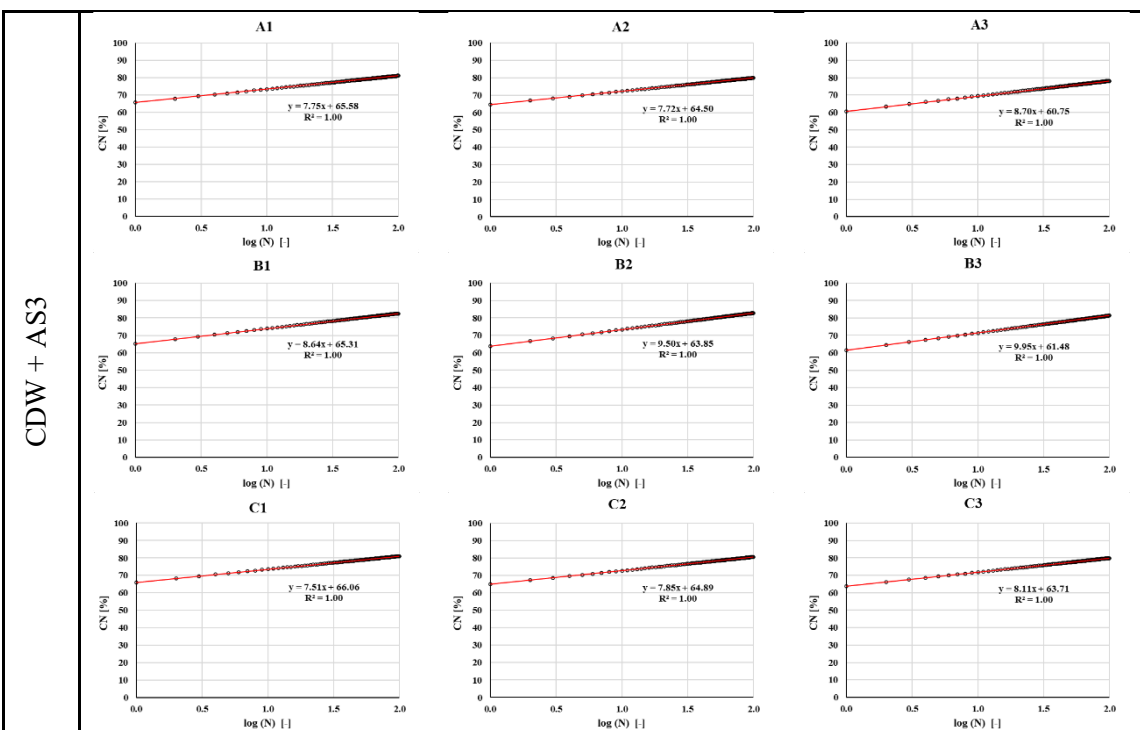
	MIXTURE	N°	Mould tare	Mould + compacted sample	Mould + cured sample	Final mass	Lost water
			[g]	[g]	[g]	[g]	[g]
CDW + 3IB	CDW_3IB_A1_7	1	738.2	4074.1	4073.9	3335.7	0.2
	CDW_3IB_C4_28	2	737.3	4057.3	4054.9	3317.6	2.4
	CDW_3IB_C1_28	3	734.6	4060.8	4057.8	3323.2	3
	CDW_3IB_C2_28	4	739.7	4033.3	4031.1	3291.4	2.2
	CDW_3IB_C3_28	5	739.2	4027.1	4023.2	3284	3.9
	CDW_3IB_A4_7	6	737.8	4012	4012	3274.2	0
	CDW_3IB_A2_7	7	739.2	4021.8	4021.5	3282.3	0.3
	CDW_3IB_A3_7	8	739.8	3999.2	3999	3259.2	0.2
	CDW_3IB_B1_7	9	735.1	2498	2498	1762.9	0
	CDW_3IB_B2_7	10	737.4	2516.4	2516.4	1779	0
	CDW_3IB_B3_7	11	741.5	2492	2491.7	1750.2	0.3
CDW + 4BF	CDW_4BF_A1_7	12	736.7	3962.9	3962.9	3226.2	0
	CDW_4BF_A2_7	13	739.2	3971.1	3971.1	3231.9	0
	CDW_4BF_A3_7	14	736.6	3947.6	3947.6	3211	0
	CDW_4BF_B1_7	15	738.7	2478.3	2478.2	1739.5	0.1
	CDW_4BF_B2_7	16	738.8	2477.3	2477.3	1738.5	0
	CDW_4BF_B3_7	17	738.8	2477.6	2477.6	1738.8	0
CDW + 8BF	CDW_8BF_A1_7	18	741	3975.1	3974.8	3233.8	0.3
	CDW_8BF_A2_7	19	743.1	3976.3	3976.2	3233.1	0.1
	CDW_8BF_A3_7	20	738.2	3971.5	3971.3	3233.1	0.2
	CDW_8BF_B1_7	21	736.7	2474.6	2474.5	1737.8	0.1
	CDW_8BF_B2_7	22	738.8	2474.7	2474.6	1735.8	0.1
	CDW_8BF_B3_7	23	736.4	2474.2	2474.1	1737.7	0.1
	CDW_8BF_C1_28	30	741.9	3974.7	3974.7	3232.8	0
	CDW_8BF_C2_28	31	736.1	3973.5	3973.5	3237.4	0
	CDW_8BF_C3_28	32	737.7	3977.5	3977.5	3239.8	0
CDW + 12BF	CDW_12BF_A1_7	24	738	3983.1	3982.9	3244.9	0.2
	CDW_12BF_A2_7	25	738.3	3986.8	3986.8	3248.5	0
	CDW_12BF_A3_7	26	739.2	3990.8	3990.7	3251.5	0.1
	CDW_12BF_B1_7	27	739.4	2483.4	2483.4	1744	0
	CDW_12BF_B2_7	28	736	2479	2479	1743	0
	CDW_12BF_B3_7	29	741.3	2485.8	2485.8	1744.5	0
CDW + AS2	CDW_AS2_A1_7	33	737.5	4081.9	4081.9	3344.4	0
	CDW_AS2_A2_7	34	735.5	4072	4072	3336.5	0
	CDW_AS2_A3_7	35	739.8	4084.8	4084.8	3345	0
	CDW_AS2_B1_7	36	739.5	2540.3	2540.3	1800.8	0
	CDW_AS2_B2_7	37	741.7	2548.9	2548.9	1807.2	0
	CDW_AS2_B3_7	38	737.9	2535.5	2535.5	1797.6	0
	CDW_AS2_B1_7 Bis	36	742.1	2549.6	2549.6	1807.5	0

	MIXTURE	N°	Mould tare	Mould + compacted sample	Mould + cured sample	Final mass	Lost water
			[g]	[g]	[g]	[g]	[g]
CDW + AS3	CDW_AS2_B2_7 Bis	37	735.7	2557	2557	1821.3	0
	CDW_AS2_C1_28	38	736.6	4089.1	4087.6	3351	1.5
	CDW_AS2_C2_28	39	735.6	4077.3	4076.3	3340.7	1
	CDW_AS2_C3_28	40	736.4	4093.1	4092.1	3355.7	1
	CDW_AS3_A1_7	41	736.1	4055.2	4055.2	3319.1	0
	CDW_AS3_A2_7	42	735.7	4061	4061	3325.3	0
	CDW_AS3_A3_7	43	741.9	4056.3	4056.3	3314.4	0
	CDW_AS3_B1_7	44	736.4	2520.6	2520.6	1784.2	0
	CDW_AS3_B2_7	45	738.5	2516.8	2516.8	1778.3	0
	CDW_AS3_B3_7	46	739.8	2516	2516	1776.2	0
	CDW_AS3_C1_28	47	738.4	4060.2	4060.2	3321.8	0
	CDW_AS3_C2_28	48	739.9	4060.2	4060.2	3320.3	0
	CDW_AS3_C3_28	49	741.1	4056.8	4056.8	3315.7	0

Workability curves







8.3. Cyclic triaxial test

RM CDW + 3IB 7 Days

RM CDW + 3IB 28 days

Specimen Sequence	Code	NAT	Confining Pressure	Cyclic Axial Stress	Maximum Axial Stress	Contact Stress	Recoverable Axial Strain	Permanent Axial Strain	Maximum Axial Load	Recoverable Axial Load	Permanent Axial Load	Octahedral stress at axial load	Octahedral stress at shear load	Octahedral stress at normal load	First invariant	Second invariant	Third invariant	RM (avg)	
		(MPa)	(kPa)	(kPa)	(%)	(%)	(kN)	(kN)	(mm)	(mm)	(kPa)	(kPa)	(kPa)	(kPa)	(kPa)	(kPa)	(kPa)	(kPa)	
s2_0	0	s2_0	416.3	103.4	93.1	103.4	0.022	0.031	0.731	0.812	0.081	206.8	103.4	137.9	48.7	413.6	534.54	2210801	
s2_1	1	s2_1	160.4	24.8	18.5	22.7	4.2	0.012	-0.013	0.146	0.178	0.033	0.0215	-0.0236	47.5	24.8	22.7	32.4	159.9
s2_2	2	s2_2	191.2	24.8	37.3	41.4	0.020	-0.013	0.293	0.324	0.032	0.0363	-0.0236	66.2	24.8	24.8	38.6	19.5	
s2_3	3	s2_3	233.4	24.8	55.9	62.1	6.2	0.024	-0.010	0.439	0.487	0.049	0.0445	-0.0184	86.9	24.8	24.8	62.1	191.4
s2_4	4	s2_4	220.1	41.4	31.0	37.0	6.0	0.014	-0.002	0.243	0.290	0.047	0.0362	-0.0028	78.4	41.4	41.4	59.5	23.5
s2_5	5	s2_5	278.0	41.4	62.0	68.9	6.9	0.022	0.000	0.487	0.541	0.054	0.0415	0.0005	110.3	41.4	37.0	53.7	134306
s2_6	6	s2_6	342.0	41.4	93.0	103.3	10.3	0.027	0.004	0.731	0.812	0.081	0.0506	0.0080	144.7	41.4	41.4	64.4	278.0
s2_7	7	s2_7	367.5	75.8	62.0	73.5	11.5	0.017	0.021	0.487	0.577	0.090	0.0314	0.0390	149.3	75.8	75.8	48.7	13698
s2_8	8	s2_8	442.4	75.8	124.0	137.8	13.8	0.028	0.027	0.974	1.083	0.108	0.0521	0.0495	213.6	75.8	137.8	121.7	348.0
s2_9	9	s2_9	489.2	75.8	185.9	206.7	20.8	0.038	0.048	1.461	1.624	0.163	0.0707	0.0884	282.5	75.8	206.7	144.7	485.79
s2_10	10	s2_10	36.3	113.7	61.9	71.4	9.5	0.017	0.064	0.486	0.561	0.075	0.0319	0.1195	185.1	113.7	113.7	71.4	97.5
s2_11	11	s2_11	40.8	113.7	93.1	103.4	10.3	0.023	0.006	0.731	0.812	0.081	0.0428	0.1223	217.1	113.7	113.7	103.4	2393433
s2_12	12	s2_12	52.8	113.7	186.0	206.7	20.7	0.035	0.080	1.461	1.624	0.163	0.0655	0.1482	320.4	113.7	113.7	206.7	404.6
s2_13	13	s2_13	417.6	137.9	93.1	103.4	10.3	0.022	0.097	0.731	0.812	0.081	0.0415	0.1799	241.3	113.7	113.7	97.4	528.1
s2_14	14	s2_14	474.2	137.9	124.0	137.8	13.8	0.026	0.100	0.974	1.082	0.108	0.0487	0.1854	275.7	137.9	137.9	103.4	587.89
s2_15	15	s2_15	589.7	137.9	248.0	275.7	27.7	0.042	0.129	1.948	2.165	0.217	0.0782	0.2398	413.6	137.9	137.9	129.8	417.3
s3_0	0	s3_0	341.0	103.4	93.0	103.4	10.3	0.027	0.040	0.731	0.812	0.081	0.0513	0.0754	206.8	103.4	103.4	48.7	365.2
s3_1	1	s3_1	94.1	24.8	18.6	22.7	4.1	0.020	-0.003	0.146	0.178	0.032	0.0372	-0.0049	47.5	24.8	24.8	22.7	442.3
s3_2	2	s3_2	131.4	24.8	37.4	41.3	3.9	0.028	-0.002	0.294	0.325	0.031	0.0353	-0.0037	66.1	24.8	24.8	41.3	489.1
s3_3	3	s3_3	179.9	24.8	55.8	62.0	6.2	0.031	0.003	0.438	0.487	0.049	0.0583	0.0060	86.8	24.8	24.8	55.5	361.8
s3_4	4	s3_4	148.1	41.4	30.7	37.0	6.2	0.021	0.010	0.241	0.290	0.049	0.0390	0.0190	78.4	41.4	37.0	33.7	412.5
s3_5	5	s3_5	213.5	41.4	61.8	68.8	7.1	0.029	0.013	0.485	0.541	0.056	0.0544	0.0237	110.2	41.4	41.4	68.8	533.85
s3_6	6	s3_6	296.8	41.4	93.0	103.2	10.3	0.031	0.021	0.333	0.486	0.057	0.0589	0.0358	144.6	41.4	41.4	41.4	180.1
s3_7	7	s3_7	29.8	75.8	61.9	73.4	11.5	0.021	0.033	0.486	0.577	0.091	0.0399	0.0625	149.2	75.8	75.8	73.4	136.4
s3_8	8	s3_8	390.2	75.8	123.9	137.8	13.8	0.032	0.040	0.973	1.082	0.108	0.0597	0.0760	213.6	75.8	137.8	121.7	492.0
s3_9	9	s3_9	471.2	75.8	185.9	206.6	20.7	0.039	0.066	1.460	1.623	0.163	0.0741	0.1241	282.4	75.8	206.6	144.7	334.40
s3_10	10	s3_10	275.6	113.7	62.1	71.5	9.4	0.023	0.069	0.488	0.562	0.074	0.0424	0.1299	185.2	113.7	113.7	71.5	148.3
s3_11	11	s3_11	329.9	113.7	92.9	103.2	10.3	0.028	0.071	0.730	0.811	0.081	0.0530	0.1331	216.9	113.7	113.7	103.2	291.4
s3_12	12	s3_12	502.7	113.7	186.0	206.7	20.7	0.037	0.086	1.461	1.624	0.163	0.0696	0.1608	320.4	113.7	206.7	182.6	502.8
s3_13	13	s3_13	342.0	137.9	92.8	103.1	10.3	0.027	0.086	0.729	0.810	0.081	0.0510	0.1620	241.0	137.9	137.9	103.1	414.2290
s3_14	14	s3_14	415.5	137.9	124.0	137.8	13.8	0.030	0.090	0.973	1.082	0.108	0.0561	0.1696	275.7	137.9	137.9	137.8	483.335
s3_15	15	s3_15	578.1	137.9	247.8	275.4	27.6	0.043	0.118	1.946	2.163	0.217	0.0806	0.2214	413.3	137.9	137.9	229.7	524.064
s3	15	s3	578.1	137.9	247.8	275.4	27.6	0.043	0.118	1.946	2.163	0.217	0.0806	0.2214	413.3	137.9	137.9	229.7	578.1

RM CDW + 4BF 7 Days

Specimen	Sequence	Code	NAT	Confining	Cyclic	Maximum	Contact	Recover	Permanent	Maxim	Contact	Octahedr	Octahedr	First	Second	Third	RM (avg)							
			Resilient Modulus	Pressure	Axial Stress	Axial Stress	Axial Strain	Axial Strain	Axial Load	Axial Load	Axial Load	at normal stress	at shear stress	stress invariant	stress invariant	stress invariant	(MPa)							
s1	0	s1.0	649.0	103.4	93.1	103.3	10.2	0.014	0.050	0.146	0.178	0.032	0.091	0.0301	47.5	24.8	48.7	413.5	534.41	2201.59	648.2			
s1	1	s1.1	381.1	24.8	18.6	22.7	4.1	0.005	0.016	0.293	0.325	0.032	0.077	0.0292	66.2	24.8	24.8	22.7	10.7	97.1	297.0	379.2		
s1	2	s1.2	391.9	24.8	37.3	41.4	4.1	0.010	0.016	0.293	0.325	0.032	0.077	0.0292	66.2	24.8	24.8	19.5	115.8	3897	40691	392.2		
s1	3	s1.3	414.4	24.8	55.8	62.0	6.2	0.013	0.017	0.438	0.487	0.049	0.125	0.0312	86.3	24.8	24.8	45.5	136.4	534.0	449.3	414.3		
s1	4	s1.4	470.2	41.4	31.0	37.0	6.0	0.007	0.023	0.243	0.290	0.047	0.122	0.0312	86.3	41.4	41.4	30.0	53.7	17.4	161.2	8204	13430	2201.59
s1	5	s1.5	483.7	61.0	62.0	68.8	6.9	0.013	0.024	0.486	0.541	0.054	0.238	0.0450	110.2	41.4	41.4	68.8	64.3	32.5	193.0	10842	188947	483.9
s1	6	s1.6	510.0	41.4	93.1	103.4	10.3	0.018	0.027	0.732	0.812	0.081	0.294	0.0495	144.8	41.4	41.4	103.4	75.9	48.7	127.0	2481.73	509.9	509.9
s1	7	s1.7	599.5	75.8	62.0	55.3	11.5	0.010	0.039	0.487	0.577	0.090	0.230	0.0493	149.3	75.8	75.8	73.5	100.3	34.6	300.9	2838.0	85784	599.6
s1	8	s1.8	614.7	75.8	123.9	137.8	14.0	0.020	0.044	0.973	1.083	0.110	0.375	0.0818	216.3	75.8	75.8	137.8	121.7	65.0	2227.49	614.4	614.4	614.4
s1	9	s1.9	606.9	75.8	185.8	206.5	20.7	0.031	0.064	1.459	1.622	0.163	0.570	0.0823	282.3	75.8	75.8	144.6	97.3	43.3	4853.9	162187.9	503.9	503.9
s1	10	s1.10	620.1	113.7	62.1	75.5	9.4	0.010	0.075	0.487	0.561	0.074	0.186	0.1386	185.2	113.7	113.7	71.5	137.5	33.7	412.6	53038	239950	620.6
s1	11	s1.11	640.8	93.1	103.3	10.2	0.028	0.076	0.731	0.812	0.080	0.240	0.1413	201.0	113.7	113.7	103.3	148.1	48.7	444.4	280826	641.2	641.2	
s1	12	s1.12	675.3	113.7	206.5	208.8	0.091	0.459	1.622	1.653	0.0512	0.1692	0.202	113.7	113.7	113.7	102.5	182.5	97.4	57.6	85746	433970	675.3	
s1	13	s1.13	672.2	137.9	93.2	103.4	10.2	0.014	0.097	0.732	0.812	0.080	0.258	0.1803	241.3	137.9	137.9	103.4	172.4	51.7	85556	488789	671.5	671.5
s1	14	s1.14	701.3	137.9	248.3	275.8	27.6	0.015	0.132	1.950	2.167	0.109	0.324	0.1846	257.5	137.9	137.9	137.9	183.8	65.0	51.5	95060	534205	701.3
s1	15	s1.15	714.2	137.9	248.3	275.8	27.6	0.015	0.132	1.950	2.167	0.109	0.324	0.1846	257.5	137.9	137.9	229.8	130.0	68.9	69.5	131260	7637849	701.3
s2	0	s2.0	497.6	103.4	93.0	103.3	10.3	0.019	0.081	0.731	0.812	0.081	0.349	0.1521	206.7	103.4	103.4	103.3	137.8	48.7	413.5	53445	2301373	497.5
s2	1	s2.1	265.4	24.8	18.6	22.7	4.1	0.007	0.043	0.146	0.178	0.032	0.091	0.0301	47.5	24.8	24.8	22.7	10.7	97.1	296.9	265.2	265.2	
s2	2	s2.2	283.7	24.8	41.4	41.4	0.013	0.044	0.293	0.325	0.032	0.091	0.0246	66.2	24.8	24.8	41.4	38.6	19.5	115.8	3897	40691	284.0	
s2	3	s2.3	313.8	24.8	55.9	62.1	6.2	0.018	0.049	0.439	0.487	0.049	0.175	0.0308	86.3	24.8	24.8	62.1	45.5	29.3	136.5	33422	313.5	313.5
s2	4	s2.4	331.2	41.4	31.0	37.0	6.0	0.009	0.056	0.243	0.290	0.047	0.175	0.0315	78.4	41.4	41.4	37.0	53.7	17.4	102.1	8204	13430	331.0
s2	5	s2.5	365.3	41.4	62.0	68.8	6.9	0.017	0.058	0.487	0.541	0.054	0.231	0.0317	110.2	41.4	41.4	68.8	64.3	32.5	193.0	10842	188947	365.6
s2	6	s2.6	405.6	41.4	93.0	103.3	10.3	0.023	0.061	0.731	0.812	0.081	0.240	0.1447	447.1	41.4	41.4	103.3	147.4	38.7	136.98	248707	405.6	405.6
s2	7	s2.7	480.0	75.8	62.0	75.5	11.5	0.013	0.076	0.487	0.571	0.059	0.241	0.1430	149.3	75.8	75.8	100.3	136.5	34.6	300.9	280826	857824	479.9
s2	8	s2.8	519.6	75.8	124.0	137.8	13.8	0.024	0.083	0.974	1.083	0.108	0.446	0.1559	213.6	75.8	75.8	137.8	121.7	65.0	345.2	381.13	1222499	519.9
s2	9	s2.9	527.8	75.8	186.0	206.8	20.7	0.035	0.115	1.461	1.624	0.163	0.659	0.2156	75.8	206.8	206.8	19.5	97.5	485.82	162284	528.0		
s2	10	s2.10	507.2	11.37	62.0	71.4	9.5	0.012	0.025	0.487	0.561	0.075	0.229	0.2345	185.1	113.7	113.7	113.7	33.7	412.5	2934343	528.0	528.0	
s2	11	s2.11	540.7	11.37	93.0	103.3	10.3	0.017	0.027	0.730	0.812	0.081	0.321	0.2379	210.0	113.7	113.7	103.3	148.1	48.7	444.4	622.83	280826	540.9
s2	12	s2.12	527.7	11.37	186.0	206.8	20.7	0.031	0.147	1.461	1.623	0.162	0.658	0.2251	320.4	113.7	113.7	113.7	182.6	97.4	54.78	48572	141773	507.8
s2	13	s2.13	563.1	13.79	93.1	103.4	10.3	0.017	0.025	0.731	0.812	0.081	0.309	0.2841	241.3	137.9	137.9	103.4	172.4	48.7	51.7	85561	4388279	562.8
s2	14	s2.14	605.6	13.79	124.0	137.8	13.8	0.020	0.055	0.974	1.082	0.108	0.446	0.2896	213.7	137.9	137.9	137.8	183.8	65.0	51.5	90549	244444	605.4
s2	15	s2.15	647.6	13.79	248.0	275.6	27.6	0.038	0.198	1.948	2.164	0.217	0.716	0.3699	413.5	137.9	137.9	137.9	19.9	689.3	133054	7526905	647.5	

RM CDW + 8BF 7 Days

RM CDW + 8BF 28 Days

Specimen Sequence	Code	NAT	Confining Pressure	Cyclic Axial Stress	Maximum Axial Stress	Contact Axial Stress	Recoverable Axial Strain	Permanent Axial Strain	Cyclic Axial Load	Maximum Axial Load	Contact Axial Load	Recoverable Axial Load	Permanent Axial Load	Octahedral Shear Stress at 63°	Octahedral Shear Stress at 33°	Octahedral Shear Stress at 15°	First stress invariant	Second stress invariant	Third stress invariant			
		(MPa)	(kPa)	(kPa)	(%)	(%)	(kN)	(kN)	(mm)	(mm)	(kPa)	(kPa)	(kPa)	(kPa)	(kPa)	(kPa)	(kPa)	(kPa)	(kPa)			
s1	0	s1_0	438.3	103.4	92.9	103.3	0.021	0.048	0.812	0.082	0.0394	0.0394	47.5	103.4	103.3	137.8	413.5	5345	2210373			
s1	1	s1_1	154.1	24.8	19.0	22.7	3.8	0.021	0.149	0.178	0.0238	0.0394	24.8	22.7	32.4	107	97.1	29214	154.5			
s1	2	s1_2	205.6	24.8	37.4	41.4	4.0	0.018	0.021	0.293	0.325	0.031	0.0338	0.0399	66.2	24.8	41.4	38.6	195.5	115.8	3899	40716
s1	3	s1_3	273.1	24.8	55.9	62.1	6.2	0.020	0.024	0.439	0.488	0.049	0.0381	0.0451	86.9	24.8	62.1	45.5	29.3	53447	273.0	
s1	4	s1_4	218.9	41.4	31.0	37.0	6.0	0.014	0.028	0.243	0.290	0.047	0.0263	0.0451	78.4	41.4	41.4	17.4	161.2	8024	134340	
s1	5	s1_5	303.1	41.4	61.7	68.8	7.1	0.020	0.030	0.485	0.541	0.056	0.0379	0.0554	110.2	41.4	41.4	64.3	32.4	193.0	10840	188913
s1	6	s1_6	407.8	41.4	93.1	103.5	10.4	0.023	0.034	0.731	0.813	0.082	0.0425	0.0630	144.9	41.4	41.4	75.9	48.8	227.7	13712	248353
s1	7	s1_7	387.4	75.8	62.0	73.4	11.4	0.016	0.043	0.487	0.577	0.089	0.0298	0.0796	149.2	75.8	73.4	100.3	34.6	300.8	283.67	857364
s1	8	s1_8	518.1	75.8	124.3	138.0	13.7	0.024	0.048	0.977	1.084	0.108	0.0446	0.0896	213.8	75.8	75.8	121.8	65.1	345.4	38158	1228418
s1	9	s1_9	634.2	75.8	186.1	206.6	20.5	0.029	0.066	1.462	1.623	0.161	0.0546	0.1225	282.4	75.8	206.6	144.7	97.4	434.0	1622684	634.9
s1	10	s1_10	371.4	113.7	62.1	71.5	9.4	0.017	0.066	0.488	0.561	0.074	0.0311	0.1231	185.2	113.7	71.5	137.5	33.7	412.6	50538	2392950
s1	11	s1_11	441.7	113.7	93.1	103.4	10.2	0.021	0.068	0.731	0.812	0.080	0.0392	0.1258	217.1	113.7	103.4	148.2	48.7	444.5	62287	2806084
s1	12	s1_12	662.5	113.7	186.3	206.9	20.6	0.028	0.080	1.463	1.625	0.161	0.0523	0.1485	320.6	113.7	206.9	182.7	97.5	548.0	85823	4144100
s1	13	s1_13	445.0	137.9	92.8	103.4	10.5	0.021	0.078	0.729	0.812	0.083	0.0388	0.1459	241.3	137.9	103.4	172.4	48.7	517.1	85556	444.7
s1	14	s1_14	539.5	137.9	123.9	137.9	14.0	0.023	0.082	0.973	1.083	0.110	0.0427	0.1519	275.8	137.9	137.9	183.9	65.0	551.6	95088	5245106
s1	15	s1_15	761.5	137.9	247.9	275.6	27.7	0.033	1.947	2.164	2.18	0.0605	0.1912	413.5	137.9	275.6	229.8	129.9	689.3	133054	760.8	
s3	0	s3_0	537.3	103.4	93.0	103.3	10.3	0.017	0.029	0.730	0.812	0.081	0.0322	0.0541	206.7	103.4	103.3	137.8	48.7	413.5	53441	2210159
s3	1	s3_1	236.2	24.8	18.7	22.7	4.0	0.008	0.000	0.147	0.178	0.031	0.0147	0.0601	47.5	24.8	22.7	32.4	107	97.1	29214	236.1
s3	2	s3_2	283.7	24.8	37.3	41.4	4.1	0.013	0.029	0.325	0.352	0.032	0.0245	0.0601	66.2	24.8	24.8	38.6	41.4	40716	154.3	
s3	3	s3_3	361.3	24.8	55.9	62.1	6.2	0.015	0.002	0.439	0.487	0.049	0.0288	0.0644	86.9	24.8	62.1	45.5	29.3	53435	361.0	
s3	4	s3_4	334.1	41.4	31.0	37.0	6.0	0.009	0.007	0.243	0.290	0.047	0.0173	0.0332	129.0	41.4	41.4	37.0	53.7	134306	333.6	
s3	5	s3_5	404.6	41.4	62.0	68.9	6.9	0.015	0.008	0.487	0.541	0.054	0.0285	0.0352	110.3	41.4	41.4	68.9	64.4	32.5	193.1	10843
s3	6	s3_6	494.1	41.4	93.0	103.3	10.3	0.019	0.011	0.731	0.812	0.081	0.0350	0.0205	144.7	41.4	103.3	75.8	48.7	227.5	13698	248079
s3	7	s3_7	491.4	75.8	62.0	73.4	11.5	0.013	0.022	0.487	0.577	0.090	0.0235	0.0400	149.2	75.8	73.4	100.3	34.6	300.8	23367	491.4
s3	8	s3_8	598.2	75.8	123.9	137.7	13.8	0.021	0.026	0.973	1.082	0.108	0.0386	0.0492	213.5	75.8	137.7	121.7	64.9	365.2	38130	122571
s3	9	s3_9	688.2	75.8	185.9	206.7	20.8	0.027	0.042	1.460	1.623	0.163	0.0502	0.0774	282.5	75.8	206.7	144.7	97.4	533.6	598.6	
s3	10	s3_10	485.4	113.7	61.9	71.4	9.5	0.013	0.048	0.486	0.561	0.075	0.0237	0.0884	185.1	71.4	71.4	412.5	33.7	2393174	485.0	
s3	11	s3_11	534.7	113.7	93.1	103.4	10.3	0.017	0.049	0.731	0.812	0.081	0.0324	0.0693	217.1	113.7	103.4	148.2	48.8	444.5	623.0	2806860
s3	12	s3_12	706.5	113.7	186.0	206.7	20.7	0.026	0.058	1.461	1.623	0.162	0.0490	0.1079	320.4	113.7	206.7	182.6	97.4	547.8	85787	4142032
s3	13	s3_13	531.5	137.9	137.9	140.4	10.4	0.018	0.064	0.812	0.882	0.109	0.0325	0.1182	241.3	137.9	103.4	172.4	48.7	517.1	488279	531.3
s3	14	s3_14	606.2	137.9	124.0	137.9	13.9	0.020	0.066	0.974	1.083	0.109	0.0380	0.1227	275.8	137.9	137.9	183.9	65.0	551.6	95077	5244346
s3	15	s3_15	781.1	137.9	248.1	275.7	27.5	0.032	0.085	1.949	2.166	0.217	0.0591	0.1573	413.6	137.9	275.7	229.8	130.0	689.4	133098	7865948

RM CDW + 12BF 7 Days

RM CDW + AS2 7 Days

Specimen Sequence	Code	NAT	Confining	Maximum Contact	Recoverable	Permanent	Cyclic	Maximum Contact	Recoverable	Permanent	Cyclic	Maximum Contact	Recoverable	Permanent	Octahedral	Octahedral	First stress	Second stress	Third stress	RM (avg)
		Resilient Modulus (MPa)	Pressure (kPa)	Axial Stress (kPa)	Axial Strain (%)	Axial Load (kN)	Axial Deformation (mm)	Axial Deformation (mm)	Axial Deformation (mm)	at shear load	at shear load	(MPa)								
s1_0	0	s1_0	713.9	103.4	92.7	103.3	10.6	0.013	0.066	0.738	0.311	0.083	0.0244	0.1235	206.7	103.4	137.8	48.7	413.5	714.5
s1_1	1	s1_1	233.0	24.8	18.5	22.7	4.2	0.008	0.005	0.145	0.178	0.033	0.0238	0.0238	24.8	22.7	32.4	19.5	97.1	232.1
s1_2	2	s1_2	293.4	24.8	37.2	41.4	4.2	0.013	0.005	0.292	0.325	0.033	0.0238	0.0238	24.8	24.8	41.4	38.6	115.8	293.1
s1_3	3	s1_3	375.9	24.8	55.9	62.0	6.2	0.015	0.008	0.439	0.487	0.048	0.0279	0.0279	24.8	24.8	62.0	45.5	29.2	375.3
s1_4	4	s1_4	416.7	41.4	30.8	36.9	6.1	0.009	0.018	0.242	0.290	0.048	0.0167	0.0167	78.3	41.4	41.4	17.4	161.1	416.2
s1_5	5	s1_5	431.2	41.4	61.8	68.8	6.9	0.014	0.021	0.486	0.540	0.054	0.0270	0.0270	110.2	41.4	41.4	68.8	64.3	1083.5
s1_6	6	s1_6	498.5	41.4	92.6	103.0	10.4	0.019	0.026	0.728	0.809	0.081	0.0349	0.0349	144.4	41.4	41.4	57.7	227.2	498.5
s1_7	7	s1_7	663.0	75.8	62.6	74.1	11.5	0.009	0.051	0.492	0.582	0.090	0.0178	0.0178	149.9	75.8	75.8	74.1	100.5	663.6
s1_8	8	s1_8	672.4	75.8	124.3	138.1	13.8	0.019	0.057	0.977	1.085	0.108	0.0348	0.0348	213.9	75.8	138.4	121.8	65.1	365.5
s1_9	9	s1_9	713.3	75.8	186.2	206.9	20.8	0.026	0.071	1.462	1.625	0.163	0.0491	0.0491	282.7	75.8	206.9	144.8	97.5	434.3
s1_10	10	s1_10	808.9	113.7	61.9	71.5	9.5	0.008	0.094	0.497	0.562	0.075	0.0144	0.0144	185.2	75.8	137.5	137.5	412.6	808.7
s1_11	11	s1_11	804.8	113.7	93.0	103.3	10.3	0.012	0.096	0.731	0.812	0.081	0.0217	0.0217	217.0	113.7	113.7	148.1	48.7	444.4
s1_12	12	s1_12	822.3	113.7	185.8	206.7	20.8	0.023	0.109	1.460	1.624	0.164	0.0425	0.0425	320.4	113.7	206.7	182.6	97.4	547.8
s1_13	13	s1_13	862.5	137.9	93.0	103.3	10.3	0.011	0.128	0.730	0.811	0.081	0.0203	0.0203	241.2	137.9	137.9	172.3	517.0	862.5
s1_14	14	s1_14	874.9	137.9	124.0	137.8	13.8	0.014	0.132	0.974	1.082	0.109	0.0267	0.0267	247.3	215.7	137.9	137.9	183.8	551.5
s1_15	15	s1_15	884.1	137.9	248.0	275.6	27.6	0.028	0.152	2.165	2.198	0.217	0.0527	0.0527	284.8	275.6	29.8	129.9	689.3	1330.65
s3_0	0	s3_0	676.5	103.4	93.0	103.4	10.3	0.014	0.008	0.730	0.811	0.081	0.0259	0.0259	206.8	103.4	103.4	137.9	48.7	534.0
s3_1	1	s3_1	422.8	24.8	18.6	22.7	4.1	0.004	-0.036	0.146	0.178	0.032	0.0081	-0.0489	47.5	24.8	24.8	22.7	10.7	97.1
s3_2	2	s3_2	473.5	24.8	37.3	41.4	4.1	0.008	-0.025	0.293	0.325	0.032	0.0148	-0.0463	66.2	24.8	24.8	41.4	38.6	474.3
s3_3	3	s3_3	508.5	24.8	55.8	62.1	6.3	0.011	-0.023	0.438	0.487	0.049	0.0206	-0.0427	86.9	24.8	24.8	62.1	45.5	534.22
s3_4	4	s3_4	503.2	41.4	30.8	36.9	6.2	0.005	-0.014	0.242	0.290	0.048	0.0098	-0.0271	78.3	41.4	36.9	53.7	161.1	591.5
s3_5	5	s3_5	595.5	41.4	61.7	68.9	7.1	0.010	-0.013	0.485	0.541	0.056	0.0195	-0.0240	110.3	41.4	68.9	64.4	32.5	193.1
s3_6	6	s3_6	619.3	41.4	92.5	103.3	10.8	0.015	-0.010	0.727	0.812	0.085	0.0281	-0.0186	144.7	41.4	41.4	103.3	75.8	48.7
s3_7	7	s3_7	714.3	75.8	62.1	73.6	11.5	0.009	0.006	0.488	0.578	0.090	0.0163	0.0163	149.4	75.8	75.8	100.3	34.7	301.0
s3_8	8	s3_8	711.8	75.8	123.9	137.8	14.0	0.017	0.011	0.973	1.082	0.109	0.0327	0.0205	213.6	75.8	137.8	121.7	38.6	2839.2
s3_9	9	s3_9	727.7	75.8	185.9	206.6	20.7	0.026	0.022	1.460	1.622	0.163	0.0480	0.0480	282.4	75.8	206.6	144.7	97.4	485.54
s3_10	10	s3_10	740.3	113.7	62.0	71.4	9.4	0.008	0.033	0.487	0.561	0.074	0.0157	0.0613	185.1	113.7	113.7	71.4	137.5	530.19
s3_11	11	s3_11	752.5	113.7	93.2	103.3	10.1	0.012	0.035	0.732	0.812	0.079	0.0233	0.0050	217.0	113.7	113.7	148.1	48.7	444.4
s3_12	12	s3_12	783.2	113.7	185.9	206.6	20.7	0.024	0.044	1.460	1.623	0.163	0.0446	0.0446	230.3	113.7	206.6	182.6	97.4	547.7
s3_13	13	s3_13	772.3	137.9	93.0	103.3	10.3	0.012	0.054	0.730	0.811	0.081	0.0226	0.0226	241.2	103.3	137.9	172.3	517.0	855.59
s3_14	14	s3_14	795.2	137.9	124.0	137.9	13.8	0.016	0.057	0.974	1.083	0.109	0.0293	0.0293	275.8	137.9	137.9	137.9	183.9	772.3
s3_15	15	s3_15	822.5	137.9	248.1	275.7	27.5	0.030	0.072	1.949	2.165	0.216	0.0567	0.1345	413.6	137.9	275.7	29.8	129.9	844.5

RM CDW + AS2 28 Days

Specimen Sequence	Code	NAT	Confining Pressure	Cyclic Axial Stress	Maximum Axial Stress	Contact Axial Stress	Recoverable Axial Strain	Permanent Axial Strain	Cyclic Axial Load	Maximum Axial Load	Contact Axial Load	Deformation	Deformation	Recoverable Axial Strain	Permanent Axial Strain	Octahedral stress	Second stress invariant	Third stress invariant	First stress invariant	Octahedral stress at normal axial load	Second stress at normal axial load	Third stress at normal axial load	RM (avg.)		
		(MPa)	(kPa)	(kPa)	(kPa)	(%)	(%)	(kN)	(kN)	(kN)	(kN)	(mm)	(mm)	(kPa)	(kPa)	(kPa)	(kPa)	(kPa)	(kPa)	(kPa)	(kPa)				
s1_0	0	s1_0	607.3	103.4	93.1	103.3	10.3	0.015	0.076	0.731	0.811	0.081	0.0288	0.1434	206.7	103.4	103.3	137.8	48.7	413.5	53.441	22101.59	608.2		
s1_1	1	s1_1	255.8	24.8	37.3	41.4	0.007	0.040	0.146	0.178	0.0759	0.032	0.0242	0.0754	47.5	24.8	24.8	32.4	97.1	97.1	38.6	115.8	29202	255.2	
s1_2	2	s1_2	289.5	24.8	37.3	41.4	0.013	0.040	0.293	0.325	0.032	0.032	0.0326	0.0759	66.2	24.8	24.8	41.4	38.6	19.5	38.6	38.99	40716	289.6	
s1_3	3	s1_3	322.2	24.8	55.9	62.0	0.017	0.041	0.439	0.487	0.049	0.049	0.047	0.0947	110.3	41.4	41.4	45.5	29.2	136.4	49.22	53410	322.7		
s1_4	4	s1_4	370.9	41.4	31.0	37.0	0.008	0.020	0.243	0.290	0.047	0.047	0.057	0.0947	37.0	41.4	41.4	37.0	53.7	17.4	161.2	134340	371.5		
s1_5	5	s1_5	408.9	41.4	62.0	68.9	0.015	0.052	0.487	0.541	0.054	0.054	0.0285	0.0970	110.3	41.4	41.4	68.9	64.4	32.5	193.1	10843	188981	408.7	
s1_6	6	s1_6	452.3	41.4	92.8	103.2	0.021	0.054	0.729	0.810	0.081	0.081	0.0386	0.1023	144.6	41.4	41.4	103.2	75.8	48.6	227.4	13687	247839	452.4	
s1_7	7	s1_7	537.9	75.8	62.0	73.5	0.012	0.070	0.487	0.577	0.090	0.090	0.0217	0.1309	149.3	75.8	75.8	100.3	34.6	300.9	283.73	857594	537.4		
s1_8	8	s1_8	599.1	75.8	124.1	137.8	0.021	0.076	0.975	1.083	0.108	0.089	0.0359	0.1419	213.6	75.8	75.8	121.7	65.0	365.2	38.133	1227499	599.4		
s1_9	9	s1_9	635.6	75.8	185.8	206.6	0.029	0.090	1.459	1.623	0.164	0.0549	0.1685	282.4	75.8	75.8	206.6	144.7	97.4	434.0	485.54	16224.54	635.2		
s1_10	10	s1_10	585.8	113.7	61.9	71.5	0.011	0.099	0.486	0.562	0.075	0.0199	0.1864	185.2	71.5	71.5	113.7	137.5	33.7	412.6	550.53	2393691	584.2		
s1_11	11	s1_11	632.0	113.7	93.0	103.3	0.015	0.010	0.730	0.811	0.0277	0.0277	0.1892	0.217.0	113.7	138.1	138.1	113.7	103.3	148.1	48.7	444.4	62273	2805309	631.8
s1_12	12	s1_12	716.4	113.7	185.8	206.7	0.026	0.09	1.459	1.623	0.164	0.0487	0.2050	320.4	113.7	113.7	206.5	182.6	97.4	547.8	557.82	41417.73	716.7		
s1_13	13	s1_13	664.2	137.9	103.3	103.3	0.014	0.114	0.731	0.812	0.081	0.0263	0.2134	241.2	173.9	173.9	137.9	137.9	172.3	172.3	855.59	45867.58	665.2		
s1_14	14	s1_14	714.7	137.9	124.0	137.8	0.017	0.116	0.973	1.082	0.109	0.0326	0.2178	275.7	137.9	137.9	137.9	137.9	183.8	65.0	551.5	95054	5242824	715.1	
s1_15	15	s1_15	800.2	137.9	247.8	275.5	0.031	0.131	1.946	2.164	0.217	0.0582	0.2470	413.4	137.9	137.9	275.5	229.7	129.9	689.2	133038	7861764	800.0		
s2_0	0	s2_0	547.9	103.4	92.9	103.3	10.3	0.017	0.029	0.730	0.811	0.082	0.0320	0.0556	206.7	103.4	103.3	137.8	48.7	53.441	22101.59	448.5	448.5		
s2_1	1	s2_1	204.2	24.8	186.2	22.7	4.1	0.009	0.006	0.146	0.178	0.032	0.0172	0.0109	47.5	24.8	24.8	22.7	32.4	10.7	97.1	29227	203.7	203.7	
s2_2	2	s2_2	258.5	24.8	37.3	41.4	0.014	0.014	0.293	0.325	0.032	0.0273	0.0108	66.2	24.8	24.8	41.4	41.4	19.5	38.6	115.8	3897	40691	258.1	
s2_3	3	s2_3	344.3	24.8	55.9	62.1	0.016	0.008	0.439	0.487	0.049	0.049	0.0307	0.0157	86.9	24.8	24.8	62.1	45.5	29.3	136.5	4924	53435	344.6	
s2_4	4	s2_4	287.9	41.4	31.0	36.9	6.0	0.011	0.013	0.243	0.290	0.047	0.0203	0.0238	78.3	41.4	41.4	36.9	53.7	17.4	161.1	81.99	134237	288.0	
s2_5	5	s2_5	391.7	41.4	62.0	68.9	6.9	0.016	0.014	0.487	0.541	0.054	0.0299	0.0270	110.3	41.4	41.4	68.9	64.4	32.5	193.1	108450	189050	391.4	
s2_6	6	s2_6	505.7	41.4	92.9	103.3	10.4	0.018	0.018	0.730	0.811	0.081	0.0347	0.0345	144.7	41.4	41.4	103.3	75.8	48.7	227.5	13695	248010	506.0	
s2_7	7	s2_7	494.5	75.8	62.0	73.5	11.5	0.013	0.027	0.487	0.577	0.091	0.0237	0.0507	149.3	75.8	75.8	100.3	34.6	300.9	283.76	857709	494.3		
s2_8	8	s2_8	618.3	75.8	124.0	137.8	13.9	0.020	0.031	0.974	1.083	0.109	0.0379	0.0583	213.6	75.8	75.8	137.8	137.8	121.7	65.0	38.13	1227499	618.7	
s2_9	9	s2_9	717.6	75.8	186.0	206.6	0.026	0.040	1.460	1.623	0.162	0.0490	0.0755	282.4	75.8	75.8	206.6	144.7	97.4	434.0	48857	1622569	718.0		
s2_10	10	s2_10	483.4	113.7	61.9	71.5	9.5	0.013	0.042	0.486	0.561	0.075	0.0242	0.0801	185.2	113.7	113.7	71.5	137.5	33.7	412.6	55042	2394208	483.5	
s2_11	11	s2_11	551.8	113.7	144.4	137.9	186.0	20.7	0.025	0.052	1.461	1.624	0.163	0.0472	0.0983	320.4	113.7	113.7	206.7	182.6	97.4	444.5	62292	2806343	552.6
s2_12	12	s2_12	560.8	137.9	103.3	103.3	0.017	0.052	0.730	0.812	0.081	0.0313	0.0981	241.2	173.9	173.9	103.3	172.3	48.7	517.0	555.39	4586758	560.2		
s2_13	13	s2_13	645.5	137.9	124.0	137.8	13.8	0.019	0.055	0.974	1.082	0.109	0.0363	0.1044	275.7	137.9	137.9	137.9	137.9	183.8	65.0	551.5	95060	5243305	646.4
s2_14	14	s2_14	820.2	137.9	248.0	275.7	27.8	0.030	0.067	1.948	2.166	0.218	0.0572	0.1269	413.6	137.9	137.9	275.7	229.8	130.0	689.4	133087	7865187	819.9	

RM CDW + AS3 7 Days

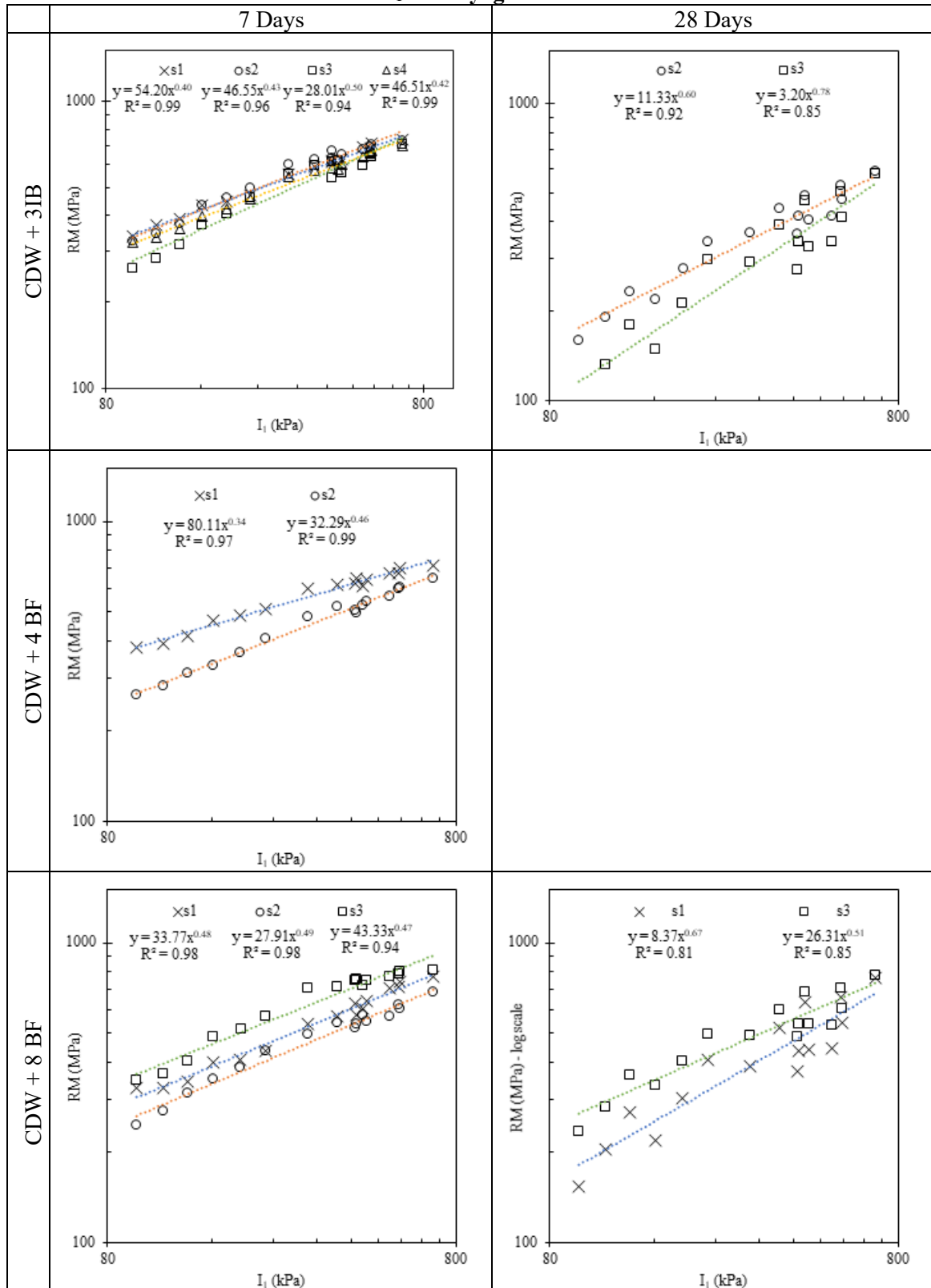
Specimen Sequence	Code	NAT	Confining Pressure	Cyclic Axial Stress	Maximum Axial Stress	Contact Axial Stress	Recoverable Axial Strain	Permanent Axial Strain	Cyclic Axial Load	Maximum Axial Load	Contact Axial Load	Recoverable Axial Load	Permanent Axial Load	Octahedral stress at normal stress	Octahedral stress at shear stress	Octahedral stress at invariant stress	First stress invariant	Second stress invariant	Third stress invariant	RM (avg.)					
		(MPa)	(kPa)	(kPa)	(kN)	(%)	(%)	(%)	(kN)	(mm)	(mm)	(mm)	(kPa)	(kPa)	(kPa)	(kPa)	(kPa)	(kPa)	(MPa)						
s2_0	0	s2_0	462.3	103.4	93.0	103.3	10.3	0.019	0.085	0.731	0.812	0.081	0.0364	0.1613	206.7	103.4	103.3	137.8	48.7	413.5	533441	2210159	482.0		
s2_1	1	s2_1	248.2	185.8	22.6	24.8	22.7	4.2	0.007	0.050	0.145	0.178	0.032	0.0252	0.0957	47.4	24.8	22.6	32.3	97.0	2968	115.8	3938	29177	247.9
s2_2	2	s2_2	280.0	24.8	37.3	41.4	4.1	0.013	0.051	0.293	0.325	0.032	0.0252	0.0957	66.2	24.8	24.8	41.4	38.6	19.5	115.8	3938	40703	279.9	
s2_3	3	s2_3	345.3	24.8	55.9	62.1	6.2	0.016	0.054	0.439	0.488	0.048	0.0306	0.1026	86.9	24.8	24.8	62.1	45.5	29.3	136.5	4924	53435	345.1	
s2_4	4	s2_4	340.5	41.4	31.0	37.0	6.0	0.009	0.063	0.243	0.290	0.047	0.0172	0.1194	78.4	41.4	41.4	68.9	64.4	32.5	193.1	104.3	134340	341.2	
s2_5	5	s2_5	411.0	41.4	62.0	68.9	6.9	0.015	0.066	0.487	0.541	0.054	0.0285	0.1241	110.3	41.4	41.4	100.3	100.3	100.3	100.3	100.3	100.3	410.9	
s2_6	6	s2_6	505.9	41.4	93.1	103.3	10.3	0.018	0.071	0.731	0.811	0.080	0.0348	0.1344	144.7	41.4	41.4	103.3	103.3	103.3	103.3	103.3	103.3	506.2	
s2_7	7	s2_7	634.2	75.8	124.1	137.9	13.8	0.019	0.087	0.486	0.577	0.091	0.0364	0.1653	149.2	75.8	75.8	75.8	75.8	75.8	75.8	633.6	633.6	633.6	
s2_8	8	s2_8	651.6	75.8	124.1	137.9	13.8	0.019	0.098	0.975	0.983	0.108	0.0360	0.1847	213.7	75.8	75.8	137.9	121.8	65.0	365.3	388.36	1227613	651.8	
s2_9	9	s2_9	701.2	75.8	186.0	206.8	20.8	0.027	0.120	1.461	1.624	0.163	0.0501	0.2272	282.6	75.8	75.8	206.8	144.7	97.5	434.2	488.85	162603	701.3	
s2_10	10	s2_10	540.3	113.7	71.5	95.5	0.111	0.128	0.561	0.574	0.0217	0.0242	0.185.2	185.2	113.7	113.7	113.7	137.5	137.5	141.26	55038	239350	540.1		
s2_11	11	s2_11	597.7	113.7	93.1	103.4	10.2	0.016	0.130	0.731	0.812	0.080	0.0295	0.2462	217.1	113.7	113.7	103.4	148.2	33.7	444.5	62287	2806084	597.0	
s2_12	12	s2_12	738.7	113.7	185.9	206.7	20.8	0.025	0.146	1.460	1.624	0.163	0.0476	0.2758	320.4	113.7	113.7	206.7	182.6	97.4	547.9	558.13	4144007	739.8	
s2_13	13	s2_13	585.2	137.9	93.1	103.4	10.3	0.016	0.149	0.731	0.812	0.081	0.0300	0.2813	241.3	137.9	137.9	103.4	172.4	48.7	517.1	555.67	4588660	584.9	
s2_14	14	s2_14	693.5	137.9	124.0	137.8	13.8	0.018	0.153	0.974	1.082	0.109	0.0338	0.2888	275.7	137.9	137.9	137.9	183.8	65.0	551.5	95060	5243305	693.4	
s2_15	15	s2_15	789.0	137.9	248.2	275.6	27.5	0.031	0.179	1.949	2.165	0.216	0.0594	0.3392	413.5	137.9	137.9	229.8	229.8	129.9	689.3	133065	7863666	788.8	
s3_0	0	s3_0	468.7	103.4	92.9	103.2	10.3	0.020	0.027	0.730	0.811	0.081	0.0383	0.0513	206.6	103.4	103.4	103.2	137.8	48.7	413.4	533425	2209304	468.9	
s3_1	1	s3_1	274.7	24.8	185.8	22.7	4.2	0.007	-0.006	0.145	0.178	0.033	0.0130	-0.0116	47.5	24.8	24.8	22.7	32.4	10.7	97.1	2969	29177	273.9	
s3_2	2	s3_2	321.6	24.8	37.3	41.3	4.1	0.012	-0.005	0.293	0.325	0.032	0.0224	-0.0100	66.1	24.8	24.8	41.3	38.6	19.5	115.7	3896	40679	321.2	
s3_3	3	s3_3	385.0	24.8	55.9	62.1	6.2	0.015	-0.002	0.439	0.487	0.049	0.0280	-0.0039	86.9	24.8	24.8	62.1	45.5	29.3	136.5	4923	53422	384.7	
s3_4	4	s3_4	350.6	41.4	31.0	36.9	5.9	0.009	0.005	0.243	0.290	0.047	0.0171	0.0091	78.3	41.4	41.4	36.9	53.7	17.4	161.1	134237	351.2	351.2	
s3_5	5	s3_5	415.5	41.4	61.9	68.8	6.9	0.015	0.007	0.486	0.541	0.055	0.0288	0.0138	110.2	41.4	41.4	68.8	64.3	32.5	193.0	10842	188947	415.4	
s3_6	6	s3_6	480.1	41.4	93.0	103.3	10.4	0.019	0.014	0.730	0.812	0.081	0.0374	0.0272	144.7	41.4	41.4	103.3	103.3	103.3	103.3	103.3	103.3	479.2	
s3_7	7	s3_7	476.3	75.8	61.9	73.4	11.5	0.013	0.029	0.486	0.577	0.091	0.0251	0.0564	149.2	75.8	75.8	75.8	137.8	48.7	413.4	533425	248044	476.5	
s3_8	8	s3_8	522.6	75.8	124.0	137.8	13.8	0.022	0.039	0.974	1.083	0.109	0.0433	0.0761	213.6	75.8	75.8	121.7	137.8	34.6	300.8	28570	857479	553.2	
s3_9	9	s3_9	626.5	75.8	186.0	206.6	20.6	0.030	0.057	1.460	1.622	0.162	0.0573	0.1108	282.4	75.8	75.8	206.6	144.7	97.4	434.0	488.51	1622339	626.5	
s3_10	10	s3_10	469.1	113.7	61.9	71.4	9.5	0.013	0.077	0.486	0.561	0.075	0.0255	0.1487	185.1	113.7	113.7	71.4	137.5	33.7	412.5	55029	2393433	468.9	
s3_11	11	s3_11	518.0	113.7	93.0	103.3	10.3	0.018	0.079	0.731	0.812	0.081	0.0347	0.1521	217.0	113.7	113.7	103.3	148.1	48.7	444.4	62283	2805826	517.7	
s3_12	12	s3_12	634.6	113.7	185.9	206.6	20.7	0.028	0.091	1.460	1.623	0.163	0.0548	0.1756	320.3	113.7	113.7	206.6	182.6	97.4	547.7	585.73	414256	654.7	
s3_13	13	s3_13	527.2	137.9	93.0	103.4	10.3	0.018	0.097	0.730	0.812	0.081	0.0341	0.1881	241.3	137.9	137.9	103.4	172.4	48.7	517.1	585.56	4587899	527.3	
s3_14	14	s3_14	590.1	137.9	124.0	137.8	13.8	0.021	0.101	0.974	1.052	0.108	0.0406	0.1940	275.7	137.9	137.9	137.8	183.8	65.0	551.5	95049	522444	589.3	
s3_15	15	s3_15	721.7	137.9	248.2	275.9	27.7	0.034	0.117	1.949	2.167	0.217	0.0664	0.2256	413.8	137.9	137.9	229.9	229.9	130.1	689.6	133148	7869371	721.6	

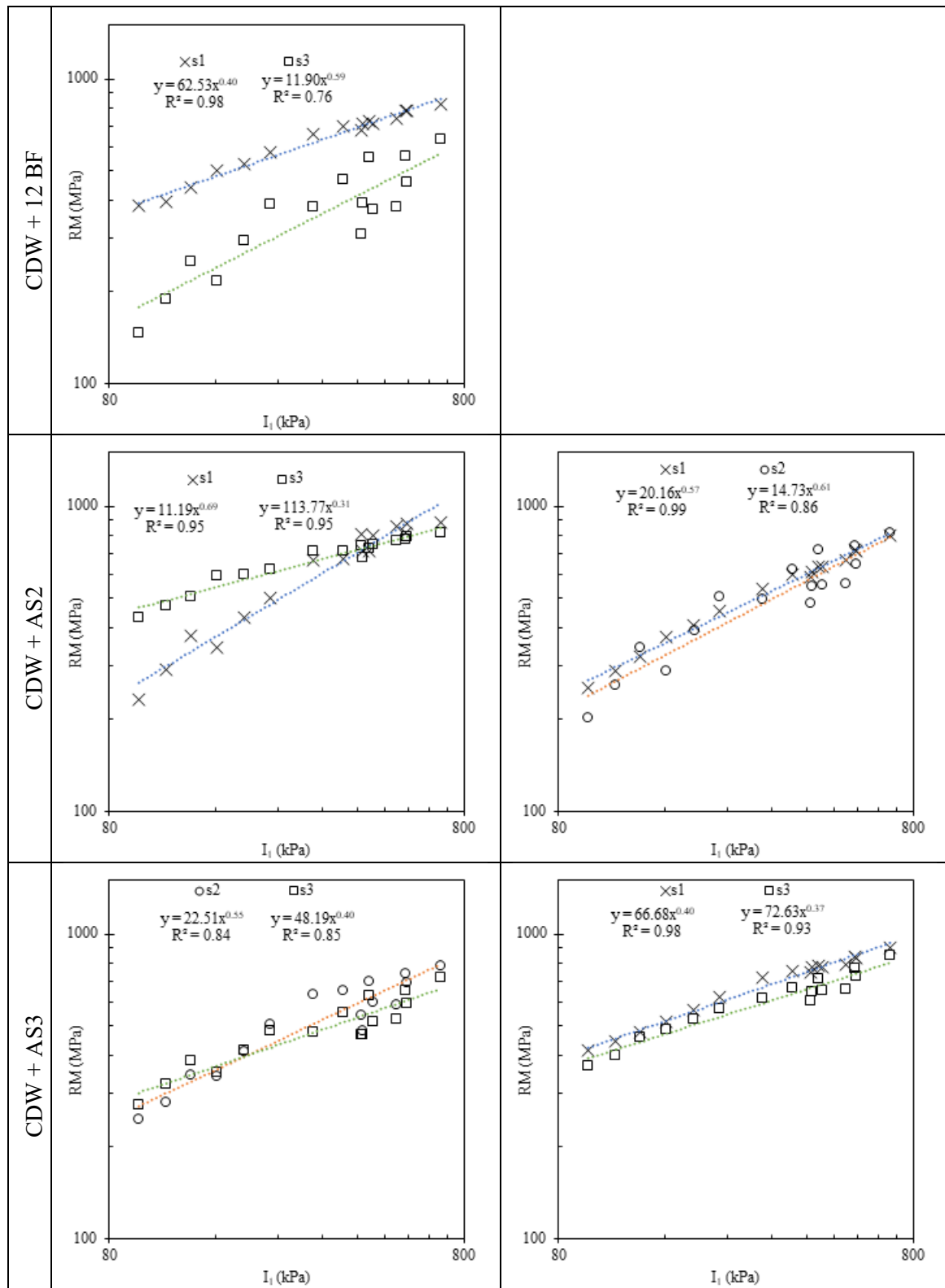
RM CDW + AS3 28 Days

Specimen Sequence	Code	NAT	Confining Pressure	Cyclic Axial Stress	Maximum Axial Stress	Contact Strain	Recoverable Axial Strain	Permanent Axial Strain	Cyclic Axial Load	Maximum Axial Load	Contact Axial Load	Recoverable Axial Load	Permanent Axial Load	Deformation	Deformation	Deformation	Octahedral shear stress at normal stress end	Octahedral shear stress at normal stress end	Octahedral shear stress at normal stress end	First invariant	Second invariant	Third invariant	RM (avg.)
		(MPa)	(kPa)	(kPa)	(kPa)	(%)	(%)	(%)	(kN)	(kN)	(kN)	(kN)	(kN)	(mm)	(mm)	(mm)	(kPa)	(kPa)	(kPa)	II	III	13	(MPa)
s1_0	0	s1_0	781.3	103.4	93.0	103.3	10.3	0.012	0.023	0.731	0.812	0.081	0.0221	0.0420	206.7	103.4	137.8	48.7	413.5	534.41	2201.59	780.4	
s1_1	1	s1_1	416.4	24.8	18.6	22.7	4.1	0.004	0.007	0.146	0.178	0.032	0.0156	0.0149	66.2	24.8	24.8	32.4	19.5	115.8	292.14	415.2	
s1_2	2	s1_2	444.1	24.8	37.3	41.4	4.1	0.008	-0.008	0.293	0.325	0.032	0.0156	0.0149	66.2	24.8	24.8	41.4	38.6	19.5	389.9	407.71	
s1_3	3	s1_3	476.2	24.8	55.8	62.1	6.2	0.012	-0.007	0.439	0.487	0.049	0.0218	-0.0138	86.9	24.8	24.8	62.1	45.5	29.3	136.5	492.3	
s1_4	4	s1_4	515.3	41.4	30.9	36.9	6.0	0.006	-0.001	0.243	0.290	0.047	0.0112	-0.0017	78.3	17.112	41.4	41.4	33.7	17.11	16.1	134.237	515.4
s1_5	5	s1_5	564.8	41.4	61.9	68.8	6.9	0.011	0.000	0.486	0.541	0.054	0.0204	-0.0004	110.2	41.4	41.4	64.3	32.4	19.3	108.40	188.913	
s1_6	6	s1_6	622.2	41.4	93.0	103.3	10.3	0.015	0.002	0.730	0.811	0.081	0.0278	0.0630	144.7	41.4	41.4	75.8	48.7	22.75	136.97	248.044	
s1_7	7	s1_7	716.8	75.8	62.0	73.5	11.5	0.009	0.013	0.487	0.577	0.090	0.0161	0.0250	149.3	75.8	75.8	100.3	34.6	30.9	83.73	857.594	
s1_8	8	s1_8	759.5	75.8	124.0	137.8	13.8	0.016	0.017	0.974	1.082	0.109	0.0304	0.0308	213.6	75.8	75.8	121.7	65.0	365.2	381.27	1227.269	
s1_9	9	s1_9	787.5	75.8	185.9	206.6	20.7	0.024	0.026	1.461	1.623	0.163	0.0439	0.0491	282.4	75.8	75.8	206.6	144.7	97.4	434.0	485.64	
s1_10	10	s1_10	752.6	113.7	62.0	71.5	9.5	0.008	0.034	0.487	0.561	0.075	0.0153	0.0632	185.2	113.7	113.7	137.5	33.7	33.7	50.38	2393.950	
s1_11	11	s1_11	782.7	113.7	93.0	103.3	10.3	0.012	0.005	0.731	0.812	0.081	0.0221	0.0649	217.0	113.7	113.7	148.1	48.7	44.4	62.83	280.826	
s1_12	12	s1_12	844.1	113.7	186.0	206.7	20.7	0.022	0.042	1.461	1.623	0.163	0.0410	0.0783	320.4	113.7	113.7	182.6	97.4	54.78	857.87	414.2032	
s1_13	13	s1_13	797.6	137.9	93.0	103.3	0.012	0.012	0.530	0.612	0.081	0.0217	0.0862	241.2	137.9	137.9	103.3	172.3	172.3	172.3	458.675		
s1_14	14	s1_14	835.9	137.9	124.0	137.9	13.8	0.015	0.048	0.974	1.083	0.109	0.0276	0.0894	275.8	137.9	137.9	137.9	137.9	137.9	137.9	797.6	
s1_15	15	s1_15	899.2	137.9	248.2	275.8	27.6	0.028	0.061	1.949	2.166	0.217	0.0513	0.128	413.7	137.9	137.9	229.8	130.0	689.5	1333.09	7566.708	
s3_0	0	s3_0	648.4	103.4	92.9	103.3	10.3	0.014	0.038	0.730	0.811	0.081	0.0269	0.0712	206.7	103.4	103.3	137.8	48.7	413.5	534.29	22095.18	
s3_1	1	s3_1	370.7	24.8	18.6	22.7	4.1	0.005	0.010	0.146	0.178	0.032	0.0184	0.0184	47.5	24.8	24.8	22.7	10.7	97.1	297.0	370.2	
s3_2	2	s3_2	399.3	24.8	37.3	41.4	4.1	0.009	0.009	0.293	0.325	0.032	0.0175	0.0177	66.2	24.8	24.8	41.4	38.6	19.5	115.8	389.7	
s3_3	3	s3_3	457.0	24.8	55.9	62.1	6.2	0.012	0.011	0.439	0.487	0.049	0.0230	0.0199	86.9	24.8	24.8	62.1	45.5	29.3	136.5	492.4	
s3_4	4	s3_4	483.3	41.4	31.0	37.0	6.0	0.006	0.017	0.244	0.291	0.047	0.0121	0.0316	78.4	41.4	41.4	37.0	53.7	17.4	161.2	83.35	
s3_5	5	s3_5	526.6	41.4	61.9	68.8	6.9	0.012	0.018	0.487	0.541	0.054	0.0221	0.0335	110.2	41.4	41.4	64.3	32.4	193.0	108.39	188.78	
s3_6	6	s3_6	566.6	41.4	92.9	103.3	10.4	0.016	0.020	0.730	0.811	0.081	0.0308	0.0372	144.7	41.4	41.4	103.3	75.8	48.7	227.5	526.6	
s3_7	7	s3_7	615.4	75.8	61.9	73.5	11.6	0.010	0.031	0.487	0.578	0.091	0.0190	0.0587	149.3	75.8	75.8	100.3	34.7	30.9	283.83	857.939	
s3_8	8	s3_8	667.3	75.8	124.2	137.8	13.7	0.019	0.035	0.975	1.083	0.107	0.0350	0.0662	213.6	121.7	121.7	137.8	381.30	1227.384	666.8	614.5	
s3_9	9	s3_9	714.1	75.8	185.8	206.5	20.6	0.026	0.046	1.460	1.622	0.162	0.0489	0.0864	282.3	75.8	75.8	206.5	144.6	97.3	433.9	485.39	
s3_10	10	s3_10	603.0	113.7	61.9	71.5	9.6	0.010	0.053	0.486	0.561	0.075	0.0193	0.0992	185.2	113.7	113.7	113.7	137.5	33.7	412.6	503.33	
s3_11	11	s3_11	651.0	113.7	92.9	103.3	10.4	0.014	0.054	0.730	0.811	0.082	0.0268	0.1017	217.0	113.7	113.7	148.1	44.4	44.4	622.78	280.567	
s3_12	12	s3_12	768.2	113.7	186.3	206.8	20.5	0.024	0.061	1.463	1.624	0.161	0.0456	0.152	320.5	113.7	113.7	182.6	97.5	547.9	858.05	414.036	
s3_13	13	s3_13	657.2	137.9	93.1	103.4	10.3	0.014	0.064	0.731	0.812	0.081	0.0267	0.1207	241.3	137.9	137.9	103.4	172.4	48.7	517.1	855.61	
s3_14	14	s3_14	730.0	137.9	124.0	137.8	13.8	0.017	0.066	0.974	1.082	0.108	0.0319	0.1249	275.7	137.9	137.9	183.8	65.0	551.5	950.66	524.5585	
s3_15	15	s3_15	847.7	137.9	248.0	275.6	27.7	0.029	0.078	1.948	2.165	0.217	0.0250	0.1474	413.5	137.9	137.9	229.8	129.9	689.3	13307.1	7566.4046	

8.3.1. Resilient modulus dyagrams

I₁-RM dyagrams





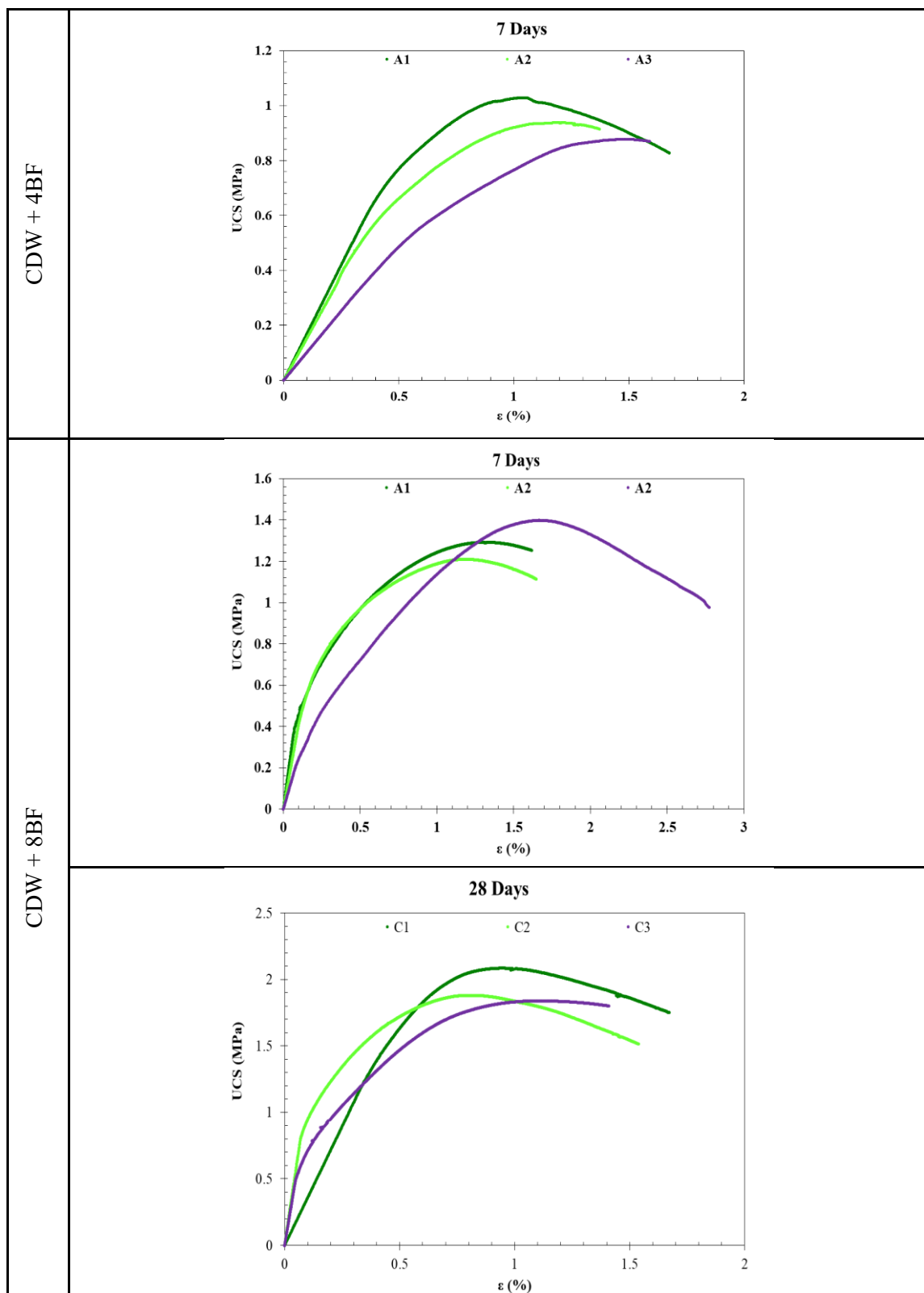
8.4. UCS and ITS

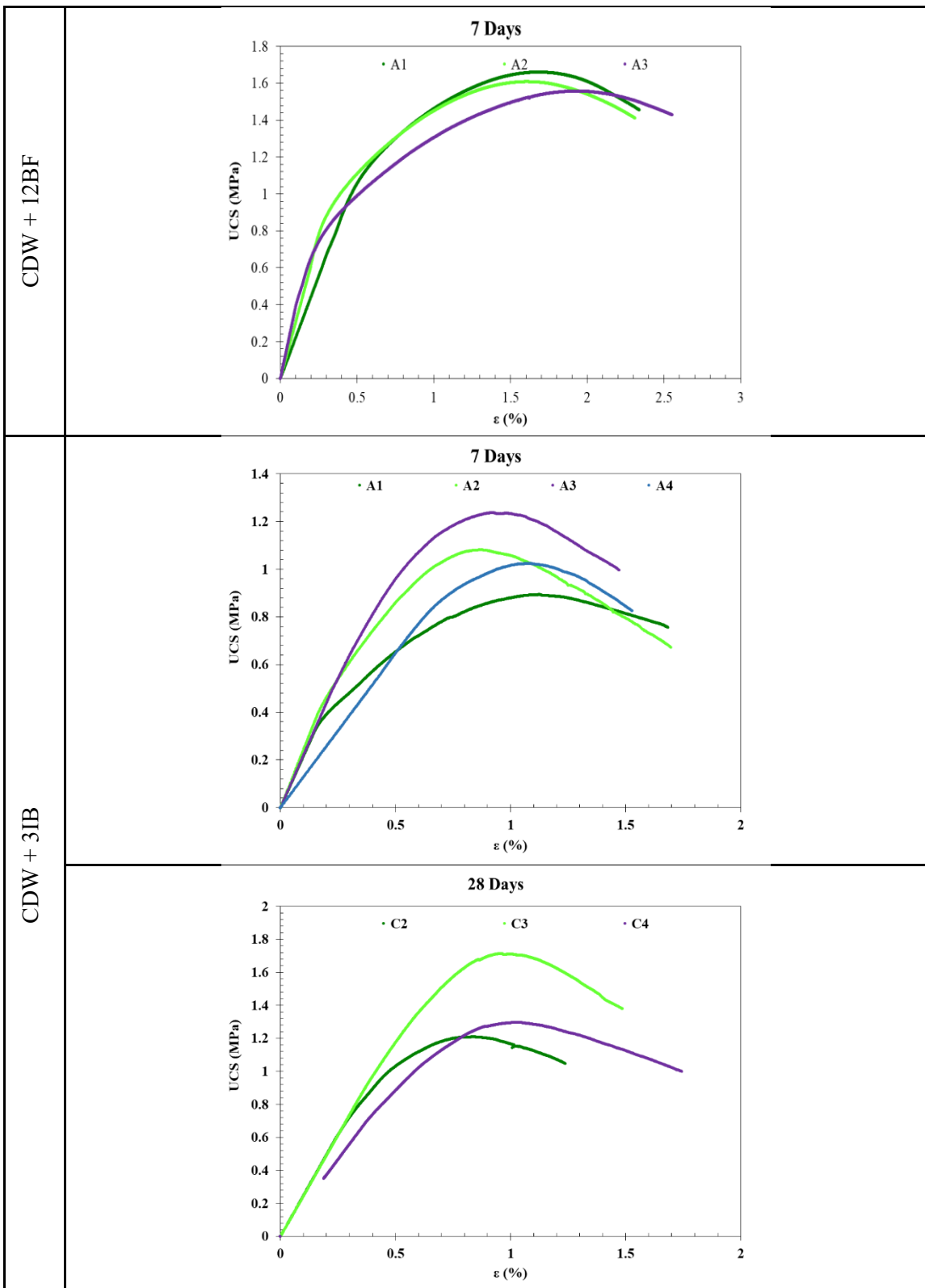
UCS and ITS sample parameters

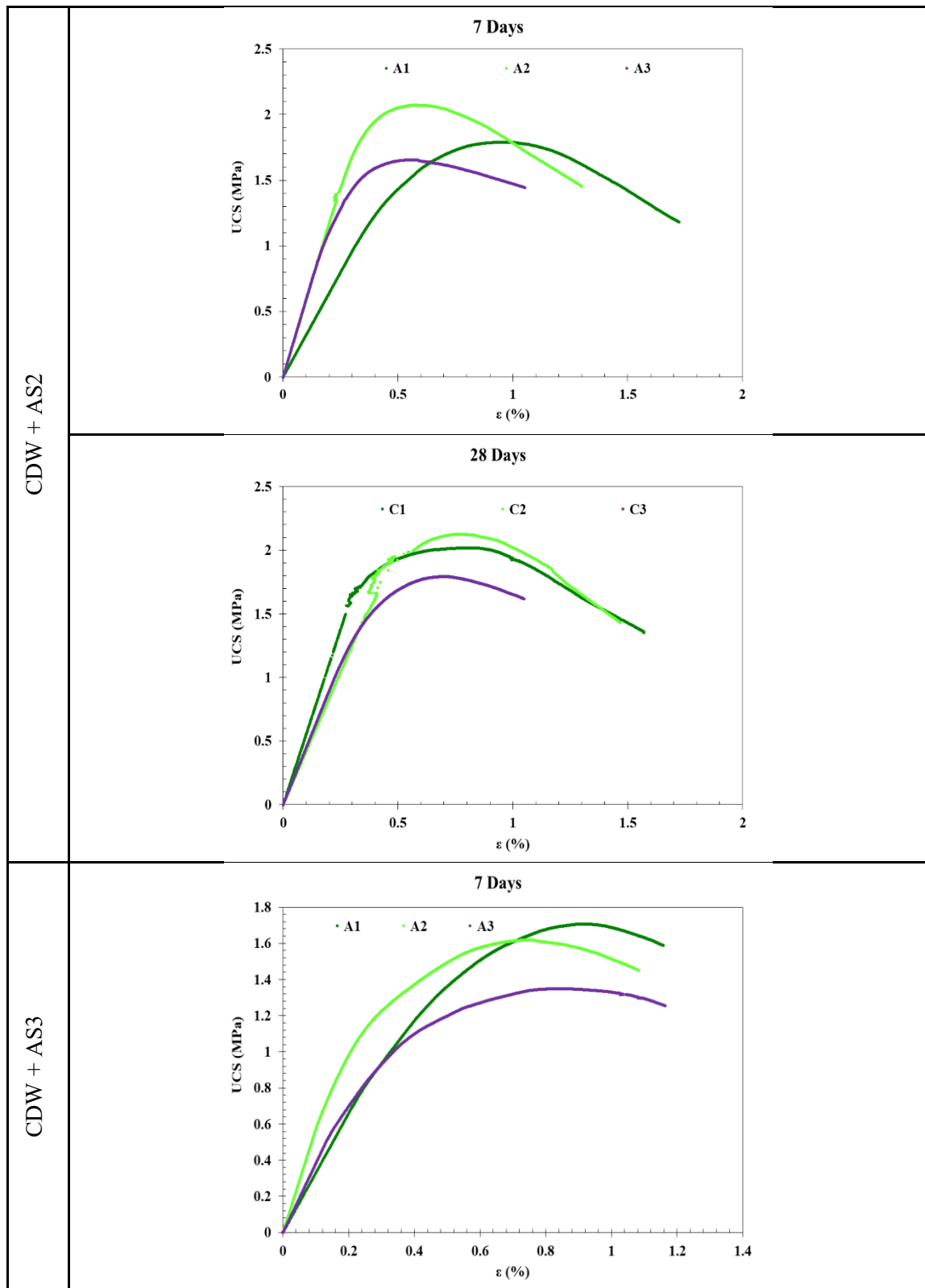
	SAMPLE	h	Mould tare	Mould + wet sample	Mould + dry sample	Water content	Dry mass	Effective W
		[mm]	[g]	[g]	[g]	[g]	[g]	[%]
CDW + 3IB	CDW_3IB_A1_7	196	583.1	3900	3655.3	244.7	3072.2	8.0%
	CDW_3IB_C4_28	193	584.3	3872.1	3631.6	240.5	3047.3	7.9%
	CDW_3IB_C1_28	194	1039.3	4349.5	4107.1	242.4	3067.8	7.9%
	CDW_3IB_C2_28	191	580.3	3862.9	3626.1	236.8	3045.8	7.8%
	CDW_3IB_C3_28	188	1025.4	4298.4	4061.1	237.3	3035.7	7.8%
	CDW_3IB_A4_7	191	415.4	3665.1	3424.6	240.5	3009.2	8.0%
	CDW_3IB_A2_7	193	742.6	3998.6	3755	243.6	3012.4	8.1%
	CDW_3IB_A3_7	186	1039.3	4282.7	4042.5	240.2	3003.2	8.0%
	CDW_3IB_B1_7	100	203.9	1948.4	1816.1	132.3	1612.2	8.2%
	CDW_3IB_B2_7	100	27.9	1803.6	1667.2	136.4	1639.3	8.3%
	CDW_3IB_B3_7	100	27.8	1773.9	1650.4	123.5	1622.6	7.6%
CDW + 4BF	CDW_4BF_A1_7	186	1039.2	4255.7	4016.1	239.6	2976.9	8.0%
	CDW_4BF_A2_7	187	401	3617.9	3376.3	241.6	2975.3	8.1%
	CDW_4BF_A3_7	191	410.2	3606.7	3372	234.7	2961.8	7.9%
	CDW_4BF_B1_7	100	399.7	2135	2007.3	127.7	1607.6	7.9%
	CDW_4BF_B2_7	101	401.7	2136.4	2006.2	130.2	1604.5	8.1%
	CDW_4BF_B3_7	101	203.8	1923	1795.2	127.8	1591.4	8.0%
CDW + 8BF	CDW_8BF_A1_7	186	584.4	3809.9	3572.3	237.6	2987.9	8.0%
	CDW_8BF_A2_7	186	584.1	3809.4	3570	239.4	2985.9	8.0%
	CDW_8BF_A3_7	186	1039.2	4264.4	4027.1	237.3	2987.9	7.9%
	CDW_8BF_B1_7	100	399.4	2130.6	2004.3	126.3	1604.9	7.9%
	CDW_8BF_B2_7	100	401.5	2132.1	2007.7	124.4	1606.2	7.7%
	CDW_8BF_B3_7	100	399.3	2129.8	2004	125.8	1604.7	7.8%
	CDW_8BF_C1_28	186	742.8	3967.1	3735.2	231.9	2992.4	7.7%
	CDW_8BF_C2_28	186	490.2	3721	3488.1	232.9	2997.9	7.8%
	CDW_8BF_C3_28	186	1039.3	4272.6	4037	235.6	2997.7	7.9%
CDW + 12BF	CDW_12BF_A1_7	186	490.8	3712.7	3484.9	227.8	2994.1	7.6%
	CDW_12BF_A2_7	186	496.5	3738.5	3509.2	229.3	3012.7	7.6%
	CDW_12BF_A3_7	186	1039.2	4277.2	4042.7	234.5	3003.5	7.8%
	CDW_12BF_B1_7	100	399.5	2140.1	2015.5	124.6	1616	7.7%
	CDW_12BF_B2_7	100	399.5	2138.7	2017.7	121	1618.2	7.5%
	CDW_12BF_B3_7	100	401.7	2142	2018.9	123.1	1617.2	7.6%
CDW + AS2	CDW_AS2_A1_7	188	1039.3	4367.4	4215.6	151.8	3176.3	4.8%
	CDW_AS2_A2_7	188	489.6	3816.7	3658	158.7	3168.4	5.0%
	CDW_AS2_A3_7	188	490.4	3827.8	3670.4	157.4	3180	4.9%
	CDW_AS2_B1_7	100	399.5	2197.3	2112.5	84.8	1713	5.0%
	CDW_AS2_B2_7	100	400.2	2204.5	2122.9	81.6	1722.7	4.7%
	CDW_AS2_B3_7	100	401.6	2193.8	2110.4	83.4	1708.8	4.9%

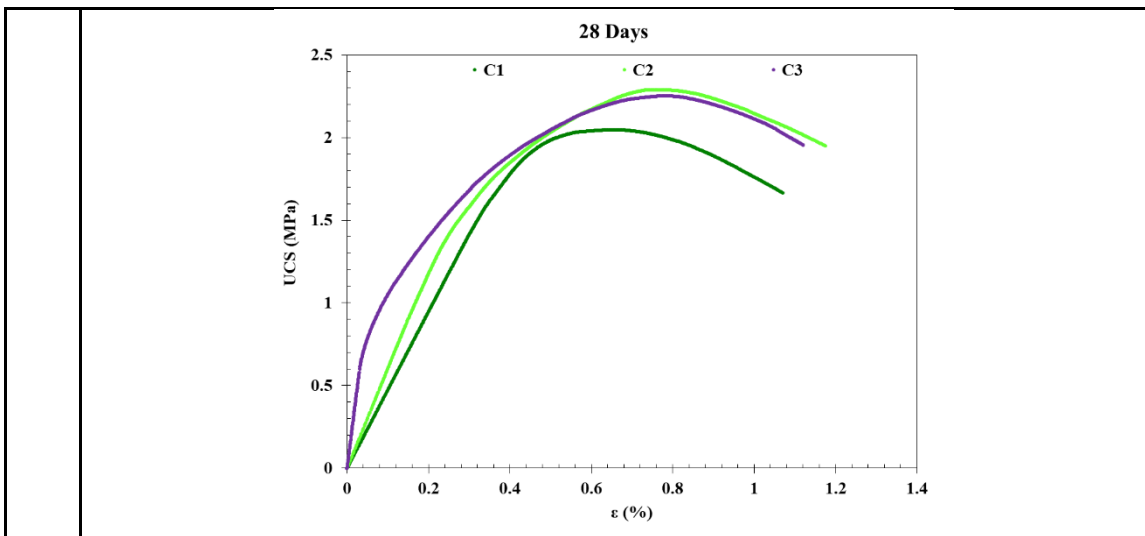
	SAMPLE	h [mm]	Mould tare [g]	Mould + wet sample [g]	Mould + dry sample [g]	Water content [g]	Dry mass [g]	Effective W [%]
	CDW_AS2_B1_7 Bis	100	399.6	2205.3	2115.1	90.2	1715.5	5.3%
	CDW_AS2_B2_7 Bis	100	401.5	2221.6	2128.5	93.1	1727	5.4%
	CDW_AS2_C1_28	188	742.8	4083	3925.3	157.7	3182.5	5.0%
	CDW_AS2_C2_28	189	496.8	3828.9	3670.8	158.1	3174	5.0%
	CDW_AS2_C3_28	192	605.3	3950.5	3788.8	161.7	3183.5	5.1%
CDW + AS3	CDW_AS3_A1_7	187	564.8	3875.3	3724.8	150.5	3160	4.8%
	CDW_AS3_A2_7	189	1039.4	4360.3	4205.9	154.4	3166.5	4.9%
	CDW_AS3_A3_7	192	742.6	4049.6	3897.1	152.5	3154.5	4.8%
	CDW_AS3_B1_7	100	399.5	2181.2	2096.2	85	1696.7	5.0%
	CDW_AS3_B2_7	101	401.6	2181.7	2096.9	84.8	1695.3	5.0%
	CDW_AS3_B3_7	100	496.7	2276.9	2187.9	89	1691.2	5.3%
	CDW_AS3_C1_28	186.4	490.4	3806.7	3665.9	140.8	3175.5	4.4%
	CDW_AS3_C2_28	187.4	590.8	3905.4	3769.1	136.3	3178.3	4.3%
	CDW_AS3_C3_28	188.3	565.1	3874.5	3736.1	138.4	3171	4.4%

UCS stress-strain curves









8.5. Preliminary site operations

8.5.1. LWD test simulation

Test	Diameter [mm]	Weight [kg]	H [in]	Drop [-]	Stress [kPa]	Def. [μm]	E _{LWD} [MPa]	Rubber [Y/N]
p0	300	10	13	1	49	869	15	Y
				2	29	575	13	Y
				3	50	832	16	Y
				4	49	829	16	Y
				5	49	807	16	Y
				6	50	828	16	Y
				7	49	784	16	Y
				8	50	834	16	Y
p1	300	10	23	1	72	1115	17	Y
				2	72	1141	17	Y
				3	71	1167	16	Y
				4	72	1187	16	Y
				5	73	1182	16	Y
				6	71	1146	16	Y
				7	73	1136	17	Y
				8	72	1154	16	Y
p2	300	10	33	1	94	1422	17	Y
				2	94	1505	16	Y
				3	96	1441	18	Y
				4	96	1427	18	Y
				5	94	1409	18	Y
				6	94	1341	18	Y
				7	97	1420	18	Y
				8	98	1365	19	Y
p3	300	10	13	1	50	749	18	N
				2	51	759	18	N
				3	51	738	18	N
				4	51	762	18	N
				5	51	760	18	N
				6	49	755	17	N
				7	51	754	18	N
				8	51	753	18	N
p4	300	10	23	1	71	944	20	N
				2	73	963	20	N
				3	71	937	20	N
				4	73	966	20	N
				5	71	964	19	N
				6	70	1002	18	N
				7	73	991	19	N
				8	72	969	20	N
p5	300	10	33	1	96	1135	22	N
				2	96	1109	23	N
				3	97	1138	22	N
				4	97	1137	22	N
				5	97	1143	22	N
				6	97	1130	23	N
				7	98	1139	23	N
				8	96	1137	22	N
p6	300	15	13	1	69	1017	18	Y
				2	73	957	20	Y
				3	73	967	20	Y
				4	73	922	21	Y
				5	71	932	20	Y
				6	71	927	20	Y
				7	73	933	21	Y
				8	73	951	20	Y
				1	111	1252	23	Y

Test	Diameter [mm]	Weight [kg]	H [in]	Drop [-]	Stress [kPa]	Def. [μm]	E _{LWD} [MPa]	Rubber [Y/N]
p7	300	15	23	2	110	1269	23	Y
				3	112	1254	24	Y
				4	113	1248	24	Y
				5	113	1248	24	Y
				6	113	1248	24	Y
				7	113	1235	24	Y
				8	112	1231	24	Y
				1	10	133	20	Y
p8	300	15	33	2	150	1393	28	Y
				3	150	1431	28	Y
				4	150	1475	27	Y
				5	149	1521	26	Y
				6	149	1462	27	Y
				7	149	1923	20	Y
				8	150	1630	24	Y
				9	151	1450	27	Y
				1	70	860	21	N
p9	300	15	13	2	71	851	22	N
				3	71	885	21	N
				4	71	884	21	N
				5	71	891	21	N
				6	71	876	21	N
				7	69	870	21	N
				8	71	886	21	N
				1	110	1132	26	N
p10	300	15	23	2	111	1175	25	N
				3	113	1199	25	N
				4	113	1205	25	N
				5	111	1212	24	N
				6	112	1219	24	N
				7	112	1228	24	N
				8	114	1234	24	N
				1	149	1465	27	N
p11	300	15	33	2	147	1441	27	N
				3	148	1412	28	N
				4	149	1405	28	N
				5	149	1428	27	N
				6	148	1461	27	N
				7	149	1440	27	N
				8	146	1473	26	N
				1	94	938	26	Y
p12	300	20	13	2	95	951	26	Y
				3	96	997	25	Y
				4	95	1031	24	Y
				5	96	1088	23	Y
				6	96	1116	23	Y
				7	96	1115	23	Y
				8	96	1068	24	Y
				1	151	1501	26	Y
p13	300	20	23	2	152	1522	26	Y
				3	152	1487	27	Y
				4	151	1507	26	Y
				5	150	1476	27	Y
				6	151	1513	26	Y
				7	150	1447	27	Y
				8	153	1413	29	Y
				1	203	1748	31	Y
p14	300	20	33	4	199	1670	31	Y
				7	199	1858	28	Y
				9	200	1636	32	Y
				1	95	1069	23	N
p15	300	20	13	2	95	1079	23	N
				3	96	1077	23	N

Test	Diameter [mm]	Weight [kg]	H [in]	Drop [-]	Stress [kPa]	Def. [μm]	E _{LWD} [MPa]	Rubber [Y/N]
p16	300	20	23	4	97	1074	24	N
				5	97	1078	24	N
				6	96	1082	23	N
				7	95	1085	23	N
				8	95	1041	24	N
				1	152	1343	30	N
				2	153	1347	30	N
				3	153	1341	30	N
				4	153	1355	30	N
				5	152	1361	29	N
p17	300	20	33	6	153	1368	29	N
				7	151	1367	29	N
				8	153	1373	29	N
				1	202	1501	35	N
				2	205	1520	36	N
				3	202	1526	35	N
				4	200	1530	34	N
				5	199	1540	34	N
p18	150	10	13	6	200	1538	34	N
				7	203	1537	35	N
				8	205	1546	35	N
				1	202	824	32	N
				2	196	823	31	N
				3	200	828	32	N
				4	202	806	33	N
				5	205	835	32	N
p19	150	10	23	6	198	813	32	N
				7	204	835	32	N
				8	199	812	32	N
				1	292	1018	38	N
				2	290	1089	35	N
				3	287	1084	35	N
				4	293	1057	36	N
				5	287	1039	36	N
p20	150	10	33	6	288	1048	36	N
				7	285	1048	36	N
				8	295	1045	37	N
				1	392	1164	44	N
				2	392	1158	45	N
				3	391	1156	45	N
				4	393	1136	46	N
				5	391	1181	44	N
p21	150	15	13	6	383	1178	43	N
				7	394	1176	44	N
				8	386	1179	43	N
				1	284	1078	35	N
				2	291	1028	37	N
				3	282	1037	36	N
				4	291	1028	37	N
				5	289	1040	37	N
p22	150	15	23	6	288	1046	36	N
				7	289	1033	37	N
				8	290	1044	37	N
				1	458	1203	50	N
				2	454	1240	48	N
				3	456	1248	48	N
				4	447	1262	47	N
				5	452	1274	47	N
p23	150	15	33	6	451	1263	47	N
				7	457	1262	48	N
				8	452	1294	46	N
p23	150	15	33	1	595	1358	58	N
				2	586	1456	53	N

Test	Diameter [mm]	Weight [kg]	H [in]	Drop [-]	Stress [kPa]	Def. [μm]	E _{LWD} [MPa]	Rubber [Y/N]
p24	150	20	13	3	588	1479	52	N
				4	582	1514	51	N
				5	592	1510	52	N
				6	585	1446	53	N
				7	591	1480	53	N
				8	584	1541	50	N
				1	384	1237	41	N
				2	390	1187	43	N
p25	150	20	23	3	386	1235	41	N
				4	390	1238	41	N
				5	387	1220	42	N
				6	391	1216	42	N
				7	392	1216	42	N
				8	387	1201	42	N
				1	587	1438	54	N
				2	589	1471	53	N
p26	150	20	33	3	588	1461	53	N
				4	589	1419	55	N
				5	586	1450	53	N
				6	589	1497	52	N
				7	590	1461	53	N
				8	587	1522	51	N
				1	772	-	-	N
				2	764	1935	52	N
p27	200	10	13	3	756	-	-	N
				1	115	661	31	N
				2	115	688	29	N
				3	112	693	28	N
				4	116	698	29	N
				5	115	697	29	N
				6	116	697	29	N
				7	113	694	29	N
p28	200	10	23	8	116	681	30	N
				1	165	887	33	N
				2	168	871	34	N
				3	166	871	33	N
				4	165	876	33	N
				5	165	874	33	N
				6	165	876	33	N
				7	162	880	32	N
p29	200	10	33	8	164	879	33	N
				1	218	1031	37	N
				2	219	1047	37	N
				3	218	1063	36	N
				4	222	1055	37	N
				5	222	1076	36	N
				6	222	1067	37	N
				7	221	1024	38	N
p30	200	15	13	8	221	1084	36	N
				1	157	912	30	N
				2	163	872	33	N
				3	163	862	33	N
				4	160	857	33	N
				5	159	865	32	N
				6	162	827	34	N
				7	163	868	33	N
p31	200	15	23	8	161	864	33	N
				1	255	1069	42	N
				2	257	1103	41	N
				3	255	1121	40	N
				4	252	1124	39	N
				5	254	1134	39	N
				6	252	1132	39	N
				7	250	1108	40	N

Test	Diameter [mm]	Weight [kg]	H [in]	Drop [-]	Stress [kPa]	Def. [μm]	E _{LWD} [MPa]	Rubber [Y/N]
p32	200	15	33	8	251	1124	39	N
				1	337	1252	47	N
				2	334	1263	46	N
				3	337	1278	46	N
				4	333	1295	45	N
				5	336	1240	48	N
				6	333	1328	44	N
				7	335	1316	45	N
				8	333	1328	44	N
				1	215	1043	36	N
p33	200	20	13	2	220	966	40	N
				3	218	1000	38	N
				4	218	1083	35	N
				5	214	1083	35	N
				6	220	1083	36	N
				7	223	1110	35	N
				8	218	1113	34	N
				1	341	1350	44	N
p34	200	20	23	2	342	1380	43	N
				3	335	1371	43	N
				4	340	1381	43	N
				5	340	1400	43	N
				6	340	1372	43	N
				7	340	1373	43	N
				8	340	1367	44	N
				1	35	220	28	N
p35	200	20	33	2	440	1523	51	N
				3	438	1546	50	N
				4	443	1560	50	N
				5	441	1575	49	N
				6	439	1599	48	N
				7	442	1585	49	N
				8	443	1604	48	N
				9	441	1599	48	N

8.5.2. LWD test on multi-layer

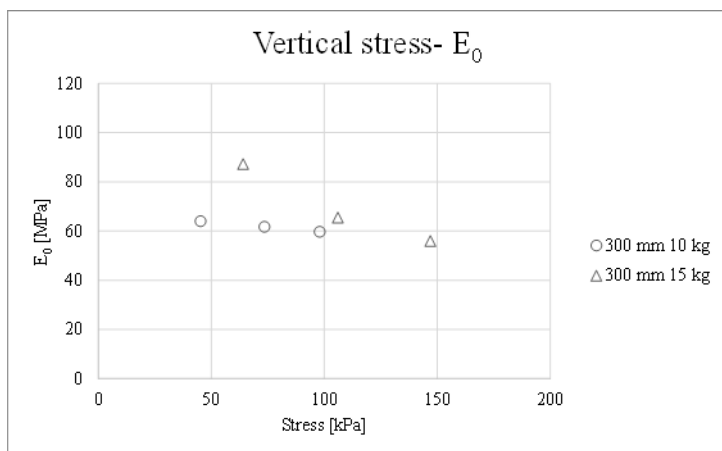
For each point are represented two tables, the first table represents the raw data (8 drops), and the second represents the average values plotted in the diagram, the average values are computed from the last four drops out of a total of eight.

Subgrade:

Point 1:

Test	Diameter [mm]	Weight [kg]	H [in]	Drop [-]	Stress [kPa]	Def. [μm]	E _{LWD} [MPa]
p1	300	10	13	1	54	512	28
				2	52	255	53
				3	30	122	65
				4	21	72	78
				5	38	162	62
				6	52	211	64
				7	52	208	65
				8	39	157	65
p2	300	10	23	1	74	344	57
				2	75	324	61
				3	74	321	60
				4	72	318	59
				5	75	313	63
				6	73	316	61
				7	72	309	61
				8	74	313	62
p3	300	10	33	1	96	476	53
				2	97	457	56
				3	99	450	58
				4	96	416	61
				5	97	445	57
				6	98	432	59
				7	98	423	61
				8	99	417	62
p4	300	15	13	1	72	261	72
				2	73	245	79
				3	36	174	54
				4	73	242	79
				5	73	235	82
				6	55	148	99
				7	56	175	85
				8	72	230	83
p5	300	15	23	1	114	475	63
				2	113	480	62
				3	114	464	65
				4	114	462	65
				5	84	328	68
				6	114	470	64
				7	114	459	65
				8	112	455	65
p6	300	15	33	1	147	710	54
				2	146	738	52
				3	148	725	54
				4	146	713	54
				5	147	697	55
				6	148	693	56
				7	146	683	56
				8	147	679	57

Point 1			
Diameter [mm]		Stress [kPa]	E _o [MPa]
300	p1	45.25	64
	p2	73.5	61.75
	p3	98	59.75
	p4	64	87.25
	p5	106	65.5
	p6	147	56

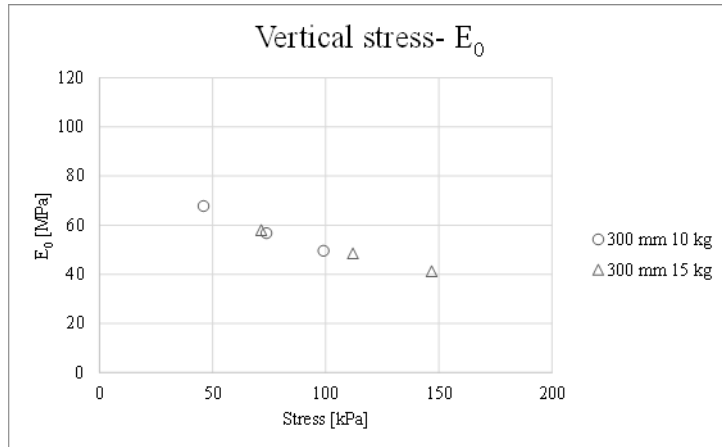


Point 2:

Test	Diameter [mm]	Weight [kg]	H [in]	Drop [-]	Stress [kPa]	Def. [μm]	E _{LWD} [MPa]
p1	300	10	13	1	51	299	45
				2	50	228	58
				3	49	217	59
				4	51	214	63
				5	51	201	67
				6	51	200	67
				7	51	201	67
				8	31	116	70
p2	300	10	23	1	72	376	50
				2	72	354	54
				3	74	350	56
				4	72	346	55
				5	74	342	57
				6	73	343	56
				7	74	347	56
				8	74	338	58
p3	300	10	33	1	98	563	46
				2	98	528	49
				3	98	536	48
				4	97	534	48
				5	100	535	49
				6	98	535	48
				7	99	506	52
				8	99	534	49
p4	300	15	13	1	73	367	52
				2	72	363	52
				3	72	337	56
				4	72	336	56
				5	72	316	60
				6	72	328	58

Test	Diameter [mm]	Weight [kg]	H [in]	Drop [-]	Stress [kPa]	Def. [μm]	E _{LWD} [MPa]
				7	71	328	57
				8	71	326	57
p5	300	15	23	1	112	641	46
				2	112	622	47
				3	112	624	47
				4	112	620	48
				5	111	621	47
				6	113	604	49
				7	112	595	50
p6	300	15	33	1	144	970	39
				2	143	961	39
				3	144	949	40
				4	144	946	40
				5	146	944	41
				6	146	936	41
				7	149	941	42
				8	146	932	41

Point 2			
Diameter [mm]		Stress [kPa]	E _o [MPa]
300	p1	46	67.75
	p2	73.75	56.75
	p3	99	49.5
	p4	71.5	58
	p5	112	48.5
	p6	146.75	41.25

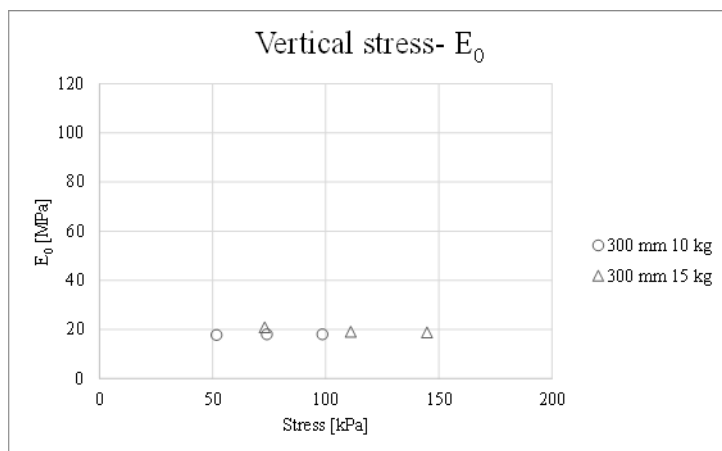


Point 3:

Test	Diameter [mm]	Weight [kg]	H [in]	Drop [-]	Stress [kPa]	Def. [μm]	E _{LWD} [MPa]
p1	300	10	13	1	51	1561	9
				2	51	939	14
				3	52	863	16
				4	52	784	17
				5	51	793	17
				6	52	786	17
				7	52	736	19
				8	52	757	18

Test	Diameter [mm]	Weight [kg]	H [in]	Drop [-]	Stress [kPa]	Def. [μm]	E _{LWD} [MPa]
p2	300	10	23	1	72	1183	16
				2	74	1160	17
				3	72	1131	17
				4	73	1116	17
				5	75	1100	18
				6	73	1108	17
				7	75	1093	18
				8	73	1035	19
p3	300	10	33	1	96	1495	17
				2	97	1489	17
				3	98	1484	17
				4	97	1460	17
				5	98	1444	18
				6	98	1437	18
				7	99	1430	18
				8	99	1413	18
p4	300	15	13	2	71	983	19
				3	72	942	20
				4	71	962	19
				5	72	949	20
				6	72	943	20
				7	73	938	20
				8	73	931	21
				9	73	899	21
				10	73	928	21
				1	110	1566	18
p5	300	15	23	2	110	1570	18
				3	112	1555	19
				4	112	1553	19
				5	110	1562	19
				6	111	1543	19
				7	112	1544	19
				8	111	1541	19
				1	144	2095	18
p6	300	15	33	2	145	2035	19
				3	144	2097	18
				4	144	2095	18
				5	144	2083	18
				6	144	2016	19
				7	146	2063	19
				8	145	2060	19

Point 3			
Diameter [mm]		Stress [kPa]	E _o [MPa]
300	p1	51.75	17.75
	p2	74	18
	p3	98.5	18
	p4	73	20.75
	p5	111	19
	p6	144.75	18.75

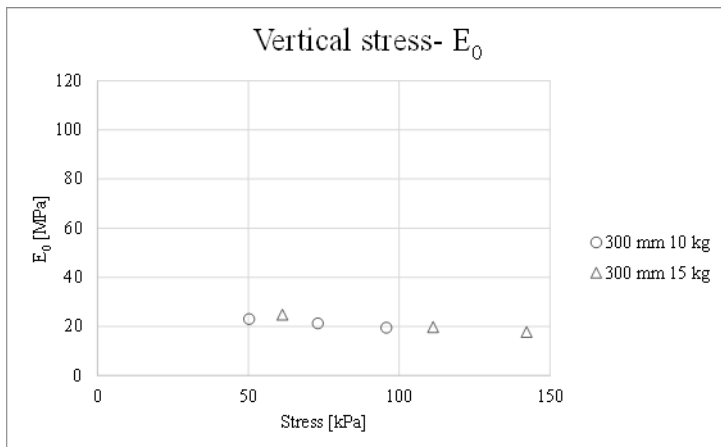


Point 4:

Test	Diameter [mm]	Weight [kg]	H [in]	Drop [-]	Stress [kPa]	Def. [μm]	E _{LWD} [MPa]
p1	300	10	13	2	50	1183	11
				3	49	664	19
				4	50	608	22
				5	50	598	22
				6	49	585	22
				7	51	572	23
				8	50	561	23
				9	51	563	24
				1	72	1077	18
p2	300	10	23	2	73	990	19
				3	73	901	21
				4	74	938	21
				5	73	929	21
				6	73	880	22
				7	74	909	21
				8	72	889	21
				1	94	1385	18
p3	300	10	33	2	96	1361	19
				3	96	1358	19
				4	97	1346	19
				5	96	1327	19
				6	95	1264	20
				7	95	1296	19
				8	97	1302	20
				1	71	848	22
p4	300	15	13	2	70	798	23
				3	70	812	23
				4	55	596	24
				5	31	302	27

Test	Diameter [mm]	Weight [kg]	H [in]	Drop [-]	Stress [kPa]	Def. [μm]	E _{LWD} [MPa]
				6	72	797	24
				7	72	799	24
				8	70	775	24
p5	300	15	23	1	109	1469	20
				2	111	1491	20
				3	111	1474	20
				4	110	1488	19
				5	111	1489	20
				6	110	1493	19
				7	112	1484	20
				8	112	1480	20
p6	300	15	33	1	140	2143	17
				2	143	2164	17
				3	143	2176	17
				4	143	2097	18
				5	143	2149	18
				6	141	2135	17
				7	142	2071	18
				8	143	2102	18

Point 4			
Diameter [mm]		Stress [kPa]	E _o [MPa]
300	p1	50.25	23
	p2	73	21.25
	p3	95.75	19.5
	p4	61.25	24.75
	p5	111.25	19.75
	p6	142.25	17.75

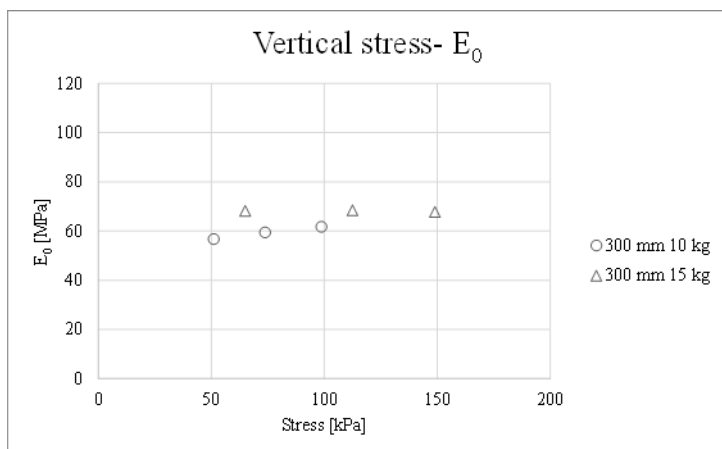


Layer 1:

Point 1:

Test	Diameter [mm]	Weight [kg]	H [in]	Drop [-]	Stress [kPa]	Def. [μm]	E_{LWD} [MPa]
p1	300	10	13	1	52	542	25
				2	51	301	45
				3	51	271	50
				4	51	256	52
				5	51	246	55
				6	51	237	57
				7	51	236	57
				8	51	233	58
p2	300	10	23	1	74	392	50
				2	73	344	56
				3	56	271	54
				4	73	348	55
				5	74	338	58
				6	74	330	59
				7	74	319	61
				8	73	322	60
p3	300	10	33	1	98	465	55
				2	98	460	56
				3	100	457	58
				4	99	441	59
				5	99	412	63
				6	99	430	61
				7	99	424	61
				8	98	418	62
p4	300	15	13	1	71	299	63
				2	73	290	66
				3	73	285	67
				4	71	289	65
				5	43	181	63
				7	73	279	69
				8	72	265	72
				9	72	274	69
p5	300	15	23	1	113	451	66
				2	113	448	66
				3	114	452	66
				4	114	441	68
				5	112	441	67
				6	113	416	72
				7	112	437	67
				8	113	436	68
p6	300	15	33	1	150	616	64
				2	149	605	65
				3	148	602	65
				4	148	599	65
				5	149	588	67
				6	150	583	68
				7	149	579	68
				8	148	573	68

Point 1			
Diameter [mm]		Stress [kPa]	E _o [MPa]
300	p1	51	56.75
	p2	73.75	59.5
	p3	98.75	61.75
	p4	65	68.25
	p5	112.5	68.5
	p6	149	67.75

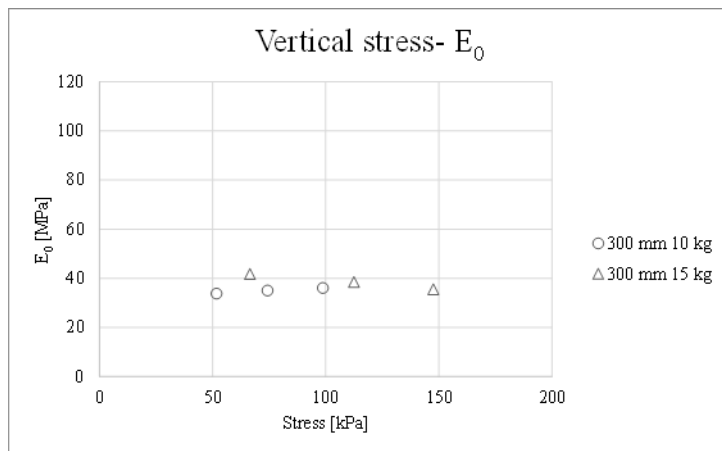


Point 2:

Test	Diameter [mm]	Weight [kg]	H [in]	Drop [-]	Stress [kPa]	Def. [μm]	E _{LWD} [MPa]
p1	300	10	13	1	48	943	13
				2	51	527	25
				3	52	470	29
				4	52	436	31
				5	52	425	32
				6	52	418	33
				7	52	389	35
				8	51	382	35
p2	300	10	23	1	74	605	32
				2	73	580	33
				3	74	587	33
				4	74	578	34
				5	72	570	33
				6	74	563	35
				7	74	557	35
				8	77	553	37
p3	300	10	33	1	97	759	34
				2	99	754	35
				3	100	752	35
				4	99	743	35
				5	99	736	35
				6	98	724	36
				7	99	719	36
				8	99	711	37
p4	300	15	13	1	72	492	38
				2	72	468	40
				3	72	466	41
				4	71	446	42
				5	70	444	42
				6	70	439	42

Test	Diameter [mm]	Weight [kg]	H [in]	Drop [-]	Stress [kPa]	Def. [μm]	E_{LWD} [MPa]
				7	72	451	42
				8	54	352	41
p5	300	15	23	1	111	768	38
				2	113	779	38
				3	113	783	38
				4	113	791	38
				5	113	787	38
				6	112	767	39
				7	113	787	38
				8	112	752	39
p6	300	15	33	1	146	1096	35
				2	147	1120	34
				3	148	1078	36
				4	146	1111	35
				5	148	1116	35
				6	146	1104	35
				7	148	1095	36
				8	148	1084	36

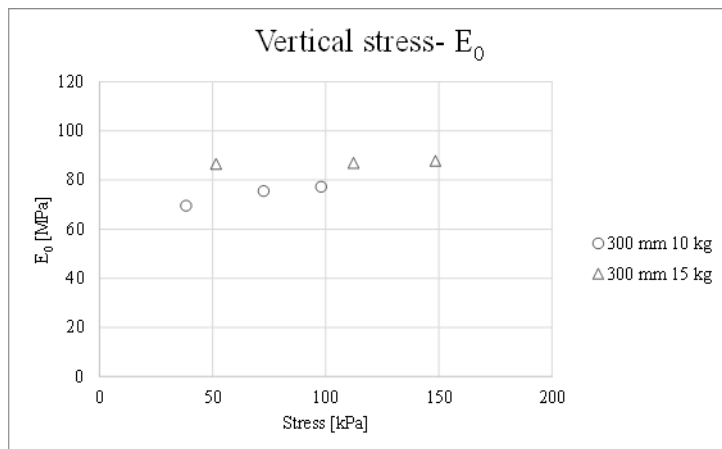
Point 2			
Diameter [mm]		Stress [kPa]	E_o [MPa]
300	p1	51.75	33.75
	p2	74.25	35
	p3	98.75	36
	p4	66.5	41.75
	p5	112.5	38.5
	p6	147.5	35.5



Point 3:

Test	Diameter [mm]	Weight [kg]	H [in]	Drop [-]	Stress [kPa]	Def. [μm]	E _{LWD} [MPa]
p1	300	10	13	1	51	278	48
				2	51	201	67
				3	51	185	73
				4	38	148	68
				5	39	149	69
				6	36	145	65
				7	39	142	72
				8	39	142	72
p2	300	10	23	1	74	278	70
				2	74	262	74
				3	74	259	75
				4	74	257	76
				5	70	256	72
				6	74	250	78
				7	72	254	75
				8	74	254	77
p3	300	10	33	1	97	349	73
				2	99	343	76
				3	97	330	77
				4	99	345	76
				5	98	343	75
				6	98	329	78
				7	96	335	75
				8	100	324	81
p4	300	15	13	2	72	240	79
				3	71	229	82
				4	72	225	84
				5	55	163	89
				6	41	127	85
				7	55	169	86
				8	55	168	86
p5	300	15	23	1	112	352	84
				2	113	345	86
				3	114	349	86
				4	113	342	87
				5	111	344	85
				6	113	335	89
				7	113	341	87
				8	112	340	87
p6	300	15	33	1	150	462	85
				2	149	461	85
				3	147	452	86
				4	152	447	90
				5	149	453	87
				6	149	451	87
				7	148	443	88
				8	148	438	89

Point 3			
Diameter [mm]		Stress [kPa]	E_o [MPa]
300	p1	38.25	69.5
	p2	72.5	75.5
	p3	98	77.25
	p4	51.5	86.5
	p5	112.25	87
	p6	148.5	87.75

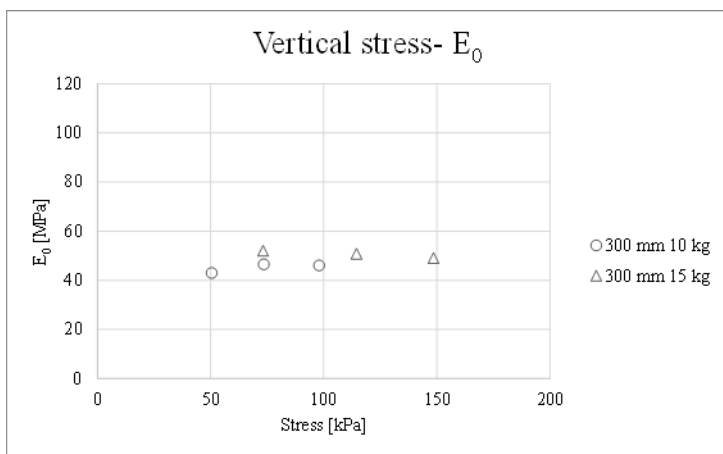


Point 4:

Test	Diameter [mm]	Weight [kg]	H [in]	Drop [-]	Stress [kPa]	Def. [μm]	E_{LWD} [MPa]
p1	300	10	13	1	52	714	19
				2	49	384	34
				3	50	344	38
				4	51	336	40
				5	49	324	40
				6	51	316	42
				7	51	293	46
				8	51	309	44
p2	300	10	23	1	74	474	41
				2	73	456	42
				3	78	443	46
				4	74	436	45
				5	72	428	45
				6	74	422	46
				7	74	408	48
				8	74	415	47
p3	300	10	33	1	98	585	44
				2	99	578	45
				3	99	570	46
				4	99	568	46
				5	97	563	45
				6	99	536	48
				7	97	586	44
				8	99	556	47
p4	300	15	13	1	73	403	47
				2	73	389	50
				3	73	385	50
				4	73	369	52
				5	73	374	52
				6	73	372	52
				7	73	370	52

Test	Diameter [mm]	Weight [kg]	H [in]	Drop [-]	Stress [kPa]	Def. [μm]	E _{LWD} [MPa]
				8	74	370	52
p5	300	15	23	1	113	605	49
				2	112	583	51
				3	114	598	50
				4	112	598	49
				5	115	598	50
				6	114	595	50
				7	115	575	52
				8	114	587	51
p6	300	15	33	1	148	807	48
				2	149	802	49
				3	149	809	49
				4	149	795	49
				5	147	802	48
				6	149	797	49
				7	148	791	49
				8	150	790	50

Point 4			
Diameter [mm]		Stress [kPa]	E _o [MPa]
300	p1	50.5	43
	p2	73.5	46.5
	p3	98	46
	p4	73.25	52
	p5	114.5	50.75
	p6	148.5	49



Layer 2:

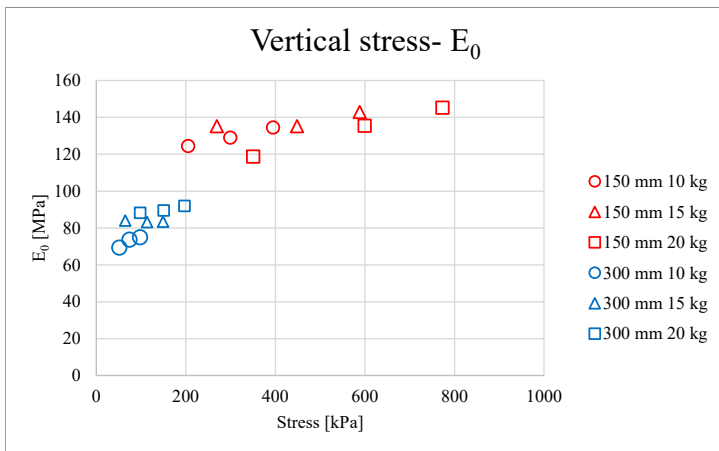
Point 1:

Test	Diameter [mm]	Weight [kg]	H [in]	Drop [-]	Stress [kPa]	Def. [μm]	E _{LWD} [MPa]
p7	150	20	13	1	385	425	119
				2	395	415	125
				3	395	415	125
				4	393	388	133
				5	243	280	114
				6	394	408	127
				7	380	441	113
				8	384	417	121
p8	150	20	23	1	602	642	123
				2	611	611	132
				3	600	559	141
				4	604	590	135
				5	600	586	135
				6	603	581	137
				7	599	584	135
				8	596	581	135
p9	150	20	33	1	764	706	142
				2	766	714	141
				3	776	695	147
				4	780	689	149
				5	770	706	144
				6	768	708	143
				7	774	705	145
				8	281	327	113
p4	150	15	13	2	174	207	111
				3	283	316	118
				4	289	295	129
				5	221	250	116
				7	284	214	175
				8	283	309	121
				1	448	449	131
				2	455	451	133
p5	150	15	23	3	456	444	135
				4	451	441	135
				5	450	444	133
				6	453	433	138
				7	458	435	139
				8	433	435	131
				1	590	546	142
				2	596	550	143
p6	150	15	33	3	584	557	138
				4	598	536	147
				5	588	544	142
				6	593	539	145
				7	587	542	143
				8	586	545	142
				1	206	225	121
				2	205	219	123
p1	150	10	13	3	165	181	120
				4	74	65	150
				5	203	215	124
				6	206	217	125
				7	204	217	124
				8	207	218	125
				1	289	310	123
				2	291	305	126
p2	150	10	23	3	233	254	121
				4	290	305	125
				5	299	306	129

Test	Diameter [mm]	Weight [kg]	H [in]	Drop [-]	Stress [kPa]	Def. [μm]	E _{LWD} [MPa]
p3	150	10	33	6	298	303	129
				7	301	306	129
				8	299	304	129
				1	398	378	139
				2	391	383	134
				3	400	394	134
				4	399	391	134
				5	389	382	134
p1	300	10	13	6	399	387	136
				7	390	389	132
				8	401	389	136
				1	52	422	32
				2	49	228	57
				3	51	210	64
				4	51	204	65
				5	49	198	65
p2	300	10	23	6	52	196	70
				7	52	195	70
				8	52	188	73
				1	72	294	65
				2	73	276	70
				3	73	273	70
				4	72	269	71
				5	74	268	73
p3	300	10	33	6	73	263	73
				7	74	263	74
				8	74	258	75
				1	99	370	71
				2	99	360	72
				3	98	357	72
				4	97	350	73
				5	97	334	76
p4	300	15	13	6	98	348	74
				7	97	343	75
				8	98	341	75
				1	73	249	77
				2	73	237	81
				3	71	235	80
				4	71	231	81
				5	72	227	83
p5	300	15	23	6	57	180	84
				7	57	177	85
				8	73	228	84
				1	115	377	80
				2	114	369	82
				3	114	366	82
				4	113	364	82
				5	114	361	83
p6	300	15	33	6	112	353	84
				7	113	360	82
				8	114	358	84
				1	148	456	85
				2	149	495	79
				3	150	486	81
				4	148	472	82
				5	150	475	83
p7	300	20	13	6	150	475	83
				7	148	469	83
				8	149	465	85
				1	99	297	88
				2	99	296	88
				3	99	293	89
				4	98	292	89

Test	Diameter [mm]	Weight [kg]	H [in]	Drop [-]	Stress [kPa]	Def. [μm]	E _{LWD} [MPa]
				5	99	292	89
				6	99	291	89
				7	97	289	88
				8	97	292	87
p8	300	20	23	1	153	449	90
				2	151	443	90
				3	151	442	90
				4	152	441	91
				5	151	446	89
				6	150	440	90
				7	150	445	89
				8	151	443	90
p9	300	20	33	1	194	604	85
				2	195	584	88
				3	192	566	89
				4	194	583	88
				5	192	558	91
				6	196	567	91
				7	204	572	94
				8	196	564	92

Point 1			
Diameter [mm]		Stress [kPa]	E _o [MPa]
150	p7	350.25	118.75
	p8	599.5	135.5
	p9	773	145.25
	p4	269.25	135.25
	p5	448.5	135.25
	p6	588.5	143
	p1	205	124.5
	p2	299.25	129
	p3	394.75	134.5
300	p1	51.25	69.5
	p2	73.75	73.75
	p3	97.5	75
	p4	64.75	84
	p5	113.25	83.25
	p6	149.25	83.5
	p7	98	88.25
	p8	150.5	89.5
	p9	197	92



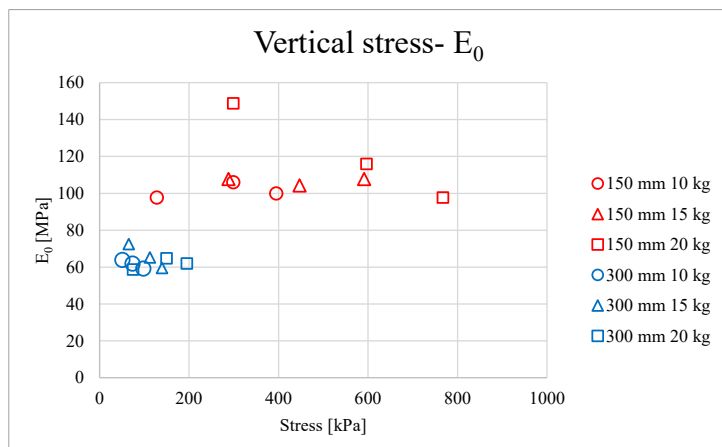
Point 2:

Test	Diameter [mm]	Weight [kg]	H [in]	Drop [-]	Stress [kPa]	Def. [μm]	E_{LWD} [MPa]
p7	150	20	13	1	390	566	91
				2	388	551	93
				3	387	539	94
				4	391	532	97
				5	394	513	101
				6	306	263	153
				7	311	228	179
				8	185	151	162
p8	150	20	23	1	597	671	117
				2	577	722	105
				3	593	781	100
				4	591	751	104
				5	595	703	112
				6	595	662	118
				7	599	683	115
				8	597	659	119
p9	150	20	33	1	774	943	108
				2	766	1013	100
				3	765	1070	94
				4	757	1092	91
				5	761	1071	94
				6	770	1051	97
				7	771	1018	100
				8	767	1012	100
p4	150	15	13	1	288	380	100
				2	284	368	102
				3	283	370	100
				4	288	365	104
				5	285	357	105
				6	290	346	110
				7	288	355	107
				8	290	350	109
p5	150	15	23	1	451	564	105
				2	438	570	101
				3	444	558	105
				4	449	574	103
				5	452	542	110
				6	444	570	102
				7	445	575	102
				8	447	572	103
p6	150	15	33	1	575	769	99
				2	585	736	105
				3	589	743	104
				4	587	738	105
				5	594	737	106

Test	Diameter [mm]	Weight [kg]	H [in]	Drop [-]	Stress [kPa]	Def. [μm]	E _{LWD} [MPa]
p1	150	10	13	6	590	734	106
				7	592	691	113
				8	588	732	106
				1	206	270	100
				2	206	263	103
				3	160	226	93
				4	123	184	88
				5	91	118	102
p2	150	10	23	6	89	130	90
				7	126	178	93
				8	206	255	106
				1	289	371	103
				2	298	374	105
				3	293	393	98
				4	296	392	99
				5	300	369	107
p3	150	10	33	6	299	373	106
				7	299	372	106
				8	298	374	105
				1	399	485	108
				2	397	496	105
				3	396	503	104
				4	389	514	100
				5	398	525	100
p4	300	10	13	6	391	516	100
				7	391	516	100
				8	399	525	100
				1	52	710	19
				2	50	259	51
				3	41	197	55
				4	30	145	55
				5	51	216	63
p5	300	10	23	6	51	210	64
				7	50	210	63
				8	51	204	66
				1	74	345	56
				2	74	332	59
				3	72	322	59
				4	74	306	64
				5	73	320	60
p3	300	10	33	6	73	309	62
				7	74	308	63
				8	73	305	63
				1	97	454	56
				2	99	442	59
				3	97	436	59
				4	99	436	60
				5	99	439	60
p4	300	15	13	6	97	440	58
				7	97	432	59
				8	98	430	60
				1	71	291	65
				2	73	278	69
				3	72	265	72
				4	74	24	825
				5	57	214	70
p5	300	15	23	6	57	204	74
				7	73	269	72
				8	74	263	74
				1	114	464	65
				2	112	464	63
				3	114	462	65
				4	112	461	64

Test	Diameter [mm]	Weight [kg]	H [in]	Drop [-]	Stress [kPa]	Def. [μm]	E _{LWD} [MPa]
				5	112	450	66
				6	111	458	64
				7	112	457	65
				8	114	455	66
p6	300	15	33	1	146	667	58
				2	148	665	59
				3	148	658	59
				4	147	653	59
				5	149	648	60
				6	149	629	62
				7	147	646	60
				8	114	534	56
p7	300	20	13	1	98	406	64
				2	77	327	62
				3	62	242	68
				4	98	391	66
				5	96	390	65
				6	50	319	42
				7	55	236	62
				8	98	393	66
p8	300	20	23	1	150	629	63
				2	150	623	63
				3	87	531	43
				4	149	598	65
				5	150	615	64
				6	150	605	65
				7	148	607	64
				8	150	597	66
p9	300	20	33	1	193	758	67
				2	193	857	59
				3	191	850	59
				4	194	842	61
				5	191	837	60
				6	191	834	60
				7	191	828	61
				8	208	823	67

Point 2		
Diameter [mm]	Stress [kPa]	E _o [MPa]
150	p7	299 148.75
	p8	596.5 116
	p9	767.25 97.75
	p4	288.25 107.75
	p5	447 104.25
	p6	591 107.75
	p1	128 97.75
	p2	299 106
	p3	394.75 100
300	p1	50.75 64
	p2	73.25 62
	p3	97.75 59.25
	p4	65.25 72.5
	p5	112.25 65.25
	p6	139.75 59.5
	p7	74.75 58.75
	p8	149.5 64.75
	p9	195.25 62



Point 3:

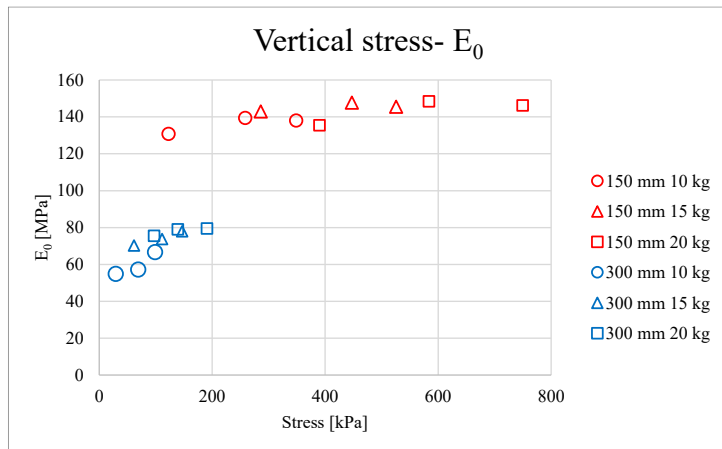
Test	Diameter [mm]	Weight [kg]	H [in]	Drop [-]	Stress [kPa]	Def. [μm]	E _{LWD} [MPa]
p7	150	20	13	1	388	483	106
				2	384	431	117
				3	393	415	125
				4	385	395	128
				5	389	392	131
				6	390	380	135
				7	392	374	138
				8	389	370	138
p8	150	20	23	1	593	531	147
				2	590	580	134
				3	590	541	143
				4	587	529	146
				5	582	533	144
				6	579	522	146
				7	590	525	148

Test	Diameter [mm]	Weight [kg]	H [in]	Drop [-]	Stress [kPa]	Def. [μm]	E _{LWD} [MPa]
p9	150	20	33	8	583	492	156
				1	764	637	158
				2	760	679	147
				3	759	700	143
				4	756	675	147
				5	756	623	160
				6	727	734	130
				7	751	723	137
				8	764	636	158
p4	150	15	13	1	284	276	135
				2	221	216	135
				3	140	139	133
				4	286	258	145
				5	283	256	145
				6	288	267	142
				7	285	265	142
				8	287	264	143
p5	150	15	23	1	451	418	142
				2	452	402	148
				3	451	391	152
				4	454	378	158
				5	446	398	148
				6	449	404	146
				7	443	405	144
				8	451	387	153
p6	150	15	33	1	589	511	152
				2	563	528	140
				3	586	529	146
				4	590	489	159
				5	582	524	146
				6	589	521	149
				7	342	353	128
				8	203	232	115
p1	150	10	13	2	114	137	109
				3	209	193	142
				4	156	172	119
				5	162	160	133
				6	117	124	124
				7	121	133	120
				8	91	82	146
				1	296	267	146
p2	150	10	23	2	292	271	142
				3	296	268	146
				4	226	225	132
				5	294	266	146
				6	220	204	142
				7	294	273	142
				8	225	232	128
				1	398	359	146
p3	150	10	33	2	390	369	139
				3	396	376	139
				4	389	368	139
				5	390	368	140
				6	397	357	146
				7	209	214	128
				8	399	381	138
				1	52	469	29
p1	300	10	13	2	51	273	49
				3	40	220	48
				4	38	215	47
				5	17	102	44
				6	10	40	66
				7	40	199	53

Test	Diameter [mm]	Weight [kg]	H [in]	Drop [-]	Stress [kPa]	Def. [μm]	E _{LWD} [MPa]
				8	50	232	57
p2	300	10	23	1	74	373	52
				2	72	362	52
				3	74	330	59
				4	72	329	58
				5	72	325	58
				6	57	278	54
				7	74	323	60
				8	72	332	57
p3	300	10	33	1	98	448	58
				2	100	439	60
				3	99	418	62
				4	98	407	63
				5	99	404	65
				6	99	395	66
				7	99	382	68
				8	98	379	68
p4	300	15	13	1	72	276	69
				2	72	273	69
				3	44	178	65
				4	23	18	336
				5	72	267	71
				6	73	266	72
				7	57	216	69
				8	45	171	69
p5	300	15	23	1	113	398	75
				2	113	399	75
				3	111	407	72
				4	111	410	71
				5	111	403	73
				6	111	397	74
				7	112	401	74
				8	111	396	74
p6	300	15	33	1	147	547	71
				2	146	540	71
				3	146	517	74
				4	147	527	73
				5	147	466	83
				6	147	505	77
				7	147	515	75
				8	147	505	77
p7	300	20	13	1	97	352	73
				2	97	335	76
				3	97	339	75
				4	97	334	76
				5	96	332	76
				6	98	337	77
				7	98	346	75
				8	97	346	74
p8	300	20	23	1	148	475	82
				2	147	479	81
				3	146	474	81
				4	148	461	85
				5	117	416	74
				6	147	499	78
				7	147	490	79
				8	145	448	85
p9	300	20	33	1	189	636	78
				2	190	619	81
				3	190	609	82
				4	196	613	84
				5	191	632	80
				6	190	637	79
				7	191	646	78

Test	Diameter [mm]	Weight [kg]	H [in]	Drop [-]	Stress [kPa]	Def. [μm]	E_{LWD} [MPa]
				8	191	622	81

Point 3			
Diameter [mm]		Stress [kPa]	E_o [MPa]
150	p7	390	135.5
	p8	583.5	148.5
	p9	749.5	146.25
	p4	285.75	143
	p5	447.25	147.75
	p6	525.75	145.5
	p1	122.75	130.75
	p2	258.25	139.5
	p3	348.75	138
300	p1	29.25	55
	p2	68.75	57.25
	p3	98.75	66.75
	p4	61.75	70.25
	p5	111.25	73.75
	p6	147	78
	p7	97.25	75.5
	p8	139	79
	p9	190.75	79.5



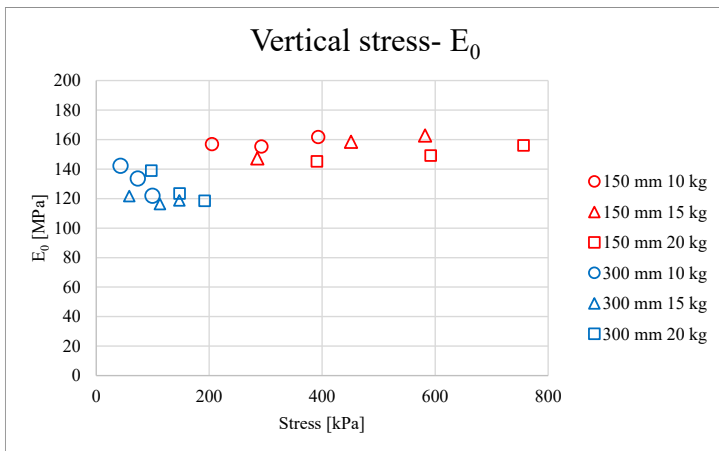
Point 4:

Test	Diameter [mm]	Weight [kg]	H [in]	Drop [-]	Stress [kPa]	Def. [μm]	E_{LWD} [MPa]
p7	150	20	13	1	383	600	84
				2	389	395	130
				3	389	393	130
				4	386	370	137
				5	391	358	144
				6	392	357	145
				7	389	349	147
				8	391	356	145
p8	150	20	23	1	595	536	146
				2	593	533	146
				3	584	525	146
				4	595	515	152
				5	585	515	150
				6	599	576	137
				7	590	504	154
				8	595	503	156
p9	150	20	33	1	765	650	155
				2	757	673	148
				3	763	648	155
				4	766	633	159
				5	756	628	158
				6	755	659	151
				7	753	651	152
				8	762	614	163
p4	150	15	13	1	273	256	140
				2	281	249	149
				3	286	265	142
				4	281	264	140
				5	279	266	138
				6	280	233	158
				7	291	267	143
				8	291	255	150
p5	150	15	23	1	449	375	158
				2	452	368	162
				3	447	374	157
				4	452	356	167
				5	454	374	160
				6	450	372	159
				7	450	373	159
				8	450	379	156
p6	150	15	33	1	592	470	166
				2	587	475	163
				3	581	437	175
				4	590	456	170
				5	586	475	162
				6	583	473	162
				7	579	463	165
				8	581	471	162
p1	150	10	13	1	202	178	149
				2	154	137	148
				3	160	137	154
				4	206	167	162
				5	205	172	157
				6	205	171	158
				7	204	174	154
				8	206	170	159
p2	150	10	23	1	298	225	174
				2	294	250	155
				3	292	250	154
				4	295	248	157
				5	294	242	160
				6	289	252	151
				7	295	249	156

Test	Diameter [mm]	Weight [kg]	H [in]	Drop [-]	Stress [kPa]	Def. [μm]	E _{LWD} [MPa]
p3	150	10	33	8	292	249	154
				1	396	312	167
				2	395	320	162
				3	394	324	160
				4	395	321	162
				5	397	321	163
				6	393	320	162
				7	394	320	162
				8	388	319	160
p1	300	10	13	1	51	93	144
				2	50	95	138
				3	21	58	98
				4	49	86	151
				5	29	58	131
				6	50	90	148
				7	41	73	149
				8	51	97	139
				9	30	59	133
				1	74	150	131
p2	300	10	23	2	73	153	126
				3	75	153	129
				4	74	153	127
				5	73	149	130
				6	73	149	128
				7	73	133	145
				8	74	147	132
				1	99	209	125
p3	300	10	33	2	100	210	125
				3	100	202	130
				4	99	222	117
				5	99	218	119
				6	100	209	126
				7	99	207	126
				1	70	177	104
p4	300	15	13	2	55	114	126
				3	28	79	93
				4	54	108	133
				5	73	145	132
				6	73	164	117
				7	44	95	120
				8	44	98	118
				1	113	278	107
p5	300	15	23	2	113	279	107
				3	112	284	104
				4	112	279	106
				5	113	272	110
				6	114	261	114
				7	112	258	114
				8	112	233	127
				1	146	350	109
p6	300	15	33	2	147	348	111
				3	142	346	108
				4	148	347	112
				5	148	341	115
				6	148	338	115
				7	146	313	123
				8	147	317	122
				1	95	202	124
p7	300	20	13	2	98	196	131
				3	96	190	133
				4	96	200	126
				5	97	189	135

Test	Diameter [mm]	Weight [kg]	H [in]	Drop [-]	Stress [kPa]	Def. [μm]	E _{LWD} [MPa]
p8	300	20	23	6	98	182	141
				7	98	183	141
				8	97	183	139
				1	149	327	119
				2	149	318	123
				3	148	311	125
				4	146	309	125
				5	147	299	130
				6	148	316	123
p9	300	20	33	7	146	322	119
				8	149	320	122
				1	190	449	111
				2	190	432	116
				3	190	430	116
				4	193	430	118
				5	192	427	119
				6	191	427	118
				7	192	422	119
				8	193	431	118

Point 4			
Diameter [mm]		Stress [kPa]	E _o [MPa]
150	p7	390.75	145.25
	p8	592.25	149.25
	p9	756.5	156
	p4	285.25	147.25
	p5	451	158.5
	p6	582.25	162.75
	p1	205	157
	p2	292.5	155.25
	p3	393	161.75
300	p1	43	142.25
	p2	73.25	133.75
	p3	99.25	122
	p4	58.5	121.75
	p5	112.75	116.25
	p6	147.25	118.75
	p7	97.5	139
	p8	147.5	123.5
	p9	192	118.5



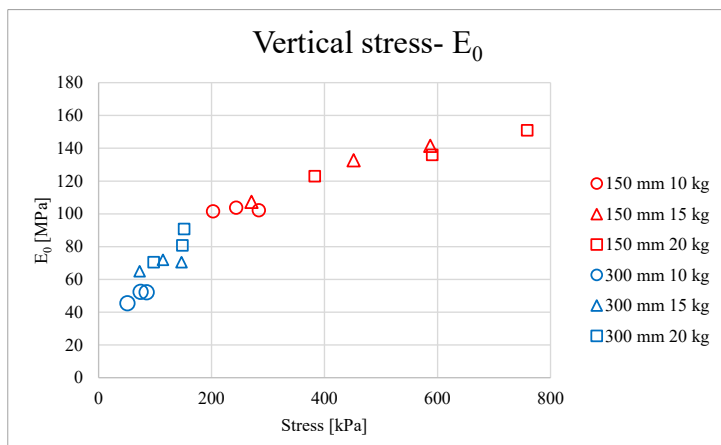
Point 5:

Test	Diameter [mm]	Weight [kg]	H [in]	Drop [-]	Stress [kPa]	Def. [μm]	E_{LWD} [MPa]
p7	150	20	13	1	389	415	124
				2	390	414	124
				3	388	420	122
				4	384	425	119
				5	387	413	123
				6	381	412	122
				7	388	416	123
				8	374	398	124
p8	150	20	23	1	566	645	116
				2	593	604	129
				3	593	585	133
				4	593	575	136
				5	587	582	133
				6	592	575	135
				7	591	567	137
				8	592	560	139
p9	150	20	33	1	758	685	146
				2	768	707	143
				3	762	706	142
				4	766	699	144
				5	758	623	160
				6	762	670	150
				7	760	679	147
				8	755	674	147
p4	150	15	13	1	288	374	101
				2	283	364	102
				3	283	357	104
				4	287	339	111
				5	284	351	107
				6	222	283	103
				7	289	348	109
				8	288	346	110
p5	150	15	23	1	76	99	101
				2	448	450	131
				3	452	450	132
				4	453	444	134
				5	452	448	133
				6	443	452	129
				7	457	448	134
				8	453	440	135
p6	150	15	33	1	584	533	144
				2	589	541	143
				3	581	541	141
				4	594	532	147
				5	588	545	142

Test	Diameter [mm]	Weight [kg]	H [in]	Drop [-]	Stress [kPa]	Def. [μm]	E _{LWD} [MPa]
p1	150	10	13	6	588	550	141
				7	586	549	140
				8	586	541	143
				1	203	280	96
				2	207	278	98
				3	204	281	96
				4	207	267	102
				5	206	256	106
p2	150	10	23	6	199	265	99
				7	200	268	98
				8	206	264	103
				1	290	341	112
				2	296	336	116
				3	297	339	115
				4	299	340	116
				5	297	336	116
p3	150	10	33	6	292	346	111
				7	232	309	99
				8	153	227	89
				1	392	404	128
				2	399	407	129
				3	395	413	126
				4	397	423	123
				5	288	353	107
p4	300	10	13	6	281	372	99
				7	288	379	100
				8	278	355	103
				1	54	1063	13
				2	21	188	29
				3	30	242	33
				4	39	262	39
				5	51	311	43
p5	300	10	23	6	51	292	46
				7	50	290	45
				8	52	285	48
				1	72	414	46
				2	72	396	48
				3	75	386	51
				4	73	360	54
				5	73	366	52
p3	300	10	33	6	75	367	54
				7	74	367	53
				8	74	379	51
				1	98	444	58
				2	97	460	56
				3	99	462	56
				4	98	458	56
				5	97	484	53
p4	300	15	13	6	72	393	48
				7	73	385	50
				8	98	443	58
				1	72	310	61
				2	57	239	63
				3	46	213	56
				4	33	179	48
				5	73	294	66
p5	300	15	23	6	72	294	65
				7	73	300	64
				8	73	296	65
				1	113	437	68
				2	112	418	70
				3	113	414	72
				4	114	413	73

Test	Diameter [mm]	Weight [kg]	H [in]	Drop [-]	Stress [kPa]	Def. [μm]	E _{LWD} [MPa]
				5	114	409	73
				6	114	415	72
				7	113	416	71
				8	114	418	72
p6	300	15	33	1	149	518	75
				2	150	522	76
				3	147	513	76
				4	148	467	84
				5	148	552	70
				6	147	570	68
				7	147	559	69
				8	146	516	75
p7	300	20	13	1	97	387	66
				2	77	323	63
				3	96	363	69
				4	97	370	69
				5	98	371	69
				6	98	362	71
				7	96	359	71
				8	98	359	71
p8	300	20	23	1	148	481	81
				2	149	487	80
				3	150	484	81
				4	149	481	81
				5	147	482	80
				6	150	486	81
				7	148	482	81
				8	149	485	81
p9	300	20	33	1	192	603	84
				2	181	596	80
				3	192	599	84
				4	190	599	84
				5	193	582	88
				6	191	596	84
				7	33	82	105
				8	188	577	86

Point 5			
Diameter [mm]		Stress [kPa]	E_0 [MPa]
150	p7	590.5	136
	p8	382.5	123
	p9	758.75	151
	p4	270.75	107.25
	p5	451.25	132.75
	p6	587	141.5
	p1	202.75	101.5
	p2	243.5	103.75
	p3	283.75	102.25
300	p1	51	45.5
	p2	74	52.5
	p3	85	52.25
	p4	72.75	65
	p5	113.75	72
	p6	147	70.5
	p7	97.5	70.5
	p8	148.5	80.75
	p9	151.25	90.75



Point 6:

Test	Diameter [mm]	Weight [kg]	H [in]	Drop [-]	Stress [kPa]	Def. [μm]	E_{LWD} [MPa]
p7	150	20	13	1	391	722	71
				2	301	418	95
				3	108	147	97
				4	34	29	154
				5	389	487	105
				6	379	472	106
				7	382	477	105
				8	380	462	108
p8	150	20	23	1	587	755	102
				2	578	734	104
				3	582	737	104
				4	582	729	105
				5	581	718	106
				6	586	712	108
				7	580	707	108

Test	Diameter [mm]	Weight [kg]	H [in]	Drop [-]	Stress [kPa]	Def. [μm]	E _{LWD} [MPa]
p9	150	20	33	8	587	701	110
				1	760	951	105
				2	746	950	103
				3	748	944	104
				4	747	929	106
				5	748	928	106
				6	754	924	107
				7	754	840	118
				8	757	913	109
p4	150	15	13	1	285	359	104
				2	284	352	106
				3	284	362	103
				4	278	356	103
				5	281	344	107
				6	291	329	117
				7	224	271	109
				8	289	314	121
p5	150	15	23	1	453	507	118
				2	452	520	114
				3	449	518	114
				4	447	508	116
				5	450	516	115
				6	449	517	114
				7	447	506	116
				8	445	504	116
p6	150	15	33	1	586	643	120
				2	577	653	116
				3	571	675	111
				4	589	660	117
				5	586	657	117
				6	580	645	118
				7	584	643	120
				8	574	642	118
p1	150	10	13	1	204	241	111
				2	200	241	109
				3	88	93	125
				4	83	88	124
				5	81	90	118
				6	121	141	113
				7	121	152	105
				8	122	149	108
p2	150	10	23	1	291	330	116
				2	290	342	112
				3	289	347	110
				4	294	344	112
				5	294	337	115
				6	292	339	113
				7	293	338	114
				8	291	323	118
p3	150	10	33	1	387	427	119
				2	398	440	119
				3	393	431	120
				4	281	338	109
				5	277	334	109
				6	215	269	105
				7	390	438	117
				8	386	431	118
p1	300	10	13	1	50	245	54
				2	51	222	60
				3	49	221	58
				4	51	214	62
				5	39	175	59
				6	39	175	59

Test	Diameter [mm]	Weight [kg]	H [in]	Drop [-]	Stress [kPa]	Def. [μm]	E _{LWD} [MPa]
				7	51	208	65
				8	49	207	63
p2	300	10	23	1	73	339	57
				2	72	327	58
				3	74	283	69
				4	55	253	58
				5	73	323	60
				6	57	248	60
				7	74	330	59
				8	74	338	58
p3	300	10	33	1	98	471	55
				2	97	457	56
				3	72	330	57
				4	99	458	57
				5	72	328	58
				6	73	325	59
				7	100	440	60
				8	96	414	61
p4	300	15	13	1	72	291	65
				2	56	217	68
				3	56	213	69
				4	43	163	70
				5	44	158	73
				6	43	160	70
				7	44	156	74
				8	43	160	70
p5	300	15	23	1	113	455	65
				2	112	456	65
				3	112	459	64
				4	113	449	66
				5	112	446	66
				6	114	443	68
				7	112	433	68
				8	113	428	69
p6	300	15	33	1	145	613	62
				2	145	608	63
				3	144	607	63
				4	146	618	62
				5	145	608	63
				6	149	589	67
				7	146	602	64
				8	146	579	67
p7	300	20	13	1	96	374	68
				2	75	286	69
				3	96	373	68
				4	95	371	68
				5	97	380	67
				6	76	281	71
				7	75	283	70
				8	76	271	74
p8	300	20	23	1	147	569	68
				2	147	569	68
				3	146	564	68
				4	146	560	68
				5	147	581	67
				6	146	588	66
				7	146	517	74
				8	146	558	69
p9	300	20	33	1	187	770	64
				2	186	779	63
				3	188	779	64
				4	187	764	64
				5	189	771	64
				6	189	767	65

Test	Diameter [mm]	Weight [kg]	H [in]	Drop [-]	Stress [kPa]	Def. [μm]	E_{LWD} [MPa]
				7	189	758	66
				8	187	751	66

Point 6			
Diameter [mm]		Stress [kPa]	E_o [MPa]
150	p7	382.5	106
	p8	583.5	108
	p9	753.25	110
	p4	271.25	113.5
	p5	447.75	115.25
	p6	581	118.25
	p1	111.25	111
	p2	292.5	115
	p3	317	112.25
300	p1	44.5	61.5
	p2	69.5	59.25
	p3	85.25	59.5
	p4	43.5	71.75
	p5	112.75	67.75
	p6	146.5	65.25
	p7	81	70.5
	p8	146.25	69
	p9	188.5	65.25

